

Electronic Thesis and Dissertation Repository

12-7-2021 5:30 PM

The Use of CT to Assess Shoulder Kinematics and Measure Glenohumeral Arthrokinematics

Baraa Daher, *The University of Western Ontario*

Supervisor: Lalone, Emily, *The University of Western Ontario*

A thesis submitted in partial fulfillment of the requirements for the Master of Engineering Science degree in Biomedical Engineering

© Baraa Daher 2021

Follow this and additional works at: <https://ir.lib.uwo.ca/etd>



Part of the [Biomechanics and Biotransport Commons](#)

Recommended Citation

Daher, Baraa, "The Use of CT to Assess Shoulder Kinematics and Measure Glenohumeral Arthrokinematics" (2021). *Electronic Thesis and Dissertation Repository*. 8295.
<https://ir.lib.uwo.ca/etd/8295>

This Dissertation/Thesis is brought to you for free and open access by Scholarship@Western. It has been accepted for inclusion in Electronic Thesis and Dissertation Repository by an authorized administrator of Scholarship@Western. For more information, please contact wlsadmin@uwo.ca.

Abstract

Recently, studies have started employing dynamic four-dimensional computed tomography (4DCT) imaging as a biomechanical assessment tool. These studies would benefit from the valuable work that has been done in the past using three-dimensional computed tomography (3DCT). Thus, a structured review was conducted to examine the extent and range of methods employing CT imaging to measure shoulder kinematics. The findings of the review were utilized to conduct a study that employed 4DCT imaging to measure glenohumeral joint congruency and arthrokinematics during internal rotation to the back in a population of healthy individuals. The results of this work show the importance of anterior-posterior translation throughout the motion to achieve maximum range of motion. In conclusion, the use of 4DCT as a biomechanical measuring tool has shown to be a reliable technique in quantifying joint congruency and arthrokinematics of the glenohumeral joint and shows promise for future studies.

Keywords

Computed tomography, four-dimensional computed tomography, shoulder, glenohumeral joint, kinematics, arthrokinematics, joint congruency, proximity maps, joint surface area, contact center translation.

Summary for Lay Audience

The shoulder is the most mobile joint in the human body with a wide range of motion. Thus, it is more susceptible to injury and disorders which affect the shoulder's function. Its special range of motion makes the assessment of shoulder motion a challenging task. Static imaging techniques, such as x-ray and computed tomography (CT), can only visualize the position of the bones when the shoulder is stationary. This is a problem when developing treatment plans after injuries, as an understanding of dynamic healthy motion is required to develop treatment plans. As new studies emerge that employ dynamic imaging and replace traditional static techniques, these studies would benefit from the valuable work that has been done in the past. To inform researchers of previously used techniques and their associated limitations, a literature review was conducted. The review (Chapter 2) outlined current gaps and discrepancies in research studies and made recommendations for future studies investigating shoulder motion pathways while using computed tomography (CT) imaging. These recommendations were then utilized in a subsequent study (Chapter 3) that uses a dynamic imaging modality called four-dimensional computed tomography (4DCT) as a motion measuring tool while participants rotated their shoulder behind their back. This motion is important in activities of daily living, such as washing the back and opposite shoulder, using a back pocket, managing toileting and clasping a brassiere. Yet, studies have shown that patients could not fully perform this motion after undergoing a shoulder surgery called reverse shoulder arthroplasty, as the shoulder was limited to only rotate. Thus, this thesis used dynamic 4DCT to measure the movement of shoulder bones surfaces in healthy adults. The results explain the importance of translation in performing the motion, which is restricted after the surgery thus limiting the motion. The use of 4DCT as a measuring tool has shown to be a reliable technique in quantifying the motion of shoulder bones surfaces. Dynamic measuring of healthy shoulder motion can help clinicians and researchers in the development of pre- and post-operative treatment plans and enhance implant designs.

Co-Authorship Statement

Chapter 1:

Baraa Daher – Sole author

Chapter 2:

Baraa Daher – Study design, literature review, data extraction, data analysis, wrote manuscript

James Hunter – Data extraction revision, reclassification of motions to standard terms, reviewed manuscript

George Athwal – Study design, reviewed manuscript

Yara Hosein – Study design, reviewed manuscript

Emily Lalone – Study design, literature review, reviewed manuscript

Chapter 3:

Baraa Daher – Study design, data collection, data analysis, statistical analysis, wrote manuscript

James Hunter – Data collection, data analysis, reviewed manuscript

George Athwal – Study design, data interpretation, reviewed manuscript

Yara Hosein – Study design, data interpretation, reviewed manuscript

Emily Lalone – Study design, data interpretation, reviewed manuscript

Chapter 4:

Baraa Daher – Sole author

Dedication

*To my parents,
for their endless sacrifices,
their invaluable support,
and their encouragement to go on every adventure, especially this one:*

Mohamad Daher and Hanadi Senjab

*To my siblings,
my biggest support group,
for their love and laughter,
for our night cruises,
and for always having my back:*

Salim, Sara, Abdullah, and Maria

I would move mountains for each and every one of you

الحمد لله الذي بنعمته تتم الصالحات
أهدي ثمرة جهدي هذا
إلى معلم البشرية أجمعين،
المهادي الأمين،
محمد صلى الله عليه و سلم

إلى من نذرت حياتها لنا فنسيت نفسها،
إلى التي في لمسة يدها رحمة الله و في نظرة عينيها طمأنينة الدنيا،
إلى التي جاورت قلبها قبل أن تراني عيناها،
إلى أعظم هبة وهبها الله لي،
إلى أعذب لفظ تلفظت به شفاه البشرية،
إلى من أتلمس خطواتي برضاها،
إلى نور عيني و ضياء حياتي،
إلى شمسي التي لا ينقطع دفؤها،
إلى أمي هنادي سنجاب

إلى من أضاء أول قنديل في حياتي،
إلى من حصد الأشواك ليمد لنا الطريق و حمانا من عواصف الأقدار،
إلى حبيبي و روح قلبي، عبق طفولتي و دفء حياتي،
إلى سندي و مصدر قوتي و فخري،
إلى من في ابتسامته أختصر أجمل معاني السعادة،
إلى من أتلمس خطواتي برضاه،
إلى من هو أحب النعم لقلبي،
إلى قمري الذي لا يغيب،
إلى أبي محمد ضاهر

إلى من قال فيهم الشاعر: "أخاك أخاك إن من لا أخأ له ... كساع إلى الهيجا بغير سلاح"
إلى نجوم سمائي المتألثة وسندي في الحياة،
إلى إخوتي و أخواتي: سليم، سارة، عبد الله، و مارية

إلى وطني، ذلك الحب الذي لا يتوقف و ذلك العطاء الذي لا ينضب

Acknowledgments

I would like to thank everyone who made this work possible with their assistance and support. First, I would like to express my deepest gratitude to my mentor Dr Emily Lalone for her exceptional guidance and continuous support. I cannot begin to think where I would be without your help and the lessons one can only learn from a supervisor with such passion and expertise. Your immense knowledge and passion for research, invaluable advice, tremendous patient, and constant encouragement have pushed me to heights I never thought possible. I am forever grateful to have done my master's degree under your supervision. I would also like to extend my gratitude to my advisory committee members, Dr George Athwal and Dr Yara Hosein. Your guidance, invaluable input and feedback, encouragement, and constant motivation have pushed me past my limits and expanded my knowledge. I consider myself fortunate to have learned from you and your experiences.

I would also like to take this opportunity to thank my colleagues at the Human Biomechanics Laboratory: James, Elizabeth, Lauren, Puneet, Sydney and Carla. Special thanks to James Hunter for helping me with data collection and analysis. Thank you to the summer student, Natalie Loewen, for her help in keeping this project move smoothly. I would also like to thank all my friends who have always stood by my side and supported me through this journey: Safa Hammadia, Aya Stif, Lina Tawfik, Sara Alsaadi, Mona Abdulhamid, Dania Alakrad, and Hadeel Rajeh.

I'm extremely grateful for my beloved family for their endless love, support and encouragement to further my education. To my parents: Mohamad Daher and Hanadi Senjab, I would not be where I am today without your support and love. I can never pay you back for your sacrifices in this world. To my siblings: Salim, Sara, Abdullah, and Maria, growing up with you is one of the greatest gifts. Thank you Salim for being my go-to person when things go south. You pushed me out of my comfort zone where I found joy in the field of biomedical engineering. Thank you Sara for converting my STL files to VTK and for accompanying me through this journey. Your sense of humor added colours to data analysis. Thank you Abdullah for always sending me memes and keeping me up-to-date with social trends. Thank you Maria for doing the little favours I ask of you. Whether it is getting me food from the kitchen or going on errands with me.

Lastly, I would like to thank everyone I met through this journey, the Faculty of Engineering and all its staff for supporting me and being my home on campus.

Table of Contents

Abstract	II
Summary for Lay Audience	III
Co-Authorship Statement	IV
Dedication	V
Acknowledgments	VI
Table of Contents	VII
List of Tables	XI
List of Figures	XII
List of Abbreviations	XIII
Chapter 1: Introduction	1
1.1 The shoulder	1
1.2 Anatomy	2
<i>1.2.1 Bones</i>	<i>2</i>
1.2.1.1 Clavicle	2
1.2.1.2 Scapula	7
1.2.1.3 Humerus	9
<i>1.2.2 Ligaments and Joint Capsule</i>	<i>10</i>
<i>1.2.3 Muscles</i>	<i>11</i>

1.2.3.1 Scapulohumeral Muscles _____	11
1.2.3.2 Humerothoracic Muscles _____	13
1.2.3.3 Scapulothoracic Muscles _____	13
1.2.3.4 Biarticular Muscles _____	14
1.3 Joints _____	18
1.4 The glenohumeral joint _____	19
<i>1.4.1 Anatomy</i> _____	19
<i>1.4.2 Glenohumeral Biomechanics</i> _____	20
<i>1.4.4 Osteoarthritis</i> _____	22
1.4.4.1 Surgical Treatment _____	23
1.4.4.1.1 Anatomic Total Shoulder Arthroplasty _____	23
1.4.4.1.2 Reverse Shoulder Arthroplasty _____	24
1.5 Methods to Quantify Articular Contact _____	25
<i>1.5.1 Direct Approaches</i> _____	25
<i>1.5.2 In-Direct Approaches</i> _____	26
1.6 Imaging Modalities _____	27
<i>1.6.1 Radiographs</i> _____	27
<i>1.6.2 Fluoroscopy</i> _____	28
<i>1.6.3 Computed Tomography</i> _____	29
<i>1.6.4 Four-Dimensional Computed Tomography</i> _____	30
1.7 Thesis Rationale _____	31
1.8 Objectives and Hypothesis _____	32
<i>1.8.1 Objectives</i> _____	32
<i>1.8.2 Hypothesis</i> _____	32
1.9 Thesis Overview _____	33

1.10 References _____	34
Chapter 2: How does Computed Tomography Inform our Understanding of Shoulder Kinematics? A Structured Review _____	41
2.1 Introduction _____	41
2.2 Methods _____	43
2.2.1 Literature Search and Study Identification _____	43
2.2.2 Study Selection _____	43
2.2.3 Data Collection Process _____	44
2.3 Results _____	45
2.3.1 Study Demographics _____	45
2.3.2 Population of Individuals Studied _____	60
2.3.3 Joints Studied and Approach Used _____	61
2.3.4 CT Scanning Use _____	73
2.3.5 Motion Description _____	87
2.4 Discussion _____	98
2.5 Limitations _____	101
2.6 Conclusion _____	102
2.7 References _____	104
Chapter 3: Four-Dimensional Computed Tomography Scanning Allows for the Visualization and Measurement of Glenohumeral Joint Arthrokinematics _____	108
3.1 Introduction _____	108
3.2 Methods _____	110
3.2.1 Study Protocol _____	110

3.2.2 <i>Three-Dimensional Reconstruction and Registration</i>	111
3.2.3 <i>Measuring Glenohumeral Joint Congruency</i>	112
3.2.4 <i>Measuring Glenohumeral Arthrokinematics</i>	112
3.2.4 <i>Reliability Analysis</i>	114
3.2.4.1 <i>Arthrokinematics Reliability</i>	114
3.2.4.2 <i>Model-Making Comparison</i>	115
3.3 Results	115
3.3.1 <i>Glenohumeral Joint Congruency</i>	115
3.3.2 <i>Glenohumeral Arthrokinematics</i>	121
3.3.3 <i>Reliability Analysis</i>	127
3.3.3.1 <i>Arthrokinematics Reliability</i>	127
3.3.3.2 <i>Model-Making Comparison</i>	127
3.4 Discussion	130
3.5 Limitations	133
3.6 Conclusion	134
Chapter 4: General Discussion and Conclusions	139
4.1 Summary and Conclusions	139
4.2 Strengths and Limitations	142
4.3 Current and Future Directions	145
4.4 Conclusions	146
4.5 References	147
Curriculum Vitae	148

List of Tables

Table 2.1: Summary of Studies Measuring the Kinematics of the Shoulder _____	46
Table 2.2: Study Demographics _____	54
Table 2.3: Kinematics Measurement _____	63
Table 2.4: Studies Purpose and Outcome Measures _____	74
Table 2.5: CT Scanner Information _____	84
Table 2.6: Description of motion examined _____	88
Table 2.7: Planar Glenohumeral Motions Examined _____	92
Table 2.8: Combined Glenohumeral Motions Examined _____	94
Table 2.9: Range of Motion Reporting _____	96
Table 3.1A: Proximity maps of frames 0-12 for n=7 during internal rotation to the back. A colour scale displays inter-bone distances from 0 to 6.0 mm (0 mm, red; 6 mm, blue) _____	116
Table 3.1B: Proximity maps of frames 14-26 for n=7 during internal rotation to the back. A colour scale displays inter-bone distances from 0 to 6.0 mm (0 mm, red; 6 mm, blue) _____	118
Table 3.2: Percent contact area for n=7 during internal rotation to the back _____	120
Table 3.3: Contact pathways of glenohumeral joint contact throughout the motion, total translation in y- and z-directions, and percent difference of total translation in y- and z-directions _____	123
Table 3.4: Contact pathways of glenohumeral joint contact throughout the motion, total translation in y- and z-directions, and percent difference of total translation in y- and z-directions _____	128

List of Figures

Figure 1.1: Anterior view of the right shoulder _____	4
Figure 1.2: Superior (top) and inferior (bottom) view of the right clavicle. _____	5
Figure 1.3: Anterior view of the right shoulder _____	6
Figure 1.4: Anterior (right panel), posterior (central panel) and lateral view (left panel) of the right scapula _____	8
Figure 1.5: The muscular origins and insertions on the scapula. Anterior (top) and posterior (bottom) view of a right scapula _____	15
Figure 1.6: The muscular origins and insertions on the humerus. Posterior (left) and anterior (right) view of a right humerus. _____	16
Figure 1.7: The muscles of the shoulder complex. Anterior (top) and posterior (bottom) views of a right shoulder _____	17
Figure 2.1: Literature Search and Study Identification _____	44
Figure 2.2: Number of studies by year _____	60
Figure 3.1: Internal rotation to the back: (A) Anterior view of the motion's starting point (B) Anterior view of the motion halfway through (C) Posterior view of the motion's ending point _____	111
Figure 3.2: Summary of image processing and data analysis _____	114
Figure 3.3: Average of total translation in the y- and z-direction of n=7 _____	121
Figure 3.4: Percent average of total translation in the y- and z-direction of n=7 _____	122
Figure 3.5: Registration differences of the bone models of both trials. A colour scale displays inter-bone distances from 0 to 1.0 mm (0 mm, blue; 1 mm, red) _____	129

List of Abbreviations

A – Anterior

ABD – Abduction

AC – Acromioclavicular

ADD – Adduction

CT – Computed Tomography

ER – External Rotation

EXT – Extension

FLEX – Flexion

I – Inferior

IR – Internal Rotation

ISB – International Society of Biomechanics

JSA – Joint Surface Area

L – Lateral

M – Medial

MRI – Magnetic Resonance Imaging

OA – Osteoarthritis

P – Posterior

ROM – Range of Motion

RSA – Reverse Shoulder Arthroplasty

S – Superior

SC – Sternoclavicular

SCAP – Scaption

ST – Scapulothoracic

TSA – Total Shoulder Arthroplasty

2D – Two-Dimensional

3D – Three-Dimensional

3DCT – Three-Dimensional Computed Tomography

4DCT – Four-Dimensional Computed Tomography

6DoF – Six Degrees of Freedom

Chapter 1: Introduction

This chapter provides an introduction to the shoulder's complex anatomy and biomechanics. A review of shoulder anatomy, including osteology, ligamentous and musculotendinous stabilizers is provided. The current understanding and challenges of shoulder biomechanics is presented, with an overview of the different assessment methods used in the literature. Particular attention is drawn to the importance of quantifying normal arthrokinematics of the shoulder and the current limitations with available imaging techniques. Lastly, a rationale, objectives and hypothesis of this thesis are provided.

1.1 The shoulder

The shoulder is the most mobile joint in the human body with a wide range of motion (Lefèvre-Colau et al., 2018; Patel et al., 2018). It is a complex joint that is responsible for articulation of the upper extremities with the skeleton, and it plays an important role in the function of the arms and hands, which sets humans apart from other mammals (Bakhsh and Nicandri, 2018; Patel et al., 2018). The shoulder is stabilized and strengthened by the ligaments and muscles and consists of three bones, the scapula, clavicle and humerus. Its wide range of motion requires the integrated contribution of its four joints; the acromioclavicular, sternoclavicular, scapulothoracic and glenohumeral joints (Chang et al., 2020; Marieb and Hoehn, 2018) (Figure 1.1). The acromioclavicular joint is formed by the connection of the distal end of the clavicle with the acromion process of the scapula. Additionally, the interface of the proximal end of the clavicle with the sternum forms the sternoclavicular joint. The scapulothoracic joint describes the anterior surface of the scapula as it glides over the thorax. Lastly, the articulation of the humeral head with

the glenoid cavity of the scapula forms the glenohumeral joint (Krishnan et al., 2019). Although these joints are capable of individual motions, their movements are not entirely independent. This means that the motion of shoulder joints is often constrained and coupled, a phenomenon known as shoulder rhythm (Högfors et al., 1987; Inman et al., 1996; Karlsson and Peterson, 1992; Xu et al., 2014). The shoulder allows for the following motions: rotation, abduction, adduction, circumduction, flexion, and extension (Tortora and Nielsen, 2016).

1.2 Anatomy

1.2.1 Bones

1.2.1.1 Clavicle

The clavicle, or collarbone, an s-shaped slender bone lies horizontally across the anterior part of the thorax superior to the first rib. It forms the anterior strut of the shoulder girdle that connects the upper extremities to the axial skeleton. The lateral half of the clavicle is concave anteriorly, and the medial half is convex anteriorly. The weakest point of the clavicle is its two junctions. The clavicle is curved and rougher in males, and straight and smoother in females (Tortora and Nielsen, 2016).

The lateral end of the clavicle, the acromial end, is broad, flat, and articulates with the acromion of the scapula to form the acromioclavicular joint. The rounded medial end, the sternal end, articulates with the sternum at the sternoclavicular joint (Figure 1.2). On the inferior surface of the lateral end, the conoid tubercle is the point of attachment of the conoid ligament. On the inferior surface of the medial end, the impression for the costoclavicular ligament is the point of

attachment of the costoclavicular ligament, which is the ligament that connects the clavicle to the first rib (Tortora and Nielsen, 2016) (Figure 1.3).

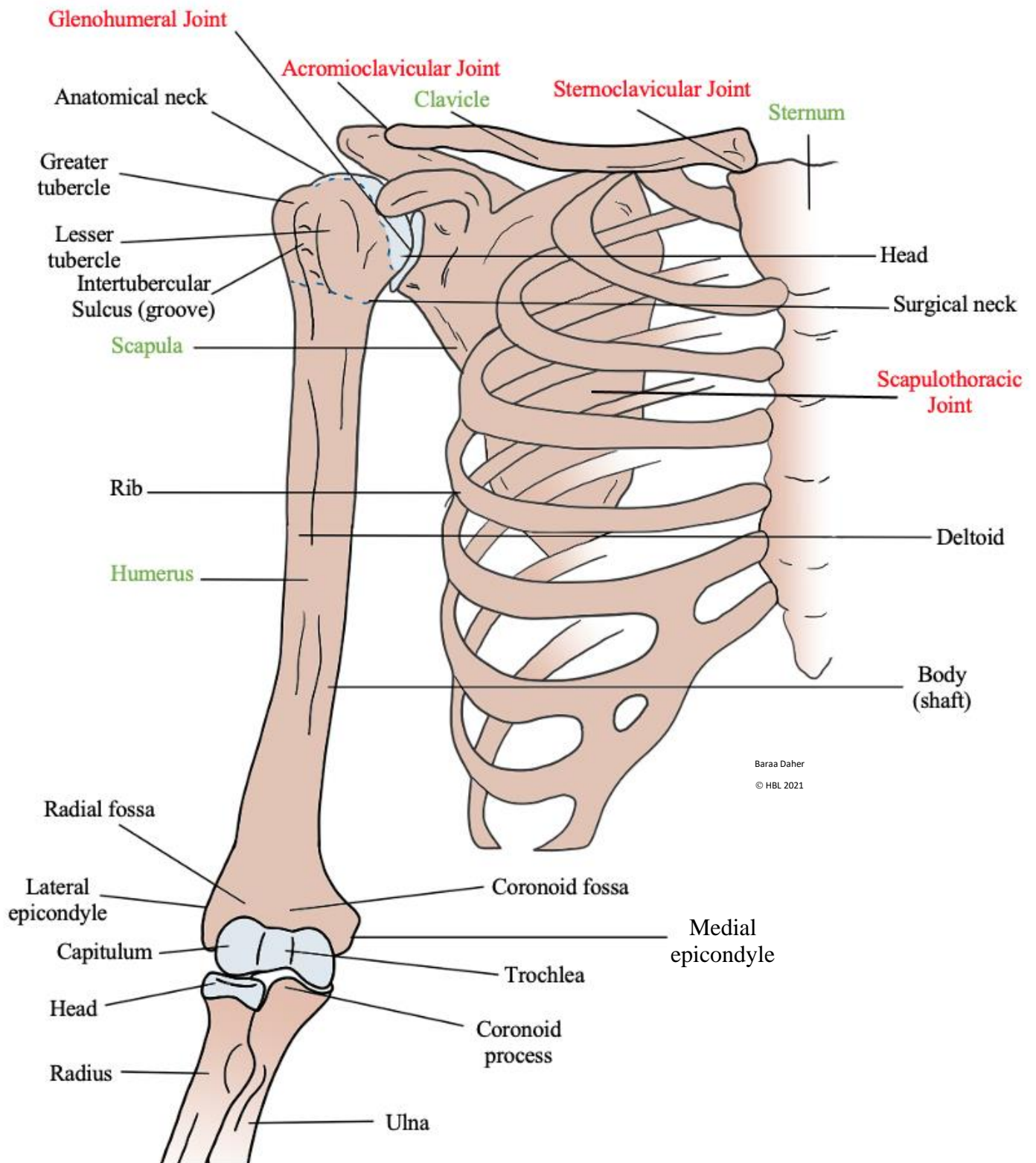


Figure 1.1: Anterior view of the right shoulder

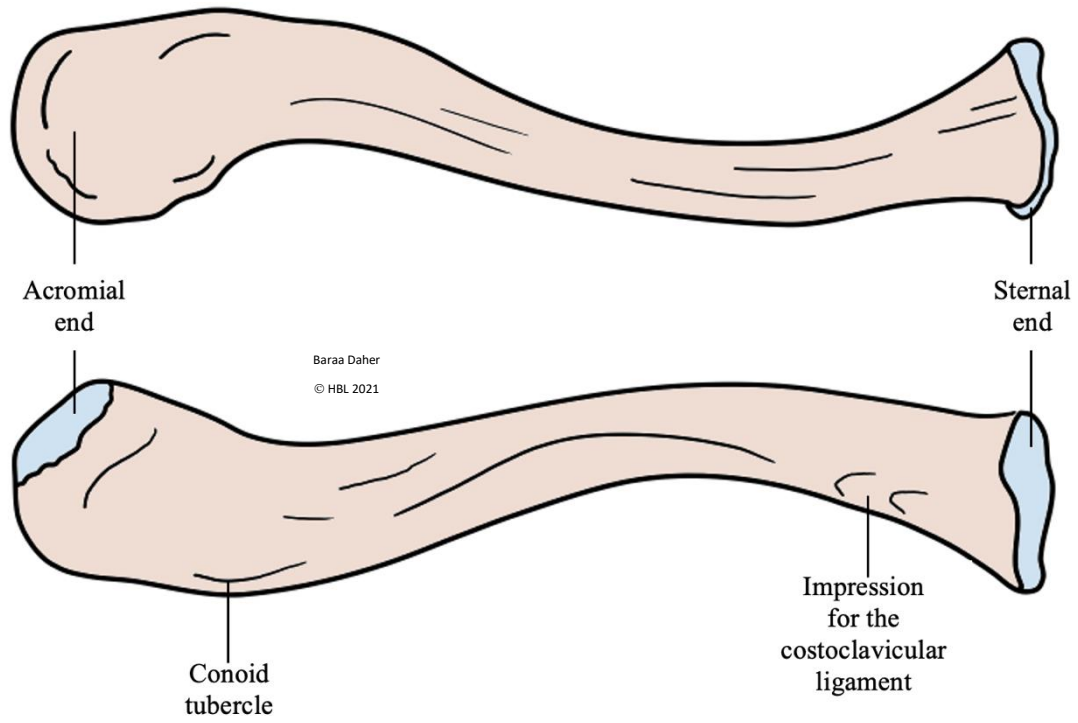


Figure 1.2: Superior (top) and inferior (bottom) view of the right clavicle.

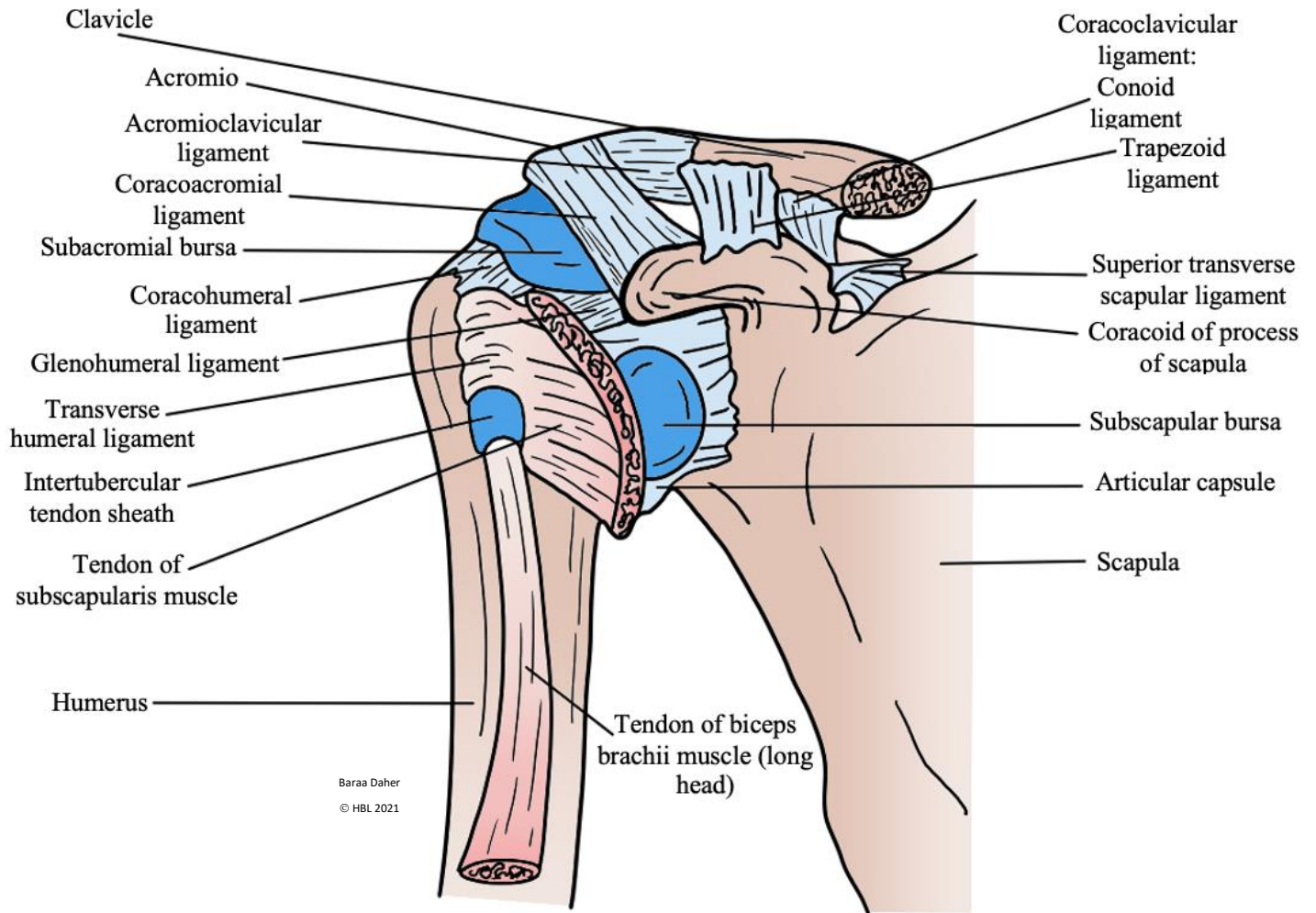


Figure 1.3: Anterior view of the right shoulder

1.2.1.2 Scapula

The scapula, or shoulder blade, is a large, flat, triangular bone with a long, narrow posterior surface. It is located on the superior end of the posterior thorax between the second and seventh ribs lateral to the vertebral (spinal) column. On the posterior surface of the scapula, a prominent ridge runs diagonally across the scapula called the spine. The acromion is a flattened projection of the lateral end of the spine of the scapula and the peak of the shoulder that is easily felt. The acromion articulates with the acromion end of the clavicle at the acromioclavicular joint. The glenoid cavity of the scapula is a shallow depression, inferior to the acromion, that articulates with the proximal head of the humerus forming the glenohumeral (shoulder) joint.

The medial, vertebral border is the thin edge of the scapula closer to the vertebral column. The lateral, axillary border, is the thick edge of the scapula closer to the arm. The inferior edge of the scapula is where the medial and lateral borders join. The superior border joins the vertebral border at the superior angle. Along the superior border, the suprascapular nerve passes through a prominent indentation called the scapular notch.

The tendons attach to a projection of the anterior surface at the lateral end of the superior border. This projection is called the coracoid process. Superior and inferior to the spine are the supraspinous and infraspinous fossae. The supraspinatus fossa serves as an attachment surface for the supraspinatus muscle of the shoulder, and the infraspinatus fossa serves as an attachment surface for the infraspinatus muscle of the shoulder. The hollowed-out area on the anterior surface called the subscapular fossa, serves as a surface of attachment for the subscapularis muscles (Tortora and Nielsen, 2016) (Figure 1.4).

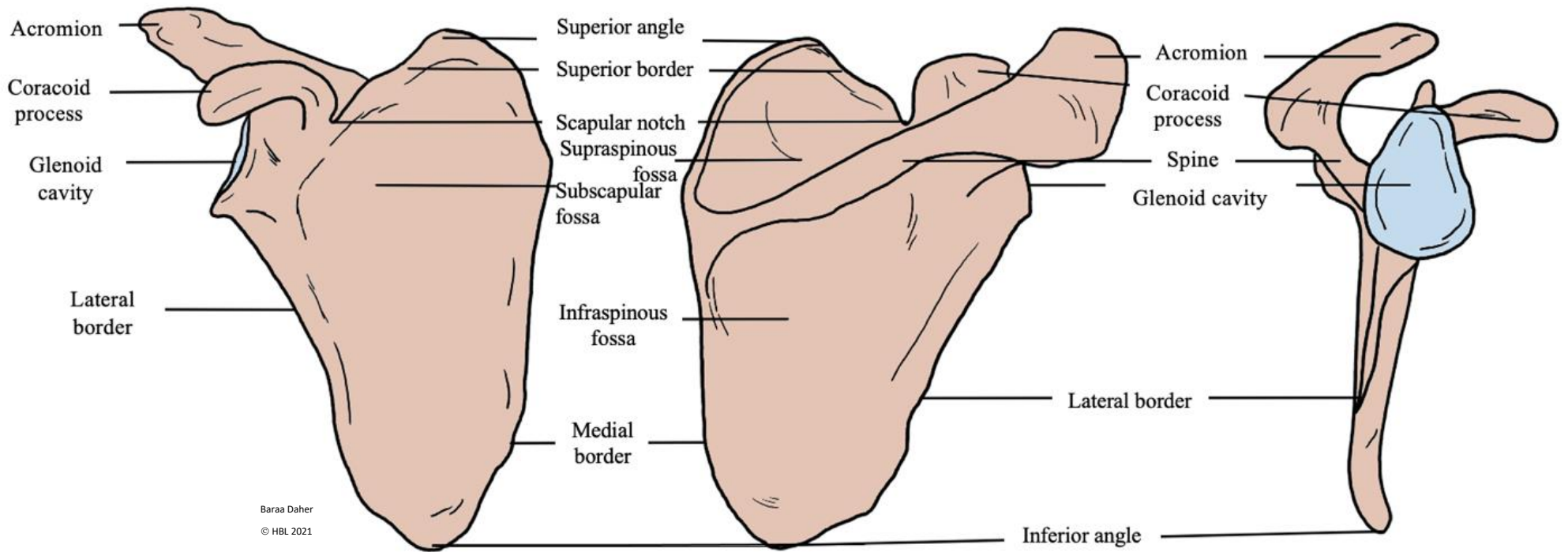


Figure 1.4: Anterior (right panel), posterior (central panel) and lateral view (left panel) of the right scapula

1.2.1.3 Humerus

The humerus, or arm bone, is the largest and longest bone of the upper extremities. It consists of a proximal end (ball-shaped), tubular shaft and a flattened distal end. Proximally, the humerus articulates with the scapula to form the glenohumeral (shoulder) joint, and distally, it articulates with both the radius and ulna to form the elbow joint. Distal to the head of the humerus is the anatomical neck, which is the site of the epiphyseal plate in the humerus. Distal to the anatomical neck is the greater tubercle, which is the most lateral palpable bony landmark of the shoulder. In addition, it is inferior to the palpable acromion of the scapula. The lesser tubercle is located anteriorly with respect to the anatomical neck. The intertubercular sulcus is an indentation running between both tubercles. Distal to the tubercles is the surgical neck where the proximal end meets the long shaft. The surgical neck is a common fracture site of the humerus (Tortora and Nielsen, 2016).

The proximal half of the shaft of the humerus is cylindrical, whereas the distal half is triangular, wide, and flat. At the middle of the shaft, on the lateral side, there is a rough, V-shaped area referred to as the deltoid tuberosity. The deltoid tuberosity serves as an attachment surface for the tendons of the deltoid muscle. The radial groove runs on the posterior side of the deltoid tuberosity and ends on its inferior side. The radial groove contains the radial nerve (Tortora and Nielsen, 2016).

On the distal end of the humerus, laterally, the capitulum articulates with the head of the radius. The anterior depression above the capitulum is called the radial fossa, and it accommodates the radial head during forearm flexion. Medial to the capitulum, a spool-shaped surface, referred to as the trochlea, articulates with the ulna. The anterior depression above the trochlea is called the coronoid fossa, and when the forearm is flexed, it receives the coronoid process of the ulna. The

large posterior depression of the distal part of the humerus is called the olecranon fossa, and when the forearm is extended, it receives the olecranon of the ulna. On the distal end of the humerus, the medial and lateral epicondyle projections are located. These surfaces serve as attachment points of most of the tendons of the forearm muscles. The ulnar nerve, the nerve responsible the sensation of pain when the elbow is hit, can be palpated on the posterior surface of the medial epicondyle (Tortora and Nielsen, 2016) (Figure 1.1).

1.2.2 Ligaments and Joint Capsule

The joint capsule and ligaments accounts for the soft tissues responsible for providing stability for the shoulder structure. The joint capsule of a synovial joint is a thin layer that surrounds the articulating surfaces of the joint and excretes lubricating synovial fluid and nutrients. In the shoulder joint, the articular capsule, or joint capsule of the glenohumeral joint is a thin, loose sac that encloses the structures of the joint, including the anatomical neck of the humerus and the glenoid cavity of the scapula. The weakest point of the articular capsule is the inferior side of the capsule (Tortora and Nielsen, 2016).

The ligaments that connect the shoulder bones and stabilizes the joints are: the acromioclavicular ligament, coracoacromial ligament, coracohumeral ligament, glenohumeral ligaments, transverse humeral ligament, coracoclavicular ligaments and superior transverse scapular ligament (Tortora and Nielsen, 2016) (Figure 1.3).

1.2.3 Muscles

The muscles of the shoulder contribute to the motion of the complex and provide stability to the overall structure. They are commonly grouped based on their insertion sites and origin, including the scapulohumeral, scapulothoracic, humerothoracic and multi-joint muscles (Figure 1.5, 1.6, 1.7)

1.2.3.1 Scapulohumeral Muscles

The scapulohumeral muscles originate on the scapula and insert on the humerus, thus playing the largest role in the stability and motion of the glenohumeral joint. The scapulohumeral muscles are composed of the deltoid, supraspinatus, subscapularis, infraspinatus, teres minor and major and coracobrachialis.

The deltoid muscle has been found to account for approximately 50% of the total required moment during glenohumeral abduction (Hess, 2000). This muscle can be divided into three sub-regions (anterior, middle, and posterior) based on their different functions. For example, the anterior and posterior deltoid muscles contribute to flexion/extension and internal/external rotation, respectively, in addition to their role in abduction (Ackland and Pandy, 2011).

The rotator cuff muscles of the shoulder provide stability to the joint throughout the motion (Culham and Peat, 1993) and are activated during both abduction and rotation moments (Neer, 1990). The cuff refers to four muscle bellies; the supraspinatus, subscapularis, infraspinatus, and teres minor muscles, and their associated tendon, joint capsule and the glenohumeral ligaments. This complex structure of muscles surrounds the glenohumeral joint from three directions, anteriorly, posteriorly, and superiorly.

The supraspinous fossa, the space between the spine and superior edge, serves as the origin of the supraspinatus muscle, which inserts on the humeral greater tuberosity. This muscle contributes to elevation motions (Howell et al., 1988; Kedgley et al., 2008; Wuelker et al., 1994a, 1994b), especially during the initiation of abduction (Ackland et al., 2008; Kedgley et al., 2007).

The infraspinatus fossa, the inferior space to the scapular spine, serves as the origin of the infraspinatus muscle, which inserts on the posterior side of the greater tuberosity. It is divided onto superior and inferior sub-regions (Ackland et al., 2008). The infraspinatus muscle contributes to stabilization rather than motion production (Ackland et al., 2008).

The subscapularis originates on the subscapular fossa, which is the entire anterior surface of the scapula, and inserts on the humeral head at the lesser tuberosity. Similar to the infraspinatus, the subscapularis is composed of a superior and inferior sub-regions that can be loaded separately (Ackland et al., 2008). The main function of the superior part is to provide joint stability and apply forward flexion moments, yet the inferior part only contributes to stabilization (Ackland and Pandy, 2011; Escamilla et al., 2009; Jenp et al., 1996). The later border of the scapula serves as the origin of the teres major and minor, with the minor located superior to the major. The teres major inserts on the anterior side of the humeral shaft, while the teres minor blends with the infraspinatus muscle and inserts on the humeral head at the greater tuberosity. Both muscles primarily contribute to humeral adduction and stability of the shoulder complex (Neer, 1990), with the teres major accounting for internal rotation and the teres minor accounting for external rotation (Ackland and Pandy, 2011). The tip of the coracoid process serves as the origin of the coracobrachialis muscle and inserts on the anteromedial side of the humeral shaft. This muscle is activated during flexion and resisted adduction (Ackland et al., 2008; Jonsson et al., 1972).

1.2.3.2 Humerothoracic Muscles

The humerothoracic muscles originate on the thoracic cage and insert on the humerus. These muscles are the latissimus dorsi and the pectoralis major. The latissimus dorsi muscle originates on the lower thoracic and upper vertebrae, pelvis's iliac crest, inferior three rib and scapula's inferior angle. This muscle inserts on the bicipital groove of the humerus and contributes to adduction, extension and internal rotation of the humerus (Ackland et al., 2008; Ackland and Pandy, 2011). The pectoralis major muscle originates on the anterior surface of the medial side of the clavicle and sternum. This muscle inserts on the lateral lip of the bicipital groove of the humerus and contributes to adduction, flexion and internal rotation of the humerus (Ackland et al., 2008; Ackland and Pandy, 2011).

1.2.3.3 Scapulothoracic Muscles

The scapulothoracic muscles originate on the thoracic cage and insert on the scapula. These muscles are the rhomboids, levator scapulae, serratus anterior, pectoralis minor and trapezius. The rhomboid and levator scapulae muscles insert on the posterior side of the scapula along the medial scapular border. Conversely, the serratus anterior muscle inserts on entire length of the anterior surface of the scapula's medial boarder. The pectoralis minor muscle inserts on the anterior surface of the coracoid process, and the trapezius muscle inserts on the superior edge of the scapular spine. Each of the scapulothoracic muscle is responsible for a different motion of the scapula relative to the trunk, including tilting and elevation of the scapula.

1.2.3.4 Biarticular Muscles

The biarticular muscles of the shoulder crosses more than one joint from origin to the point of insertion. These muscles include the triceps brachii and short and long heads of the biceps brachii. Primarily, these muscles play a role in elbow motion, but their paths across the GH joint affects the function and kinematics of the shoulder. The triceps muscles originate on the lateral border of the scapula inferior to the glenoid cavity, while crossing the elbow and GH joints. This muscle inserts on the ulna with limited contribution to the shoulder motion, yet provides resistance to inferior shear forces during adduction activities (“Rockwood and Matsen’s The Shoulder, 2 Volume Set - 4th Edition,” n.d.). The biceps short head muscle originates from the tip of the coracoid process and the long head originates from supraglenoid tubercle. Both heads meet at the deltoid tuberosity and cross the elbow to insert on the radius. Some studies have proposed that the role of the short head is to provide resistance to anterior translation of the humeral head (“Rockwood and Matsen’s The Shoulder, 2 Volume Set - 4th Edition,” n.d.).

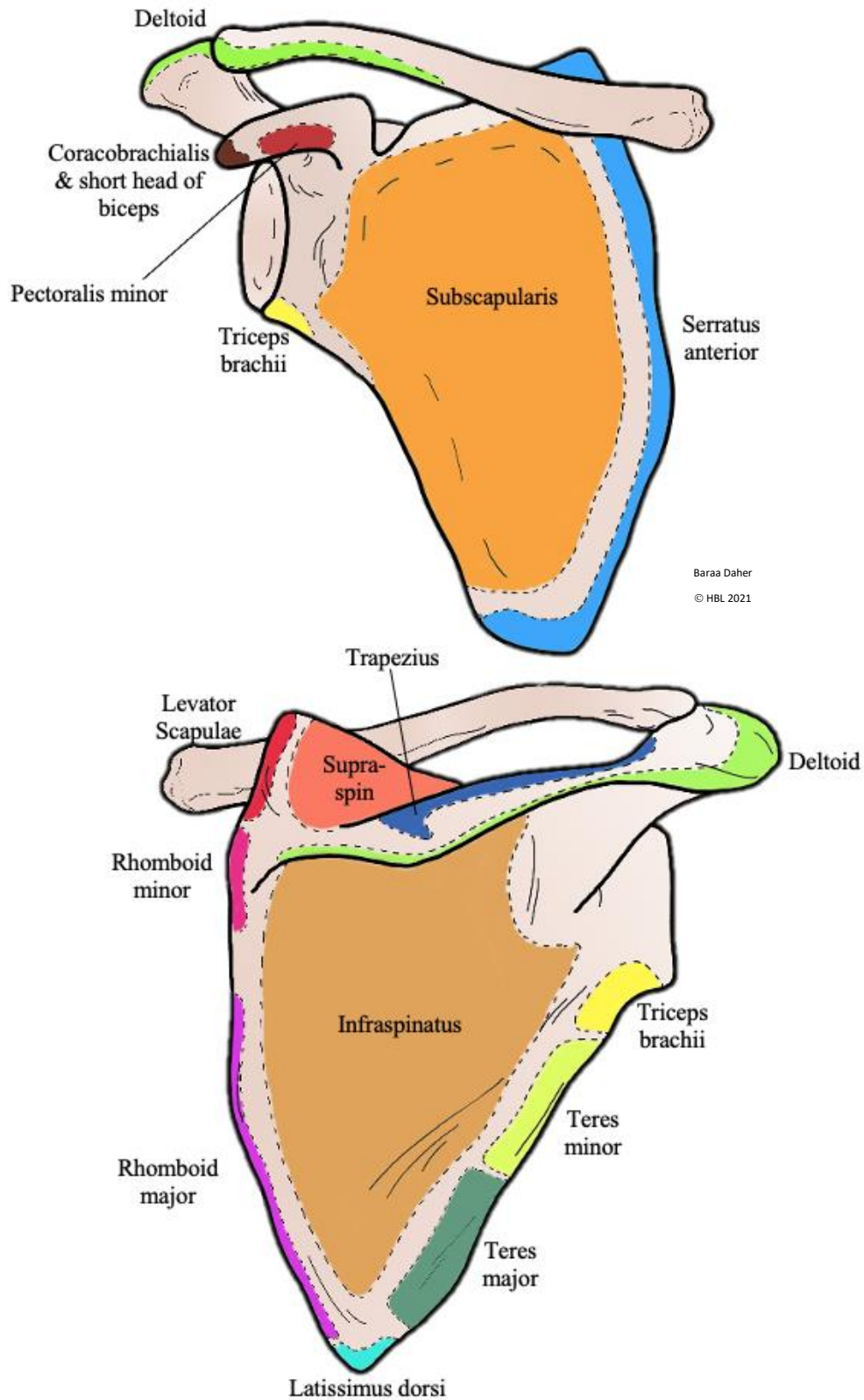


Figure 1.5: The muscular origins and insertions on the scapula. Anterior (top) and posterior (bottom) view of a right scapula

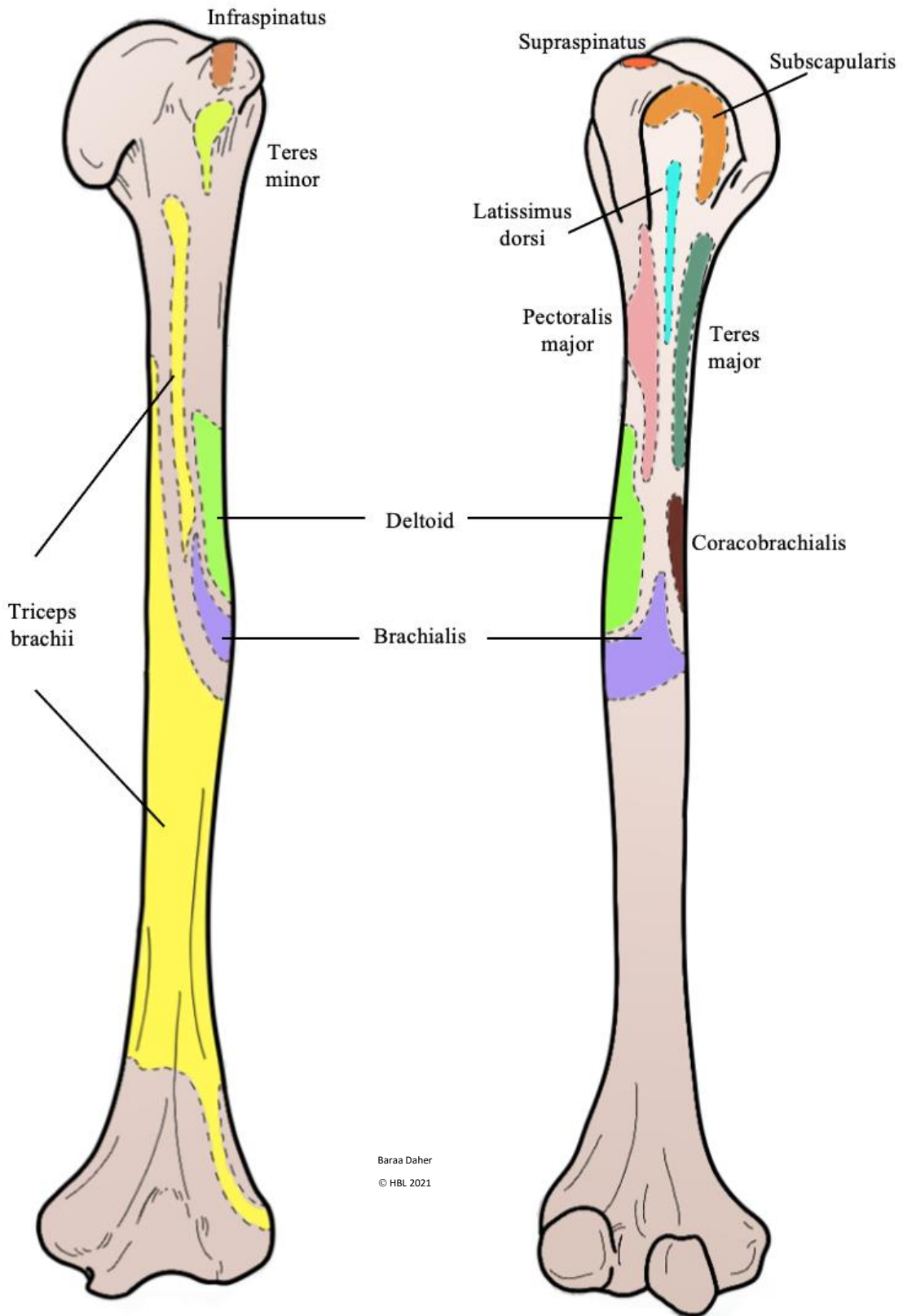


Figure 1.6: The muscular origins and insertions on the humerus. Posterior (left) and anterior (right) view of a right humerus.

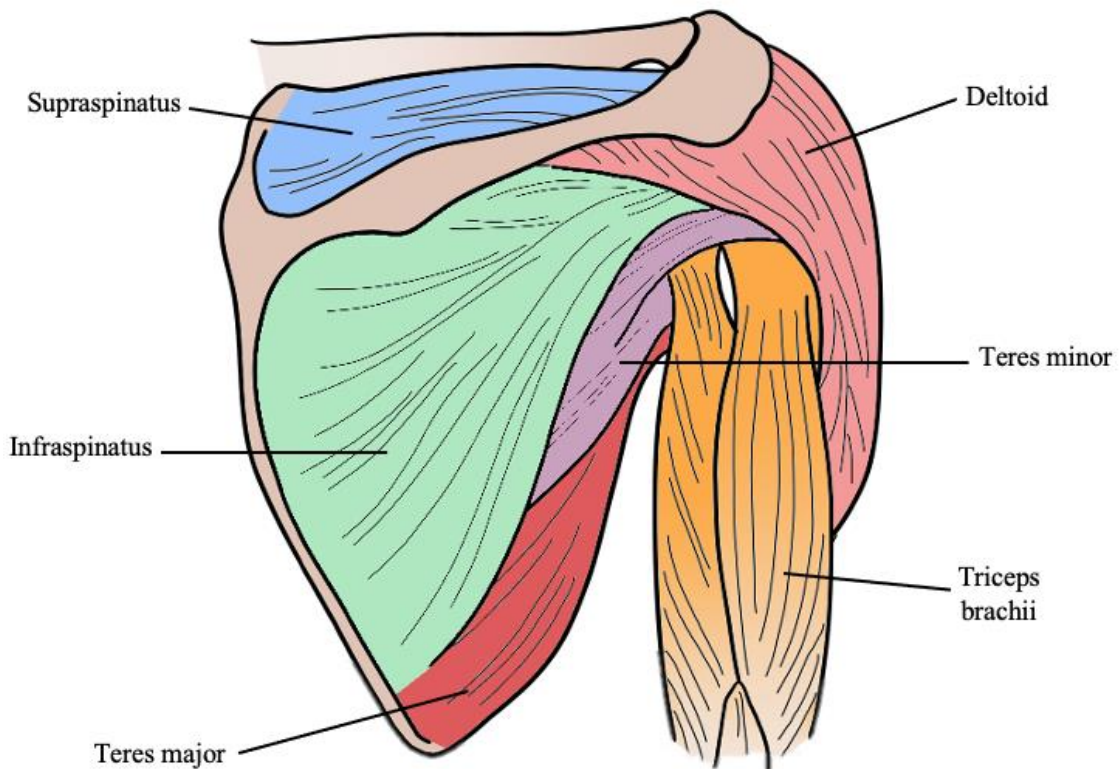
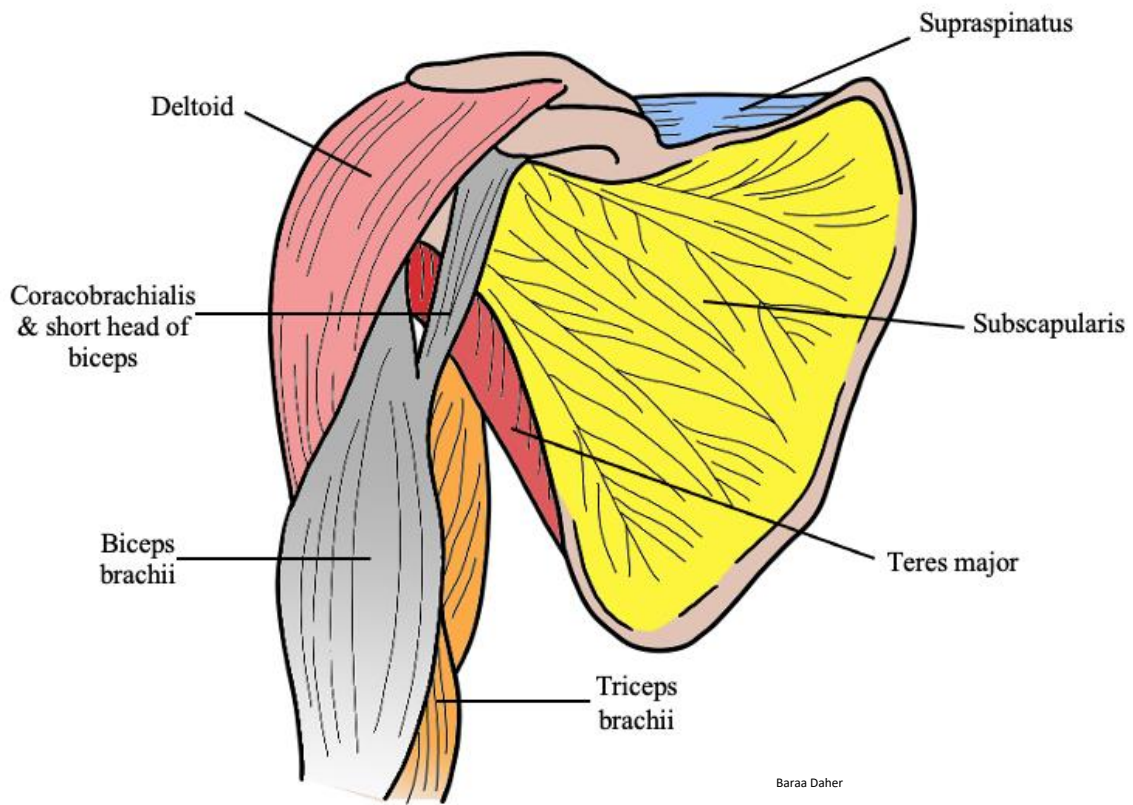


Figure 1.7: The muscles of the shoulder complex. Anterior (top) and posterior (bottom) views of a right shoulder

1.3 Joints

The joints forming the shoulder complex have two main functions; to provide stability to prevent injury and/or dysfunction and to achieve maximal range of motion (ROM) (“Rockwood and Matsen’s The Shoulder, 2 Volume Set - 4th Edition,” n.d.). The glenohumeral (GH) joint has the largest ROM, thus accounting for the majority of the motion produced by the shoulder complex (An et al., 1991; Halder et al., 2001b, 2001c, 2001a; Howell et al., 1988; Karduna et al., 1996; Ludewig et al., 2009). The shoulder allows for rotation, abduction, adduction, circumduction, flexion, and extension (Tortora and Nielsen, 2016). The articulating surfaces of this joint include the concave surface of the glenoid fossa and the convex surface of the humeral head. The surface area of the humeral head is roughly four times larger than the surface area of the glenoid (Chang et al., 2020). Hence, only a small, constantly changing portion of the humeral head is in contact with the glenoid throughout the motion, while the glenoid contact is relatively constant throughout the motion (Bey et al., 2010; Kelkar et al., 2001; Soslowsky et al., 1992; Warner et al., 1998).

The sternoclavicular (SC) and acromioclavicular (AC) joints describe the articulation between the medial and lateral sides of the clavicle with the sternum and acromion, respectively. These joints are defined as plane synovial joints based on their anatomy, yet the sternoclavicular joint functions as a ball-and-socket joint and has three degrees of freedom. The SC joint can undergo elevation/depression, protraction/retraction and rotation about the longitudinal axis (Abbott and Lucas, 1954). On the other hand, the acromioclavicular joint allows for minimal translation motion during excessive load application. Both joints contribute to the stability and motion of the scapula (Culham and Peat, 1993).

The scapulothoracic (ST) joint describes the anterior surface of the scapula as it glides over the thorax, separated by the subscapularis muscle belly. The articulation of this joint contributes to the range of motion of the shoulder complex by delaying the impingement of the greater tuberosity during abduction and increasing range of protraction during horizontal adduction (Culham and Peat, 1993). These motions contribute to the joint stability by directing the joint load within the articular surface of the glenoid, hence preventing potential damage to the soft tissue stabilizers of the shoulder (S and F, 1993).

1.4 The glenohumeral joint

1.4.1 Anatomy

The glenohumeral (shoulder) joint is a ball-and-socket, synovial joint formed by the articulation of the humerus head with the glenoid cavity of the scapula. This joint is also referred to as the humeroscapular joint. The articular capsule, or joint capsule, of the glenohumeral joint is a thin, loose sac that encloses the structures of the joint, including the anatomical neck of the humerus and the glenoid cavity of the scapula.

The glenohumeral joint consists of three main ligaments, including the coracohumeral ligament, glenohumeral ligaments and transverse humeral ligament. The coracohumeral ligament is a strong, broad band that strengthens the upper (superior) part of the joint capsule and covers the greater tubercle of the humerus and the coracoid process of the scapula. It splits into two bands, anterior and posterior, which insert into the lesser and greater tubercles of the humerus, respectively (Arai et al., 2014). This ligament does not only strengthen the superior part of the capsule, but also reinforces the anterior aspect of the joint capsule. The glenohumeral ligaments are three ligaments (superior, middle, and inferior ligament) that combine to cover the anterior

surface of the glenohumeral joint. These ligaments extend from the glenoid cavity to the anatomical neck and lesser tubercle. Although they provide minimal strength to the joint, the glenohumeral ligaments stabilize the joint when the humerus approaches or surpasses its range of motion limits. In another word, they prevent the shoulder from dislocating anteriorly. Lastly, the transverse humeral ligament is a thin band spreading from the lesser tubercle to the greater tubercle of the humerus. The ligament's role is to retain and grip into the head of the biceps brachii muscle in the intertubercular groove (Tortora and Nielsen, 2016).

The labrum of the glenohumeral joint is a thin layer of fibrocartilage surrounding the outer layer of the glenoid cavity. It enlarges and deepens the glenoid cavity of the scapula. The glenohumeral joint consists of four bursae, including the subscapular bursa, subdeltoid bursa, and subcoracoid bursa, and subcromial bursa. Bursae are sacs filled with lubrication fluid found between the bones and tendons of synovial joints (Tortora and Nielsen, 2016) (Figure 1.4).

1.4.2 Glenohumeral Biomechanics

The glenohumeral joint is the most mobile joint in the human body with a wide range of motion (ROM) in multiple planes (Bakhsh and Nicandri, 2018; Lefèvre-Colau et al., 2018; Patel et al., 2018). These motions include, flexion/extension, adduction/abduction, and internal/external rotation (Bakhsh and Nicandri, 2018; Chang et al., 2020). The shoulder movements in the sagittal plane are flexion and extension. Flexion defines the movement of the upper limb (humerus) anteriorly and its normal ROM ranges from 150° to 180°. Extension is the movement of the upper limb posteriorly and its normal ROM ranges from 40° to 60°. In the coronal plane, movement towards the midline is called adduction, and movement away from the midline is known as abduction. The normal ROM of abduction ranges from 150° to 180°. The motions in the transverse

plane are internal and external rotations, in another word, the internal and external axial rotations of the humerus. The normal ROM of internal and external rotations ranges from 50° to 90° and 60° to 90°, respectively (Bakhsh and Nicandri, 2018; Chang et al., 2020; Dutton, 2008; Norkin et al., 2009). In addition, the humerus moves about the vertical axis, which results in unique shoulder articulations including horizontal adduction, horizontal abduction, and cross-abduction. Moreover, the shoulder's wide range of motion allows for movements that are not limited to cardinal planes, such as circumduction and elevation and depression of the humerus (Krishnan et al., 2019). These complex movements require the motion of all shoulder bones, allowing for the wide range of motion. This constrained and coupled motion of the shoulder bones is known as the shoulder rhythm (Högfors et al., 1987; Karlsson and Peterson, 1992; Xu et al., 2014), and is dependent on numerous factors, such as joint anatomy, plane and arc of elevation and loading conditions (Gopura et al., 2016; Lo and Xie, 2012). The complexity of the shoulder movement poses a challenge when analyzing the kinematics of the shoulder in addition to challenges related to anatomic complexity, inconsistent clinical descriptions, measurement limitations and movement variability (Krishnan et al., 2019). Movement variability is a significant barrier in standardizing upper limb kinematics (Murphy and Häger, 2015), as it originates from both inter- and intra-subject variability (Viceconti, 2011), and since the upper arm movements are discrete, it is challenging to compare inter- and intra-subject kinematics (Rau et al., 2000). Unlike the gait cycle in the lower extremity, movements in the upper extremity are variable and are not often cyclic or characterized into discrete phases. To overcome some of these challenges, some studies examine only planar motion to simplify their analysis, but this kinematic simplification may not adequately capture full functional movements (Favre et al., 2009; Rau et al., 2000).

1.4.4 Osteoarthritis

The glenohumeral joint often becomes a source of musculoskeletal pathology, such as osteoarthritis. Osteoarthritis (OA) is a chronic, degenerative disorder of multifactorial etiology (Patel et al., 2018). It presents clinical symptoms and structural and radiological changes of the joint. These include the loss of articular cartilage, inflammation, subchondral bone remodeling and increased mechanical stress (Bijlsma et al., 2011; Patel et al., 2018; Woolf and Pfleger, 2003). Osteoarthritis of the glenohumeral joint significantly affects activities of daily living performance and quality of life, thus resulting in upper limb disability. The GH joint is characterized by a small joint surface contact area between the glenoid and the head of the humerus. Joint's muscles and ligaments ensure its stability and congruency, making it the most mobile and unstable joint of the human body. Normally, the articulation of the humeral head with the glenoid cavity is almost frictionless with the well-lubricated, smooth cartilage between the bones (Kaback et al., 2012; Soslowsky et al., 1992). The degeneration of the joint cartilage caused by osteoarthritis results in an abnormal distribution of the loads of the GH joint followed by adaptive changes in the subchondral bone. The humeral head and glenoid cavity wear down resulting in osseous articulation deformity and limited range of motion (Walch et al., 1999). Typically, cartilage damage starts at the center of the humeral head and the posterior side of the glenoid, along the growth of osteophytes around the anatomical neck of the humerus. These bony changes often result in the loss of the central position of the humeral head with respect to the glenoid, followed by posterior subluxation. In addition, the formation of osteophytes around the bones can limit rotations of the shoulder and increase bone volume (Parsons et al., 2004). Patients with OA experience pain and reduced range of motion, followed by difficulties in performing of activities

of daily living. Osteoarthritis can be treated with surgery, including anatomic total shoulder arthroplasty and reverse shoulder arthroplasty.

1.4.4.1 Surgical Treatment

1.4.4.1.1 Anatomic Total Shoulder Arthroplasty

Anatomic total shoulder arthroplasty (TSA) maintains normal anatomy of the shoulder joint (ball and socket). The humeral head is replaced with a rounded, smooth metal head with a stem inserted into the humerus, and the glenoid is replaced with a cemented polyethylene component (Sanchez-Sotelo, 2011). Previous studies have demonstrated the benefits of TSA, such as restoring active forward flexion, external rotation at the side, and internal rotation to the back. This surgery requires the rotator cuff to be intact and the glenoid to have adequate bone stock for the implant to be inserted and constrained (Latif et al., 2012; Mattei et al., 2015). Undergoing TSA with a damaged rotator cuff results in abnormal shoulder kinematics, leading to loosening of the implant (Latif et al., 2012; Mattei et al., 2015). Mild deformities of the glenoid may be corrected by leveling the surface of the glenoid and restoring its version (i.e., eccentric reaming). However, in cases of severe deformities, for example, posterior erosion of the glenoid surface, the use of total shoulder arthroplasty has a higher rate of failure as a result of glenoid implant loosening and posterior instability. In such cases that have severe erosion, reverse shoulder arthroplasty is indicated as an alternative to an unconstrained total shoulder arthroplasty (Latif et al., 2012; Mattei et al., 2015).

1.4.4.1.2 Reverse Shoulder Arthroplasty

Reverse shoulder arthroplasty (RSA) is a widely spread surgery used to treat numerous shoulder pathologies, including osteoarthritis, to relief pain and restore function (Boulahia et al., 2002; Frankle et al., 2006; Jauregui et al., 2018). Different than anatomic total shoulder arthroplasty, RSA reverses the normal anatomy of the shoulder (ball and socket) by replacing the glenoid fossa with a ball component, and the humeral head with an articular socket (Lee et al., 2020). Similar to anatomic shoulder arthroplasty, previous clinical and biomechanical studies have demonstrated the benefits of RSA, such as restoring active forward flexion of the shoulder (Berliner et al., 2015; Gerber et al., 2009; Kwon et al., 2012). However, RSA cannot restore the full range of motion of other motions. Studies have shown no significant improvement in internal and external rotation motions in patients who underwent RSA (Maier et al., 2014; Wall et al., 2007; Young et al., 2009). A recent study noted no significant improvements in external rotation at the side, external rotation at 90° of abduction, and internal rotation to the back (Kim et al., 2020). The internal rotation to the back motion is important in activities of daily living, such as washing the back and opposite shoulder, using a back pocket, managing toileting and clasping a brassiere (Kim et al., 2020). The limited motion is thought to be the consequence of inverting the anatomic concavities of the glenoid and humerus that creates a fixed structure in which is limited to only rotate/spin (Roche and Crosby, 2018). Quantifying normal arthrokinematics can explain the importance of translation to achieve maximum range of motion and underline the changes of contact area caused by OA.

1.5 Methods to Quantify Articular Contact

Quantifying normal contact mechanics of human joints can help clinicians and researchers in the development of diagnostic tools, pre- and post-operative treatment plans, and enhance implant designs.

1.5.1 Direct Approaches

Initial techniques for examining and quantifying contact area of articulating joints consisted of direct, invasive techniques, which are limited to static positions of inferring motions. These approaches include pressure-sensitive films, dye staining and silicone casting. Pressure-sensitive films technique involves the insertion of a film directly into the surfaces of articulating joints to measure the pressures applied to the joint in loaded conditions. The pressure produces a stain, in which its intensity is then calibrated to the magnitude of pressure. The drawback of pressure-sensitive films, as is true with all direct approaches; they are invasive and only used on cadaveric specimens. The second direct technique to quantify contact area, dye staining, uses dye or stain to locate and quantify the contact area. This technique is associated with numerous artifacts, such as the introduction of air bubbles in the dye material and the dye's inability to reach all the articulating surfaces. The air bubbles results in the overestimation of the measured contact area, and the dye's inability to reach all the articulating surfaces result in the underestimation of the measured contact area. The last approach to quantify contact mechanics is silicone casting, which is the gold standard when studying and measuring contact area. In this approach, the joint is distracted and injected by a casting material, such as cement. Then, the joint is held until the cast has solidified after being reduced to the intact orientation. After removing the material from the joint, the areas lacking the dried cement are quantified as the joint contact areas. This technique

alters the magnitude and orientation of contact since it requires sectioning of the surrounding soft tissue and capsule. This results in inaccurate representation of the native joint contact area and mechanics. The discussed methods require direct access into the joint, sometimes sectioning of joint's capsule and soft tissue that support the joint. These techniques are invasive and compromise the stability of the joint, thus, altering the actual contact mechanics.

1.5.2 In-Direct Approaches

In-direct, non-invasive imaging techniques have been developed to quantify bones interaction and contact that occurs at the joint. These techniques include bi-plane fluoroscopy, computed tomography (CT) and magnetic resonance imaging (MRI) (Cohen et al., 1999; Marai et al., 2004). These medical modalities provide volumetric datasets that can be reconstructed into three-dimensional models to evaluate joint surfaces using different approaches. One approach to quantify contact mechanics uses two-dimensional images to identify the overlapping pixels of each slice, or tomography (Van Ginckel et al., 2011). The downside to this technique is that it uses two-dimensional (2D) slices, which can introduce errors when examining anatomically complex structures. Another approach is proximity mapping, which is a three-dimensional (3D) technique that measures joint contact area and congruency (Anderst and Tashman, 2003; Ateshian et al., 1994; Bey et al., 2008; Goto et al., 2004; Lösch et al., 1997; Marai et al., 2006, 2004; von Eisenhart-Rothe et al., 2004). This approach uses the volumetric datasets acquired from the scans to reconstruct 3D models of the articulating joints and create proximity maps using a software algorithm (Lalone et al., 2013). The algorithm defines the contact area by measuring Joint Surface Area (JSA), which assumes that regions of higher contact pressure (or smaller inter-bone distance) resemble those of closest/high proximity (Marai et al., 2004). The algorithm measuring the inter-

bone distance was originally developed for in vitro cadaveric testing, and has been validated against a gold standard (Gammon et al., 2018). Ever since, this algorithm has been used in numerous in vitro and in vivo studies examining the contact mechanics of the wrist, elbow and shoulder (Gammon et al., 2018; Lalone et al., 2021, 2013, 2011).

1.6 Imaging Modalities

Medical imaging plays an important role in the understanding of the normal function of the shoulder, the diagnostic of diseases and injuries, and the planning of pre- and post- operative treatment plans. Previous studies examining the kinematics and arthrokinematics of the shoulder have relied on different imaging modalities, including radiographs and computed tomography (CT).

1.6.1 Radiographs

Radiographs, or x-rays, are the first line of investigation to assess suspected fracture, fracture healing and alignment of joint. They have excellent bone contrast and are cost-effective. X-rays are generated by bombarding metal anodes with accelerated electrons, which are transmitted through a phosphor screen or a film combination. The intensity of this 2D projected image depends on the amount of attenuation that is occurring as x-rays are travelling through the body. X-rays experience exponential attenuation that is in proportion to the attenuation coefficient of the body its travelling through. As a result, the images produced provide key diagnostic information due to the different attenuation factors (40-120 keV) of bone, muscle, fat and other tissues of the body (Leahy and Clackdoyle, 2005). X-rays have excellent contrast for assessing bones of the body and are cost-effective compared to other imaging modalities. The inability of x-

rays to precisely perceive articular incongruity have resulted in literature discrepancy between produced images and clinical results.

1.6.2 Fluoroscopy

Certain medical procedures use fluoroscopy imaging as guide though the internal structure. Fluoroscopy imaging provides x-ray images in a series of a movie to allow for real-time assessment of kinematics. This modality involves the injection of a contrast agent, in which its movement is tracked through the body, resulting in a moving image of the functioning organs of the body. After the x-rays pass through the body, they are received by an intensifier, which converts the radiographs to moving images displayed on a monitor. Fluoroscopy imaging have been employed to examine kinematics of the human joints, since it overcomes the limitation of static studies (Baumer et al., 2016; Bey et al., 2008; Dal Maso et al., 2016; Matsuki et al., 2016; Matsumura et al., 2019; Mozingo et al., 2019). However, like many other modalities, fluoroscopy imaging is limited by its 2D nature, making it difficult to detect complex musculoskeletal movements and abnormalities (Baumer et al., 2016; Bey et al., 2008; Dal Maso et al., 2016; Matsuki et al., 2016; Matsumura et al., 2019; Mozingo et al., 2019).

1.6.3 Computed Tomography

Three-dimensional computed tomography (3DCT)), quasi-statically (sequence scans) or dynamically by employing CT with bi-plane fluoroscopy (Baumer et al., 2016; Bey et al., 2008; Dal Maso et al., 2016; Matsuki et al., 2016; Matsumura et al., 2019; Mozingo et al., 2019) can be used to measure shoulder joints kinematics as bony landmarks and structures can be readily seen.

The technique of using fluoroscopy with CT utilizes 3D models of bones obtained from computed tomography (CT) scans, which are then matched to aspects of the acquired radiographic images acquired from fluoroscopy (Baumer et al., 2016; Bey et al., 2008; Dal Maso et al., 2016; Matsuki et al., 2016; Matsumura et al., 2019; Mozingo et al., 2019). This technique can accurately monitor real-time dynamic joint forces and 3D complex motions in in-vivo environments. The procedure of matching the 3D models to the radiographic images requires the user to manually align the models to the fluoroscopic projections as close as possible, which makes the outcome strongly operator dependent. In addition, this process is time consuming and can result in inaccurate estimations. A further problem is that fluoroscopic images obtained with 3D fluoroscopy are geometrically distorted and unsuitable for quantitative analysis without an accurate correction process.

Overall, CT techniques can overcome many challenges associated with other motion measuring techniques by providing accurate, non-invasive, 3D measures of in-vivo shoulder joint anatomy that can be used to create anatomical coordinate systems and 6 degrees of free kinematic analysis. While these techniques have been useful in producing 3D images of bony anatomy, over time, there are still many challenges associated with the ability to accurately measure dynamic motions and limited field of view and out of plane error. Thus, better imaging modality with improved image processing is required.

1.6.4 Four-Dimensional Computed Tomography

Four-dimensional computed tomography (4DCT) is a dynamic CT imaging technique, which allows for evaluation of continuous shoulder motion as opposed to sequential static 3DCT. Four-dimensional computed tomography produces 3DCT volume sequences of a moving structure captured over time (time + CT), creating a dynamic volume data set (Kwong et al., 2015). This technique has promising clinical outcomes for the visualization and measurement of kinematic musculoskeletal pathophysiology. It has currently been used to assess the glenohumeral joint (Matsumura et al., 2019), scapulothoracic joint (Bell et al., 2015), acromioclavicular (Alta et al., 2012) and sternoclavicular joint (Hislop-Jambrich et al., 2016) of the shoulder. Shoulder research using 4DCT have been used as a motion measuring tool of the glenohumeral and acromioclavicular joint (Alta et al., 2012; Matsumura et al., 2019), as a preoperative planning tool in snapping scapula syndrome (Bell et al., 2015), and as a diagnostic tool of the sternoclavicular joint instability (Hislop-Jambrich et al., 2016). This new technology is recently emerging, yet only few studies have been done at the shoulder structure, none of which have looked at the contact mechanics over time.

1.7 Thesis Rationale

The shoulder is a complex joint with a wide, coupled, and constrained motion, making shoulder biomechanics challenging to assess, especially under in-vivo conditions. Medical imaging approaches can provide a non-invasive approach that can produce three-dimensional measures of in-vivo shoulder joint. These approaches have been widely used to measure normal and pathological shoulder biomechanics. New studies are emerging that employ four-dimensional computed tomography (4DCT) and replace traditional study designs that combine biplane fluoroscopy and computed tomography (CT). These studies would benefit from the valuable work that has been done in the past to inform this new generation of CT motion analysis.

Recent research studies using 4DCT have not evaluated normal contact patterns of the glenohumeral joint during active internal rotation to the back. This motion is significant in activities of daily living and its contact mechanics is yet to be measured. Characterizing normal glenohumeral arthrokinematics of the glenoid with the humerus in healthy adults can help clinicians and researchers in the development of pre- and post-operative treatment plans and enhance implant designs.

The purpose of this thesis is to advance the biomedical engineering field by assessing the use of CT in shoulder kinematics to propose a technique that employs 4DCT. The findings of this thesis will inform researchers of previously used techniques and their associated limitations and quantify glenohumeral arthrokinematics during internal rotation to the back.

1.8 Objectives and Hypothesis

1.8.1 Objectives

1. To examine the extent and range of methods employing CT imaging to measure shoulder kinematics in research studies using a systematic literature search and structured data extraction process.
2. To describe a technique which employs 4DCT to quantify in vivo glenohumeral contact patterns during dynamic shoulder motion and examine the reliability of the proposed technique.
3. To quantify normal glenohumeral joint congruency and arthrokinematics in the healthy adult during internal rotation to the back.

1.8.2 Hypothesis

1. The use of CT imaging in the literature to assess the kinematics of the shoulder presents inconsistencies and significant gaps of data reporting due to non-standardized protocols.
2. The techniques using 4DCT will be a useful tool to visualize and quantify in vivo dynamic glenohumeral joint arthrokinematics. The proposed technique to measure glenohumeral arthrokinematics will be reliable within 0.5 mm.
3. Similar trend of glenohumeral contact patterns will be noticed throughout internal rotation to the back, however, participants will undertake different pathways and different translation distance to reach maximum range of motion.

1.9 Thesis Overview

Chapter 2 examines the extent and range of methods using CT imaging to measure shoulder kinematics in research studies using a systematic literature search and structured data extraction process.

Chapter 3 describes the use of a previously developed inter-bone distance algorithm and 4DCT images to analyze the contact area of the glenohumeral joint to measure glenohumeral joint arthrokinematics. This chapter also tests the reliability of the approach used to quantify glenohumeral arthrokinematics.

Chapter 4 provides a general discussion and summary of the work in this thesis and indicates directions for future work.

1.10 References

- Abbott, L.C., Lucas, D.B., 1954. The function of the clavicle; its surgical significance. *Ann Surg* 140, 583–599. <https://doi.org/10.1097/00000658-195410000-00014>
- Ackland, D.C., Pak, P., Richardson, M., Pandy, M.G., 2008. Moment arms of the muscles crossing the anatomical shoulder. *J Anat* 213, 383–390. <https://doi.org/10.1111/j.1469-7580.2008.00965.x>
- Ackland, D.C., Pandy, M.G., 2011. Moment arms of the shoulder muscles during axial rotation. *J Orthop Res* 29, 658–667. <https://doi.org/10.1002/jor.21269>
- Alta, T.D., Bell, S.N., Troupis, J.M., Coghlan, J.A., Miller, D., 2012. The New 4-Dimensional Computed Tomographic Scanner Allows Dynamic Visualization and Measurement of Normal Acromioclavicular Joint Motion in an Unloaded and Loaded Condition. *Journal of Computer Assisted Tomography* 36, 749–754. <https://doi.org/10.1097/RCT.0b013e31826dbc50>
- An, K.N., Browne, A.O., Korinek, S., Tanaka, S., Morrey, B.F., 1991. Three-dimensional kinematics of glenohumeral elevation. *J Orthop Res* 9, 143–149. <https://doi.org/10.1002/jor.1100090117>
- Anderst, W.J., Tashman, S., 2003. A method to estimate in vivo dynamic articular surface interaction. *J Biomech* 36, 1291–1299. [https://doi.org/10.1016/s0021-9290\(03\)00157-x](https://doi.org/10.1016/s0021-9290(03)00157-x)
- Arai, R., Nimura, A., Yamaguchi, K., Yoshimura, H., Sugaya, H., Saji, T., Matsuda, S., Akita, K., 2014. The anatomy of the coracohumeral ligament and its relation to the subscapularis muscle. *Journal of Shoulder and Elbow Surgery* 23, 1575–1581. <https://doi.org/10.1016/j.jse.2014.02.009>
- Ateshian, G.A., Kwak, S.D., Soslowky, L.J., Mow, V.C., 1994. A stereophotogrammetric method for determining in situ contact areas in diarthrodial joints, and a comparison with other methods. *J Biomech* 27, 111–124. [https://doi.org/10.1016/0021-9290\(94\)90038-8](https://doi.org/10.1016/0021-9290(94)90038-8)
- Bakhsh, W., Nicandri, G., 2018. Anatomy and Physical Examination of the Shoulder. *Sports Medicine and Arthroscopy Review* 26. <https://doi.org/10.1097/JSA.0000000000000202>
- Baumer, T.G., Giles, J.W., Drake, A., Zael, R., Bey, M.J., 2016. Measuring Three-Dimensional Thorax Motion Via Biplane Radiographic Imaging: Technique and Preliminary Results. *J Biomech Eng* 138. <https://doi.org/10.1115/1.4032058>
- Bell, S.N., Troupis, J.M., Miller, D., Alta, T.D., Coghlan, J.A., Wijeratna, M.D., 2015. Four-dimensional computed tomography scans facilitate preoperative planning in snapping scapula syndrome. *J Shoulder Elbow Surg* 24, e83-90. <https://doi.org/10.1016/j.jse.2014.09.020>
- Berliner, J.L., Regalado-Magdos, A., Ma, C.B., Feeley, B.T., 2015. Biomechanics of reverse total shoulder arthroplasty. *Journal of Shoulder and Elbow Surgery* 24, 150–160. <https://doi.org/10.1016/j.jse.2014.08.003>
- Bey, M.J., Kline, S.K., Zael, R., Kolowich, P.A., Lock, T.R., 2010. In Vivo Measurement of Glenohumeral Joint Contact Patterns. *EURASIP J Adv Signal Process* 2010, 162136. <https://doi.org/10.1155/2010/162136>

- Bey, M.J., Kline, S.K., Zauel, R., Lock, T.R., Kolowich, P.A., 2008. Measuring dynamic in-vivo glenohumeral joint kinematics: technique and preliminary results. *J Biomech* 41, 711–714. <https://doi.org/10.1016/j.jbiomech.2007.09.029>
- Bijlsma, J.W.J., Berenbaum, F., Lefeber, F.P.J.G., 2011. Osteoarthritis: an update with relevance for clinical practice. *Lancet* 377, 2115–2126. [https://doi.org/10.1016/S0140-6736\(11\)60243-2](https://doi.org/10.1016/S0140-6736(11)60243-2)
- Bouhassira, A., Edwards, T.B., Walch, G., Baratta, R.V., 2002. Early Results of a Reverse Design Prosthesis in the Treatment of Arthritis of the Shoulder in Elderly Patients With a Large Rotator Cuff Tear. *Orthopedics* 25, 129–133. <https://doi.org/10.3928/0147-7447-20020201-16>
- Chang, L.-R., Anand, P., Varacallo, M., 2020. Anatomy, Shoulder and Upper Limb, Glenohumeral Joint, StatPearls [Internet]. StatPearls Publishing.
- Cohen, Z.A., McCarthy, D.M., Kwak, S.D., Legrand, P., Fogarasi, F., Ciaccio, E.J., Ateshian, G.A., 1999. Knee cartilage topography, thickness, and contact areas from MRI: in-vitro calibration and in-vivo measurements. *Osteoarthritis and Cartilage* 7, 95–109. <https://doi.org/10.1053/joca.1998.0165>
- Culham, E., Peat, M., 1993. Functional anatomy of the shoulder complex. *J Orthop Sports Phys Ther* 18, 342–350. <https://doi.org/10.2519/jospt.1993.18.1.342>
- Dal Maso, F., Blache, Y., Raison, M., Lundberg, A., Begon, M., 2016. Glenohumeral joint kinematics measured by intracortical pins, reflective markers, and computed tomography: A novel technique to assess acromiohumeral distance. *J Electromyogr Kinesiol* 29, 4–11. <https://doi.org/10.1016/j.jelekin.2015.07.008>
- Dutton, M., 2008. *Orthopaedic Examination, Evaluation, and Intervention*, 2nd ed. ed. McGraw-Hill Medical, New York.
- Escamilla, R.F., Yamashiro, K., Paulos, L., Andrews, J.R., 2009. Shoulder muscle activity and function in common shoulder rehabilitation exercises. *Sports Med* 39, 663–685. <https://doi.org/10.2165/00007256-200939080-00004>
- Favre, P., Snedeker, J.G., Gerber, C., 2009. Numerical modelling of the shoulder for clinical applications. *Philosophical Transactions of the Royal Society A: Mathematical, Physical and Engineering Sciences* 367, 2095–2118. <https://doi.org/10.1098/rsta.2008.0282>
- Frankle, M., Levy, J.C., Pupello, D., Siegal, S., Saleem, A., Mighell, M., Vasey, M., 2006. The Reverse Shoulder Prosthesis for Glenohumeral Arthritis Associated with Severe Rotator Cuff Deficiency: A Minimum Two-Year Follow-up Study of Sixty Patients Surgical Technique. *JBJS* 88, 178–190. <https://doi.org/10.2106/JBJS.F.00123>
- Gammon, B., Lalone, E., Nishiwaki, M., Willing, R., Johnson, J., King, G.J.W., 2018. Arthrokinematics of the Distal Radioulnar Joint Measured Using Intercartilage Distance in an In Vitro Model. *J Hand Surg Am* 43, 283.e1-283.e9. <https://doi.org/10.1016/j.jhsa.2017.08.010>
- Gerber, C., Pennington, S.D., Nyffeler, R.W., 2009. Reverse Total Shoulder Arthroplasty. *JAAOS - Journal of the American Academy of Orthopaedic Surgeons* 17, 284–295.

- Gopura, R.A.R.C., Bandara, D.S.V., Kiguchi, K., Mann, G.K.I., 2016. Developments in hardware systems of active upper-limb exoskeleton robots: A review. *Robotics and Autonomous Systems* 75, 203–220. <https://doi.org/10.1016/j.robot.2015.10.001>
- Goto, A., Moritomo, H., Murase, T., Oka, K., Sugamoto, K., Arimura, T., Nakajima, Y., Yamazaki, T., Sato, Y., Tamura, S., Yoshikawa, H., Ochi, T., 2004. In vivo elbow biomechanical analysis during flexion: three-dimensional motion analysis using magnetic resonance imaging. *J Shoulder Elbow Surg* 13, 441–447. <https://doi.org/10.1016/j.jse.2004.01.022>
- Halder, A.M., Halder, C.G., Zhao, K.D., O’Driscoll, S.W., Morrey, B.F., An, K.N., 2001a. Dynamic inferior stabilizers of the shoulder joint. *Clin Biomech (Bristol, Avon)* 16, 138–143. [https://doi.org/10.1016/s0268-0033\(00\)00077-2](https://doi.org/10.1016/s0268-0033(00)00077-2)
- Halder, A.M., Kuhl, S.G., Zobitz, M.E., Larson, D., An, K.N., 2001b. Effects of the glenoid labrum and glenohumeral abduction on stability of the shoulder joint through concavity-compression : an in vitro study. *J Bone Joint Surg Am* 83, 1062–1069. <https://doi.org/10.2106/00004623-200107000-00013>
- Halder, A.M., Zhao, K.D., Odriscoll, S.W., Morrey, B.F., An, K.N., 2001c. Dynamic contributions to superior shoulder stability. *J Orthop Res* 19, 206–212. [https://doi.org/10.1016/S0736-0266\(00\)00028-0](https://doi.org/10.1016/S0736-0266(00)00028-0)
- Hess, S.A., 2000. Functional stability of the glenohumeral joint. *Man Ther* 5, 63–71. <https://doi.org/10.1054/math.2000.0241>
- Hislop-Jambrich, J., Troupis, J., Moaveni, A., 2016. The Use of a Dynamic 4-Dimensional Computed Tomography Scan in the Diagnosis of Atraumatic Posterior Sternoclavicular Joint Instability. *Journal of Computer Assisted Tomography* 40, 576–577. <https://doi.org/10.1097/RCT.0000000000000410>
- Högfors, C., Sigholm, G., Herberts, P., 1987. Biomechanical model of the human shoulder—I. Elements. *Journal of Biomechanics* 20, 157–166. [https://doi.org/10.1016/0021-9290\(87\)90307-1](https://doi.org/10.1016/0021-9290(87)90307-1)
- Howell, S.M., Galinat, B.J., Renzi, A.J., Marone, P.J., 1988. Normal and abnormal mechanics of the glenohumeral joint in the horizontal plane. *J Bone Joint Surg Am* 70, 227–232.
- Inman, V.T., Saunders, J.B. dec M., Abbott, L.C., 1996. Observations of the Function of the Shoulder Joint: *Clinical Orthopaedics and Related Research* 330, 3–12. <https://doi.org/10.1097/00003086-199609000-00002>
- Jauregui, J.J., Nadarajah, V., Shield, W.P.I., Henn, R.F.I., Gilotra, M., Hasan, S.A., 2018. Reverse Shoulder Arthroplasty: Perioperative Considerations and Complications. *JBJS Reviews* 6, e3. <https://doi.org/10.2106/JBJS.RVW.17.00152>
- Jenp, Y.N., Malanga, G.A., Growney, E.S., An, K.N., 1996. Activation of the rotator cuff in generating isometric shoulder rotation torque. *Am J Sports Med* 24, 477–485. <https://doi.org/10.1177/036354659602400412>
- Jonsson, B., Olofsson, B.M., Steffner, L.C., 1972. Function of the teres major, latissimus dorsi and pectoralis major muscles. A preliminary study. *Acta Morphol Neerl Scand* 9, 275–280.

- Kaback, L.A., Green, A., Blaine, T.A., 2012. Glenohumeral arthritis and total shoulder replacement. *Med Health R I* 95, 120–124.
- Karduna, A.R., Williams, G.R., Williams, J.L., Iannotti, J.P., 1996. Kinematics of the glenohumeral joint: influences of muscle forces, ligamentous constraints, and articular geometry. *J Orthop Res* 14, 986–993. <https://doi.org/10.1002/jor.1100140620>
- Karlsson, D., Peterson, B., 1992. Towards a model for force predictions in the human shoulder. *J Biomech* 25, 189–199. [https://doi.org/10.1016/0021-9290\(92\)90275-6](https://doi.org/10.1016/0021-9290(92)90275-6)
- Kedgley, A.E., Mackenzie, G.A., Ferreira, L.M., Drosdowech, D.S., King, G.J.W., Faber, K.J., Johnson, J.A., 2008. Humeral head translation decreases with muscle loading. *J Shoulder Elbow Surg* 17, 132–138. <https://doi.org/10.1016/j.jse.2007.03.021>
- Kedgley, A.E., Mackenzie, G.A., Ferreira, L.M., Drosdowech, D.S., King, G.J.W., Faber, K.J., Johnson, J.A., 2007. The effect of muscle loading on the kinematics of in vitro glenohumeral abduction. *J Biomech* 40, 2953–2960. <https://doi.org/10.1016/j.jbiomech.2007.02.008>
- Kelkar, R., Wang, V.M., Flatow, E.L., Newton, P.M., Ateshian, G.A., Bigliani, L.U., Pawluk, R.J., Mow, V.C., 2001. Glenohumeral mechanics: a study of articular geometry, contact, and kinematics. *J Shoulder Elbow Surg* 10, 73–84. <https://doi.org/10.1067/mse.2001.111959>
- Kim, M.S., Jeong, H.Y., Kim, J.D., Ro, K.H., Rhee, S.-M., Rhee, Y.G., 2020. Difficulty in performing activities of daily living associated with internal rotation after reverse total shoulder arthroplasty. *Journal of Shoulder and Elbow Surgery* 29, 86–94. <https://doi.org/10.1016/j.jse.2019.05.031>
- Krishnan, R., Björnsell, N., Gutierrez-Farewik, E.M., Smith, C., 2019. A survey of human shoulder functional kinematic representations. *Med Biol Eng Comput* 57, 339–367. <https://doi.org/10.1007/s11517-018-1903-3>
- Kwon, Y.W., Pinto, V.J., Yoon, J., Frankle, M.A., Dunning, P.E., Sheikhzadeh, A., 2012. Kinematic analysis of dynamic shoulder motion in patients with reverse total shoulder arthroplasty. *Journal of Shoulder and Elbow Surgery* 21, 1184–1190. <https://doi.org/10.1016/j.jse.2011.07.031>
- Kwong, Y., Mel, A.O., Wheeler, G., Troupis, J.M., 2015. Four-dimensional computed tomography (4DCT): A review of the current status and applications. *J Med Imaging Radiat Oncol* 59, 545–554. <https://doi.org/10.1111/1754-9485.12326>
- Lalone, E.A., Fox, A.-M.V., Kedgley, A.E., Jenkyn, T.R., King, G.J.W., Athwal, G.S., Johnson, J.A., Peters, T.M., 2011. The effect of CT dose on glenohumeral joint congruency measurements using 3D reconstructed patient-specific bone models. *Phys. Med. Biol.* 56, 6615–6624. <https://doi.org/10.1088/0031-9155/56/20/006>
- Lalone, E.A., MacDermid, J., King, G., Grewal, R., 2021. The Effect of Distal Radius Fractures on 3-Dimensional Joint Congruency. *J Hand Surg Am* 46, 66.e1-66.e10. <https://doi.org/10.1016/j.jhsa.2020.05.027>
- Lalone, E.A., McDonald, C.P., Ferreira, L.M., Peters, T.M., King, G.W., Johnson, J.A., 2013. Development of an image-based technique to examine joint congruency at the elbow. *Comput Methods Biomech Biomed Engin* 16, 280–290. <https://doi.org/10.1080/10255842.2011.617006>

- Latif, V., Denard, P.J., Young, A.A., Liotard, J.-P., Walch, G., 2012. Bilateral Anatomic Total Shoulder Arthroplasty Versus Reverse Shoulder Arthroplasty. *Orthopedics (Online)* 35, e479–e485. <http://dx.doi.org/10.3928/01477447-20120327-25>
- Leahy, R.M., Clackdoyle, R., 2005. 10.2 - Computed Tomography, in: Bovik, A. (Ed.), *Handbook of Image and Video Processing (Second Edition)*, Communications, Networking and Multimedia. Academic Press, Burlington, pp. 1155–XXXII. <https://doi.org/10.1016/B978-012119792-6/50128-5>
- Lee, D.H., Choi, Y.S., Potter, H.G., Endo, Y., Sivakumaran, T., Lim, T.K., Chun, T.J., 2020. Reverse total shoulder arthroplasty: an imaging overview. *Skeletal Radiol* 49, 19–30. <https://doi.org/10.1007/s00256-019-03275-0>
- Lefèvre-Colau, M.-M., Nguyen, C., Palazzo, C., Srour, F., Paris, G., Vuillemin, V., Poiraudreau, S., Roby-Brami, A., Roren, A., 2018. Recent advances in kinematics of the shoulder complex in healthy people. *Annals of Physical and Rehabilitation Medicine* 61, 56–59. <https://doi.org/10.1016/j.rehab.2017.09.001>
- Lo, H.S., Xie, S.Q., 2012. Exoskeleton robots for upper-limb rehabilitation: state of the art and future prospects. *Med Eng Phys* 34, 261–268. <https://doi.org/10.1016/j.medengphy.2011.10.004>
- Lösch, A., Eckstein, F., Haubner, M., Englmeier, K.H., 1997. A non-invasive technique for 3-dimensional assessment of articular cartilage thickness based on MRI. Part 1: Development of a computational method. *Magn Reson Imaging* 15, 795–804. [https://doi.org/10.1016/s0730-725x\(97\)00012-x](https://doi.org/10.1016/s0730-725x(97)00012-x)
- Ludewig, P., Phadke, V., Braman, J., Hassett, D., Cieminski, C., LaPrade, R., 2009. Motion of the Shoulder Complex During Multiplanar Humeral Elevation. *The Journal of Bone & Joint Surgery* 91, 378–389. <https://doi.org/10.2106/JBJS.G.01483>
- Maier, M.W., Caspers, M., Zeifang, F., Dreher, T., Klotz, M.C., Wolf, S.I., Kasten, P., 2014. How does reverse shoulder replacement change the range of motion in activities of daily living in patients with cuff tear arthropathy? A prospective optical 3D motion analysis study. *Arch Orthop Trauma Surg* 134, 1065–1071. <https://doi.org/10.1007/s00402-014-2015-7>
- Marai, G.E., Crisco, J.J., Laidlaw, D.H., 2006. A kinematics-based method for generating cartilage maps and deformations in the multi-articulating wrist joint from CT images. *Conf Proc IEEE Eng Med Biol Soc 2006*, 2079–2082. <https://doi.org/10.1109/IEMBS.2006.259742>
- Marai, G.E., Laidlaw, D.H., Demiralp, C., Andrews, S., Grimm, C.M., Crisco, J.J., 2004. Estimating joint contact areas and ligament lengths from bone kinematics and surfaces. *IEEE Trans Biomed Eng* 51, 790–799. <https://doi.org/10.1109/TBME.2004.826606>
- Marieb, E., Hoehn, K., 2018. *Human Anatomy & Physiology*, 11 edition. ed. Pearson, Hoboken, New Jersey.
- Matsuki, K., Kenmoku, T., Ochiai, N., Sugaya, H., Banks, S.A., 2016. Differences in glenohumeral translations calculated with three methods: Comparison of relative positions and contact point. *J Biomech* 49, 1944–1947. <https://doi.org/10.1016/j.jbiomech.2016.03.042>
- Matsumura, N., Oki, S., Fukasawa, N., Matsumoto, M., Nakamura, M., Nagura, T., Yamada, Y., Jinzaki, M., 2019. Glenohumeral translation during active external rotation with the shoulder

- abducted in cases with glenohumeral instability: a 4-dimensional computed tomography analysis. *Journal of Shoulder and Elbow Surgery* 28, 1903–1910. <https://doi.org/10.1016/j.jse.2019.03.008>
- Mattei, L., Mortera, S., Arrigoni, C., Castoldi, F., 2015. Anatomic shoulder arthroplasty: an update on indications, technique, results and complication rates. *Joints* 3, 72–77. <https://doi.org/10.11138/jts/2015.3.2.072>
- Mozingo, J.D., Akbari-Shandiz, M., Van Straaten, M.G., Murthy, N.S., Schueler, B.A., Holmes, D.R., McCollough, C.H., Zhao, K.D., 2019. Comparison of glenohumeral joint kinematics between manual wheelchair tasks and implications on the subacromial space: A biplane fluoroscopy study. *J Electromyogr Kinesiol* 102350. <https://doi.org/10.1016/j.jelekin.2019.08.004>
- Murphy, M.A., Häger, C.K., 2015. Kinematic analysis of the upper extremity after stroke – how far have we reached and what have we grasped? *Physical Therapy Reviews* 20, 137–155. <https://doi.org/10.1179/1743288X15Y.0000000002>
- Neer, C.S., 1990. *Shoulder Reconstruction*, 1st edition. ed. Saunders, Philadelphia.
- Norkin, C., White, D.J., Malone, T.W., Kalem, G., 2009. *Measurement of Joint Motion: A Guide to Goniometry*, 4th ed. FADavis Company, Philadelphia.
- Parsons, I.M., Weldon, E.J., Titelman, R.M., Smith, K.L., 2004. Glenohumeral arthritis and its management. *Phys Med Rehabil Clin N Am* 15, 447–474. <https://doi.org/10.1016/j.pmr.2003.12.001>
- Patel, R.M., Gelber, J.D., Schickendantz, M.S., 2018. The Weight-Bearing Shoulder: *Journal of the American Academy of Orthopaedic Surgeons* 26, 3–13. <https://doi.org/10.5435/JAAOS-D-15-00598>
- Rau, G., Disselhorst-Klug, C., Schmidt, R., 2000. Movement biomechanics goes upwards: from the leg to the arm. *Journal of Biomechanics* 33, 1207–1216. [https://doi.org/10.1016/S0021-9290\(00\)00062-2](https://doi.org/10.1016/S0021-9290(00)00062-2)
- Roche, C., Crosby, L., 2018. Kinematics and biomechanics of reverse shoulder arthroplasty, in: *Othopaedic Knowledge Update: Shoulder and Elbow*. pp. 45–54.
- Rockwood and Matsen's *The Shoulder*, 2 Volume Set - 4th Edition [WWW Document], n.d. URL <https://www.elsevier.com/books/rockwood-and-matsen-s-the-shoulder-2-volume-set/matsen/978-1-4160-3427-8> (accessed 6.8.20).
- S, L., F, M., 1993. Mechanisms of glenohumeral joint stability. *Clinical orthopaedics and related research*.
- Sanchez-Sotelo, J., 2011. Total Shoulder Arthroplasty. *Open Orthop J* 5, 106–114. <https://doi.org/10.2174/1874325001105010106>
- Soslowsky, L.J., Flatow, E.L., Bigliani, L.U., Mow, V.C., 1992. Articular geometry of the glenohumeral joint. *Clin Orthop Relat Res* 181–190.
- Tortora, G.J., Nielsen, M., 2016. *Principles of Human Anatomy*, 14th Edition. Wiley, New York.

- Van Ginckel, A., Roosen, P., Almqvist, K.F., Verstraete, K., Witvrouw, E., 2011. Effects of in vivo exercise on ankle cartilage deformation and recovery in healthy volunteers: an experimental study. *Osteoarthritis Cartilage* 19, 1123–1131. <https://doi.org/10.1016/j.joca.2011.06.009>
- Viceconti, M., 2011. *Multiscale Modeling of the Skeletal System*. Cambridge University Press, Cambridge. <https://doi.org/10.1017/CBO9781139049627>
- von Eisenhart-Rothe, R., Siebert, M., Bringmann, C., Vogl, T., Englmeier, K.-H., Graichen, H., 2004. A new in vivo technique for determination of 3D kinematics and contact areas of the patello-femoral and tibio-femoral joint. *J Biomech* 37, 927–934. <https://doi.org/10.1016/j.jbiomech.2003.09.034>
- Walch, G., Badet, R., Boulahia, A., Houry, A., 1999. Morphologic study of the glenoid in primary glenohumeral osteoarthritis. *J Arthroplasty* 14, 756–760. [https://doi.org/10.1016/s0883-5403\(99\)90232-2](https://doi.org/10.1016/s0883-5403(99)90232-2)
- Wall, B., Nové-Josserand, L., O'Connor, D.P., Edwards, T.B., Walch, G., 2007. Reverse total shoulder arthroplasty: a review of results according to etiology. *J Bone Joint Surg Am* 89, 1476–1485. <https://doi.org/10.2106/JBJS.F.00666>
- Warner, J.J., Bowen, M.K., Deng, X.H., Hannafin, J.A., Arnoczky, S.P., Warren, R.F., 1998. Articular contact patterns of the normal glenohumeral joint. *J Shoulder Elbow Surg* 7, 381–388. [https://doi.org/10.1016/s1058-2746\(98\)90027-1](https://doi.org/10.1016/s1058-2746(98)90027-1)
- Woolf, A.D., Pfleger, B., 2003. Burden of major musculoskeletal conditions. *Bull World Health Organ* 81, 646–656.
- Wuelker, N., Plitz, W., Roetman, B., Wirth, C.J., 1994a. Function of the supraspinatus muscle. Abduction of the humerus studied in cadavers. *Acta Orthop Scand* 65, 442–446. <https://doi.org/10.3109/17453679408995490>
- Wuelker, N., Schmotzer, H., Thren, K., Korell, M., 1994b. Translation of the glenohumeral joint with simulated active elevation. *Clin Orthop Relat Res* 193–200.
- Xu, X., Lin, J., McGorry, R.W., 2014. A regression-based 3-D shoulder rhythm. *J Biomech* 47, 1206–1210. <https://doi.org/10.1016/j.jbiomech.2014.01.043>
- Young, S.W., Everts, N.M., Ball, C.M., Astley, T.M., Poon, P.C., 2009. The SMR reverse shoulder prosthesis in the treatment of cuff-deficient shoulder conditions. *Journal of Shoulder and Elbow Surgery* 18, 622–626. <https://doi.org/10.1016/j.jse.2009.01.017>

Chapter 2: How does Computed Tomography Inform our Understanding of Shoulder Kinematics? A Structured Review

Chapter 2 examines the extent and range of methods employing CT imaging to measure shoulder kinematics in research studies using a systematic literature search and structured data extraction process. This chapter addresses the current gaps in data reporting, and concludes with recommendations for future studies using CT.

A version of this work has been submitted to the Journal of Medical and Biological Engineering and Computing.

2.1 Introduction

Human movement is complicated and the behavior of the single parts does not fully explain the behavior of the whole body, and vice versa (Viceconti, 2011). Thus, a single joint behavior cannot entirely account for the behavior of multiple joints (Gielen et al., 1995). This previous statement couldn't be more true than when examining the motion of the hand and upper limb, as it is difficult to reliably evaluate the kinematics of the upper limb when the hand, wrist, elbow and shoulder are moving synchronously (Rau et al., 2000). Kinematics is concerned with the motion of objects (pathway of motion) and does not reference the forces that cause the motion. Numerous challenges arise when analyzing shoulder kinematics, and these challenges are related to anatomic complexity, inconsistent clinical descriptions, measurement limitations, over-constrained systems, and movement variability (Krishnan et al., 2019).

As discussed in Chapter 1, medical imaging approaches can provide a non-invasive approach that can produce 3D measures of in-vivo shoulder joint motion (six degrees of freedom) (Baumer et al., 2016; Dal Maso et al., 2016; Matsuki et al., 2016). Recently, 4-dimensional computed tomography (4DCT) (time + 3DCT) technology has emerged and may be a useful alternative to 3DCT, as it overcomes the challenges associated with limited field of view, out of plane error, and static limitations of current imaging modalities.

Several studies have employed 4DCT scanning to assess the glenohumeral joint (Matsumura et al., 2019), scapulothoracic joint (Bell et al., 2015), acromioclavicular joint (Alta et al., 2012) and sternoclavicular joint (Hislop-Jambrich et al., 2016), but the validity of this technique and the outcome measures reported have not been examined or standardized. Critically appraising and comparing results from many studies using systematic reviews and meta-analyses is essential to further our efforts towards the biomechanical challenge of characterizing complex shoulder motion. Additionally, as new studies emerge that employ 4DCT and replace traditional study designs that combine biplane fluoroscopy and CT, these studies would benefit from the valuable work that has been done in the past to inform this new generation of CT motion analysis. Therefore, the aim of this structured review was to examine how CT scanning has been used to measure range of motion in six degrees of freedom (6DoF). Specifically, the objective was to examine the extent and range of methods employing CT imaging to measure shoulder kinematics in research studies using a systematic literature search and structured data extraction process.

2.2 Methods

2.2.1 Literature Search and Study Identification

A literature search was conducted using Evidence-based Medicine Reviews (Embase) and PubMed with publication dates up to and including February 2020. The search was limited to full-text publications, written in English, and involving adult humans. The following keywords were used to search databases for eligible studies: Shoulder OR Glenohumeral OR Scapulothoracic OR Acromioclavicular OR Sternoclavicular AND Computed Tomography OR CT OR 3DCT OR 4DCT AND Motion OR Kinematic OR Kinematics. The first step of study identification was reviewing the titles listed from both databases using the specified keywords. In total 2,058 titles were reviewed (Figure 2.1). Studies were excluded if they were non-English, involving non-humans or children. Additionally, studies were excluded if they were review articles, published in conference proceedings or as a dissertation or thesis. Included studies had to meet the criteria of using CT imaging to measure the kinematics of the shoulder.

2.2.2 Study Selection

In total, 167 studies were included for abstract screening. Studies were excluded if they were not evaluating shoulder kinematics or did not use CT scanning. After the abstract screening, 79 studies were excluded in addition to 21 duplicates. Eighty-eight full-text studies were then considered eligible for data extraction. After reading the full article, 59 studies were further excluded for not meeting the inclusion criteria (i.e., measuring shoulder kinematics), and 29 studies were included. The excluded studies used CT scanning to measure static models or abnormalities of the shoulder, rather than kinematics (Figure 2.1).

2.2.3 Data Collection Process

The data extraction and review process were conducted using a standardized data extraction procedure developed for this review, as shown in Figure 2.1. Three reviewers were involved in the data extraction and review process. Two reviewers completed detailed reviews of all articles, with consultation of the third reviewer in the case of uncertainty in the extraction process. In addition, the PRISMA checklist was used to improve transparency in this review.

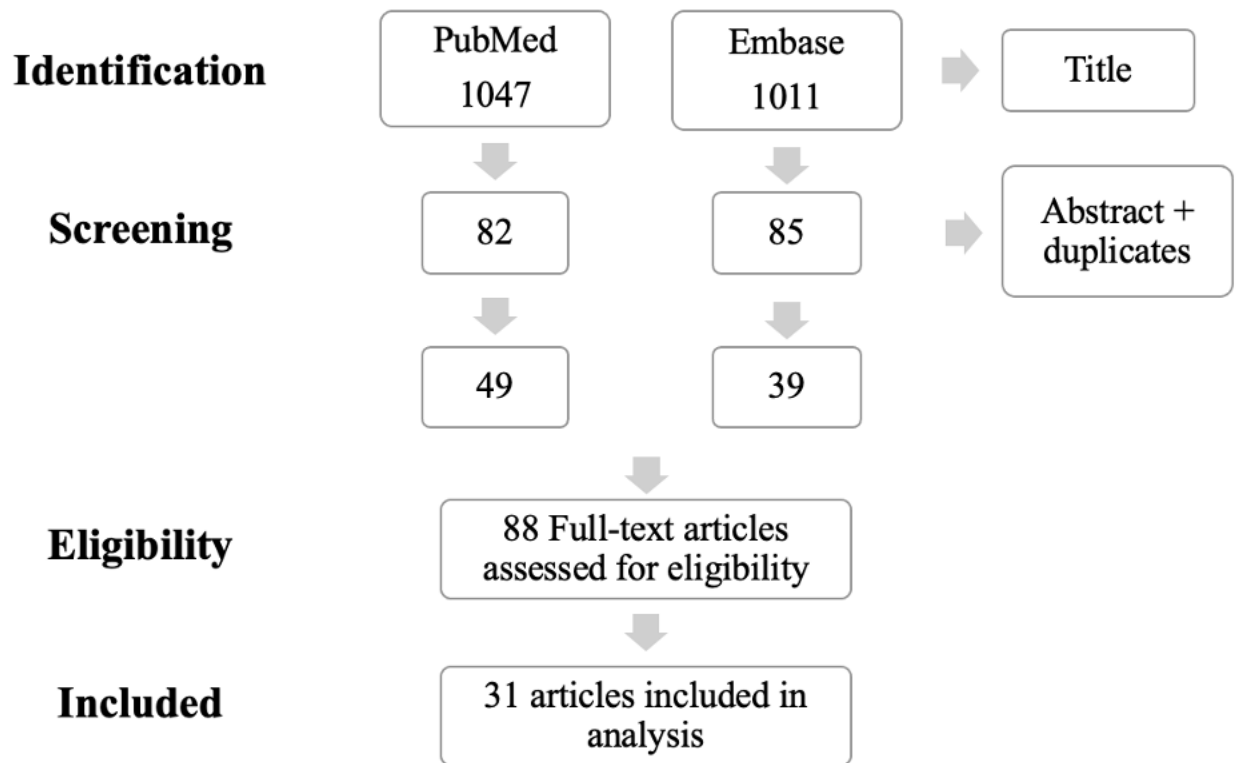


Figure 2.1: Literature Search and Study Identification

2.3 Results

2.3.1 Study Demographics

In total, 29 studies were included in the data extraction process (Figure 2.1). Table 2.1 lists the authors, titles, journal reference, study location, year of publication, start and end pages, volume and issues of each study in alphabetical order. As shown, the majority of the studies reviewed were conducted in Japan (11 studies) (Fung et al., 2001; Kijima et al., 2015; Kozono et al., 2018a, 2018b, 2017; Matsuki et al., 2016, 2014, 2012, 2011; Matsumura et al., 2019; Nishinaka et al., 2008), followed by the USA (6 studies) (Bakshi et al., 2016; Baumer et al., 2016, p.; Bey et al., 2008; Elwell et al., 2017; Giphart et al., 2013; Mozingo et al., 2019), Korea (5 studies) (Jeon et al., 2016; D. S. Kim et al., 2017; E. Kim et al., 2017, p., 2017; Kim et al., 2015), Canada (Clément et al., 2017; Dal Maso et al., 2016) and Germany (Werner et al., 2018, 2017) (2 studies), Switzerland (Lädemann et al., 2019), Belgium (Baeyens et al., 2001) and Australia (Alta et al., 2012) (1 study). The frequency of studies investigating shoulder kinematics increased in 2016 and 2017 and decreased in 2018 (Figure 2.2). Detailed information about the sample size, sex, age and participants of each study are shown in Table 2.2. The overall number of participants across all included studies was 397 participants, in which 218 participants were males and 54 participants were females. Eight studies did not report the sex of their participants, leaving the sex of 125 participants unstated. Eleven studies included males only as their participants. Almost half of the articles examined participants with a mean age of ≥ 40 years (14 studies). Ten studies examined adults with a mean age of 30-39 years, and six studies investigated adults with a mean age of 20-29 years. Two studies did not state the age group of their participants.

Table 2.1: Summary of Studies Measuring the Kinematics of the Shoulder

Article #	Title	Author	Journal	Location	Year	Start Page	End Page	Volume	Issue
1	The New 4-dimensional Computed Tomographic Scanner Allows Dynamic Visualization and Measurement of Normal Acromioclavicular Joint Motion in an Unloaded and Loaded Condition	Alta et al.	Journal of Computed Assisted Tomography	Australia	2012	749	754	36	6
2	Glenohumeral joint kinematics related to minor anterior instability of the shoulder at the end of the late preparatory phase of throwing	Baeyens et al.	Clinical Biomechanics	Belgium	2001	752	757	16	9

3	The Influence of Surgical Stabilization on Glenohumeral Abduction Using 3-Dimensional Computed Tomography in Patients With Shoulder Instability	Bakshi et al.	The Journal of Arthroscopic and Related Surgery	USA	2016	1495	1501	32	8
4	Measuring Three-Dimensional Thorax Motion Via Biplane Radiographic Imaging: Technique and Preliminary Results	Baumer et al.	Journal of Biomechanical Engineering	USA	2016	145041	145045	138	1
5	Measuring dynamic in-vivo glenohumeral joint kinematics: Technique and preliminary results	Bey et al.	Journal of Biomechanics	USA	2008	711	714	41	3
6	Three-dimensional analysis of the locked position in patients with recurrent shoulder instability.	Clément et al.	Journal of Shoulder and Elbow Surgery	Canada	2017	536	543	26	3

7	Quantifying the competing relationship between adduction range of motion and baseplate micromotion with lateralization of reverse total shoulder arthroplasty	Elwell et al..	Journal of Biomechanics	USA	2017	24	30	52	8
8	Scapular and clavicular kinematics during humeral elevation: a study with cadavers	Fung et al.	Journal of Shoulder and Elbow Surgery	Japan	2001	278	285	10	3
9	Effect of Plane of Arm Elevation on Glenohumeral Kinematics A Normative Biplane Fluoroscopy Study	Giphart et al.	The Journal of Bone and Joint Surgery	USA	2013	238	245	95	3
10	Effect of critical shoulder angle, glenoid lateralization, and humeral inclination on range of movement in reverse shoulder arthroplasty.	läderrmann et al.	Bone and Joint Research	Switzerland	2019	378	386	8	8

11	Combined effect of change in humeral neck-shaft angle and retroversion on shoulder range of motion in reverse total shoulder arthroplasty — A simulation study	Jeon et al.	Journal of Clinical Biomechanics	Korea	2016	12	19	31	--
12	In vivo 3-dimensional analysis of scapular and glenohumeral kinematics: comparison of symptomatic or asymptomatic shoulders with rotator cuff tears and healthy shoulders	Kijima et al.	Journal of Shoulder and Elbow Surgery	Japan	2015	1817	1826	24	11
13	Comparison of dynamics in 3D glenohumeral position between primary dislocated shoulders and contralateral healthy shoulders.	Kim et al.	Journal of orthopaedics	Korea	2017	195	200	14	1
14	In Vivo Analysis of Three-Dimensional Dynamic Scapular Dyskinesia in Scapular or Clavicular Fractures.	Kim et al.	Acta Med. Okayama	Korea	2017	151	159	71	2

15	Three-dimensional scapular dyskinesis in hook-plated acromioclavicular dislocation including hook motion.	Kim et al.	Journal of Shoulder and Elbow Surgery	Korea	2018	1117	1124	27	6
16	In vivo analysis of acromioclavicular joint motion after hook plate fixation using three-dimensional computed tomography	Kim et al.	Journal of Shoulder and Elbow Surgery	Korea	2015	1106	1111	24	7
17	In Vivo Kinematic Analysis of the Glenohumeral Joint During Dynamic Full Axial Rotation and Scapular Plane Full Abduction in Healthy Shoulders	Kozono et al.	European Society of Sports Traumatology, Knee Surgery, Arthroscopy (ESSKA)	Japan	2017	2032	2040	25	7
18	Dynamic kinematics of the glenohumeral joint in shoulders with rotator cuff tears	Kozono et al.	Journal of Orthopaedic Surgery and Research	Japan	2018	1	7	13	9

19	In Vivo Dynamic Acromiohumeral Distance in Shoulders With Rotator Cuff Tears	Kozono et al.	Clinical Biomechanics	Japan	2018	95	99	60	--
20	Glenohumeral joint kinematics measured by intracortical pins, reflective markers, and computed tomography: A novel technique to assess acromiohumeral distance	Maso et al.	Journal of Electromyography and Kinesiology	Canada	2016	4	11	29	--
21	In vivo 3-dimensional analysis of scapular kinematics: comparison of dominant and nondominant shoulders	Matsuki et al.	Journal of Shoulder and Elbow Surgery	Japan	2011	659	665	20	4
22	Dynamic in Vivo Glenohumeral Kinematics During Scapular Plane Abduction in Healthy Shoulders	Matsuki et al.	Journal of orthopedic & sports physical therapy	Japan	2012	96	104	42	2

23	In vivo 3D analysis of clavicular kinematics during scapular plane abduction: Comparison of dominant and non-dominant shoulders	Matsuki et al.	Gait and Posture	Japan	2014	625	627	39	1
24	Differences in Glenohumeral Translations Calculated With Three Methods: Comparison of Relative Positions and Contact Point	Matsuki et al.	Journal of Biomechanics	Japan	2016	1944	1947	49	9
25	Glenohumeral translation during active external rotation with the shoulder abducted in cases with glenohumeral instability: a 4-dimensional computed tomography analysis	Matsumura et al.	Journal of Shoulder and Elbow Surgery	Japan	2019	1903	1910	28	10
26	Comparison of glenohumeral joint kinematics between manual wheelchair tasks and implications on the subacromial space: A biplane fuoroscopy study	Mozingo et al.	Journal of Electromyography and Kinesiology	USA	2019	1	11	--	--

27	Determination of in Vivo Glenohumeral Translation Using Fluoroscopy and Shape-Matching Techniques	Nishinaka et al.	Journal of Shoulder and Elbow Surgery	Japan	2008	319	322	17	2
28	The influence of humeral neck shaft angle and glenoid lateralization on range of motion in reverse shoulder arthroplasty	Werner et al.	Journal of Shoulder and Elbow Surgery	Germany	2017	1726	1731	26	10
29	Glenosphere design affects range of movement and risk of friction-type scapular impingement in reverse shoulder arthroplasty.	Werner et al.	The Bone and Joint Journal	Germany	2018	1182	1186	100-B	9

Table 2.2: Study Demographics				
Article #	Sample Size	Sex (F:M)	Age (years)	Participants
1	16	5:11	42 ± 11	Healthy
2	6	Not stated	30-40	1st division handball players with minor anterior instability vs. control
3	39	6:33	24.6 (15- 58)	3 groups of patients with shoulder instability: failed surgical stabilization, successful surgical stabilization, and unstable shoulder with no prior surgical intervention. Compared with unaffected shoulder
4	5	Not stated	59.4 ± 9.9	Rotator cuff tear patients

5	5	0:5	65.4 ± 8.6	Repaired and contralateral shoulders of patients following rotator cuff repair
6	44 patients, 46 shoulders	Not stated	Normal laxity: 27 ± 7 Hyperlaxity: 27 ± 7 Epilepsy: 24 ± 3	18 with “normal” laxity, 18 with hyperlaxity and 8 (2 bilateral) with epilepsy
7	3 cadavers, 4 shoulders	1:2	71–78	Healthy
8	3 cadavers	Not stated	76.3 ± 6.6	Healthy
9	13	2:11	Mean age of 29 ± 6 years	Healthy
10	12	Not stated	Not stated	Scheduled to undergo RSA (type A1 glenoid)
11	3	0:3	Two males in their 20s and one male in his 40s	Healthy

12	19	8:11	Symptomatic RCTs: A mean age of 67 years (range, 62-72 years)	5 symptomatic RCT patients, 7 asymptomatic RCTs patients, 7 healthy participants
13	10 participants, 20 shoulders	0:10	23.4 ± 8.8 (17–35)	Subjects who had suffered shoulder dislocation for first time compared with the contralateral healthy shoulder.
14	20 patients, 40 shoulders	Not stated	Patients with scapular fracture: 48.2 (36-84) Patients with clavicular non-union: 54.7 (26-72)	Patients who had been treated for scapular or clavicular fracture. Compared with normal contralateral shoulder.

15	15 patients, 30 shoulders	Not stated	48.2 (36-84)	15 cases of acromioclavicular dislocation treated with a hook plate and 15 contralateral normal shoulders
16	7 participants, 14 shoulders	2:5	42 (24-60)	Patients with distal clavicular fractures fixed with hook plate of one shoulder compared with the normal (without hook plate fixation) shoulder.
17	10	0:10	32 (30-37)	Healthy
18	21	5:16	RCT: 72 ± 5 (65-75) Healthy control subjects: 32 ± 2 years (30-37)	11 rotator cuff tear patients who were scheduled to undergo rotator cuff surgery. 10 healthy controls

19	21	5:16	Patient: 72 ± 5 Control: 32 ± 2	11 rotator cuff tear patients and 10 healthy control subjects
20	4	0:4	36 (27-41) mean	Healthy
21	12	0:12	32 (27-36)	Healthy dominant vs. nondominant
22	12	0:12	32 (27-36)	Healthy
23	12	0:12	32 (27-36)	Healthy
24	15	0:15	31 (27-36)	Healthy

25	10 participants, 20 shoulders	0:10	22.5 ± 3.5	Patients with unilateral glenohumeral instability with a positive fulcrum test. Compared with contralateral shoulder
26	10	1:9	45.8 ± 12.5 (26-58)	Participants with spinal cord injury who use a manual wheelchair as their primary mode of mobility
27	9	1:8	31(27-38)	Healthy
28	20	Not stated	Not stated	Patients scheduled to undergo primary total shoulder arthroplasty for concentric osteoarthritis
29	21	18:3	71.9 (50-87)	Patients with primary glenohumeral OA eligible for total shoulder arthroplasty

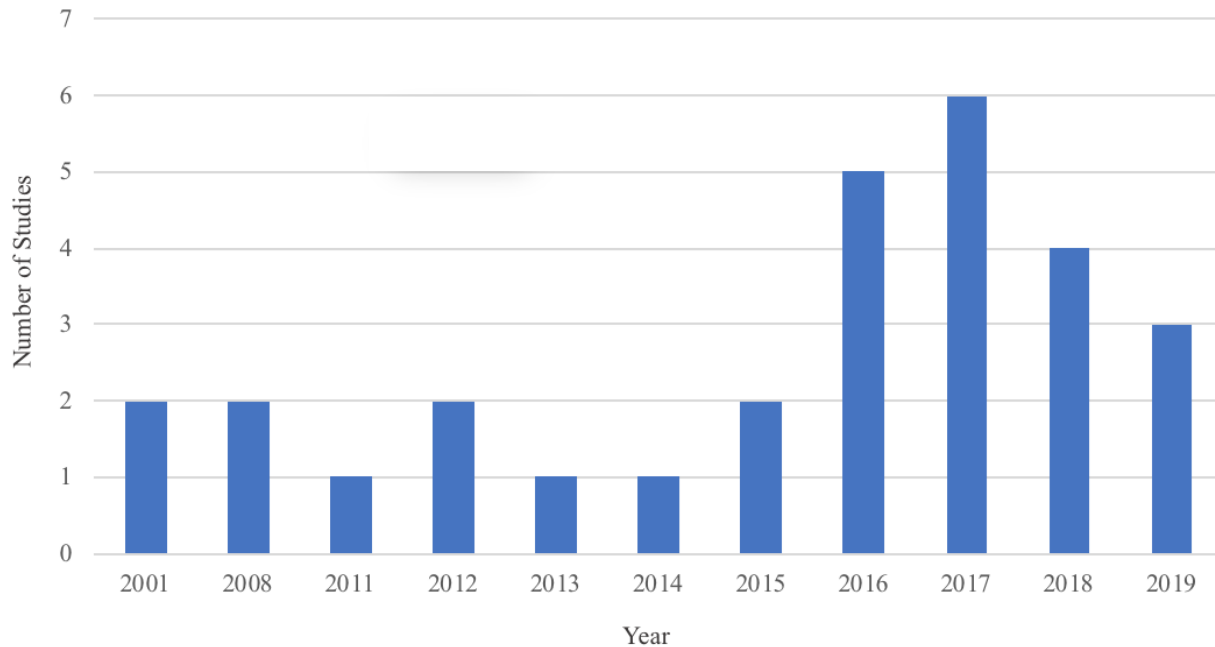


Figure 2.2: Number of studies by year

2.3.2 Population of Individuals Studied

Table 2.2 lists the participants examined in each study. Twelve studies examined healthy participants, five studies examined participants with shoulder instability, five studies examined participants with a rotator cuff tear, three studies examined participants with shoulder osteoarthritis and two studies examined shoulders with fractures. “Other” category includes studies evaluating participants with hyperlaxity or spinal cord injury who use a manual wheelchair. Of the 29 included studies, eight studies compared the results to the participants’ contralateral shoulder (Bakshi et al., 2016; Bey et al., 2008; D. S. Kim et al., 2017; E. Kim et al., 2017; Kim et al., 2018, 2015; Matsuki et al., 2011; Matsumura et al., 2019), and five studies compared the results to a control group (Baeyens et al., 2001; Elwell et al., 2017; Kijima et al., 2015; Kozono et al., 2018a, 2018b) (Table 2.2).

2.3.3 Joints Studied and Approach Used

Of the studies included in this review, several studies assessed multiple joints. Overall, the kinematics of the glenohumeral joint was measured in 22 studies (Baeyens et al., 2001; Bakshi et al., 2016; Bey et al., 2008; Clément et al., 2017; Dal Maso et al., 2016; Elwell et al., 2017; Fung et al., 2001; Giphart et al., 2013; Jeon et al., 2016; Kijima et al., 2015; D. S. Kim et al., 2017; Kozono et al., 2018a, 2018b, 2017; Lädermann et al., 2019; Matsuki et al., 2016, 2012; Matsumura et al., 2019; Mozingo et al., 2019; Nishinaka et al., 2008; Werner et al., 2018, 2017). The scapulothoracic joint kinematics was measured in eight studies (Baumer et al., 2016; Fung et al., 2001; Giphart et al., 2013; Kijima et al., 2015; E. Kim et al., 2017; Kim et al., 2018; Matsuki et al., 2012), and the acromioclavicular and sternoclavicular joints were measured across seven (Alta et al., 2012; Dal Maso et al., 2016; Fung et al., 2001; Kim et al., 2018, 2015; Kozono et al., 2018b; Matsuki et al., 2014) and two studies (Fung et al., 2001; Matsuki et al., 2014), respectively. Table 2.3 presents detailed data on the motions and joints studied and landmarks and coordinate systems used to assess motion. To measure the 6DoF kinematics, a joint coordinate system must be employed. Fourteen studies used a coordinate system that followed the International Society of Biomechanics (ISB) recommendation (Bakshi et al., 2016; Bey et al., 2008; Dal Maso et al., 2016; Fung et al., 2001; Giphart et al., 2013; E. Kim et al., 2017; Kim et al., 2018; Kozono et al., 2018a, 2018b, 2017; Lädermann et al., 2019; Matsuki et al., 2014; Matsumura et al., 2019; Mozingo et al., 2019; Wu et al., 2005) and 11 studies developed a coordinate system for various reasons (Baeyens et al., 2001; Baumer et al., 2016; Clément et al., 2017; Jeon et al., 2016; Kijima et al., 2015; D. S. Kim et al., 2017; Matsuki et al., 2016, 2012, 2011; Matsumura et al., 2019; Nishinaka et al., 2008). The other five studies did not use or develop a coordinate system to measure range of motion; however, range of motion was measured using software or by taking 2D planar

measurements of the CT scans (Alta et al., 2012; Elwell et al., 2017; Kim et al., 2015; Werner et al., 2018, 2017). One study used both ISB recommendations and a developed coordinate system (Baumer et al., 2016). The study compared and validated a rib-based thorax coordinate system against the ISB recommendations before measuring the motion.

Table 2.3: Kinematics Measurement				
Article #	Joint	Motion	Landmarks	Coordinate System
1	Acromioclavicular	<ul style="list-style-type: none"> • Neutral, adduction of the arm (unloaded) • Neutral, adduction (loaded resisted superior elevation) 	Anteroposterior translation: a line anterior to the acromion perpendicular to the joint line and a second line anterior to the clavicle parallel to this. Super-inferior translation: a horizontal line under the acromion.	Not used
2	Glenohumeral	<ul style="list-style-type: none"> • 90° abduction • 90° external rotation • Late cocking position with the arm maximally externally rotated 	4 humeral and 4 scapular landmarks 4	Veldpaus Coordinate System (F. Veldpaus, 1988)
3	Glenohumeral	<ul style="list-style-type: none"> • 0° of abduction and 0° of external rotation • 30° of abduction and 30° of external rotation • Arms maximally abducted (overhead position). 	ISB	ISB

4	Scapulothoracic	<ul style="list-style-type: none"> • Coronal-plane abduction 	Costovertebral (CV) and the sternocostal (SC) joint	<p>Compared ISB to a rib-based thorax coordinate system. The origin of the thorax coordinate system was defined as the SC joint of the superior rib. The S/I axis of the thorax coordinate system was defined as the vector from the midpoint of the inferior rib's CV and SC joints to the midpoint of the superior rib's CV and SC joints. The M/L axis was defined as a vector perpendicular to the plane created by the CV and SC joint of the superior rib and the midpoint between the SC and CV joint of the inferior rib pointing to the right. Finally, the A/P axis was defined as the cross product of the superior/inferior and M/L axes.</p>
5	Glenohumeral	<ul style="list-style-type: none"> • Coronal-plane elevation from a resting position (arm at the subject's side) to approximately 120° of humerothoracic elevation (loaded with 3lb weight) • External rotation with the arm adducted from a resting position of full internal rotation to maximal external rotation (loaded with 3lb weight) 	ISB	ISB

6	Glenohumeral	<ul style="list-style-type: none"> • 12° of abduction • 90° of external rotation • 21° of extension 	<p>Glenoid: the origin O_g was the center of the ellipse. Humerus: the centroid of the humeral head and aligned with the glenoid-centered coordinate system</p>	<p>A glenoid coordinate system (O_g, X_g, Y_g, Z_g) was defined at the scapula, as described in Ohl et al. The origin O_g was the center of the ellipse, the Z_g axis was perpendicular to the mean plane fitted to the glenoid rim, the Y_g axis was the vector from the inferior to the superior part of the ellipse, and the X_g axis was the cross product of Y_g and Z_g to form an orthonormal system. The humeral coordinate system (O_h, X_h, Y_h, Z_h) was defined at the centroid of the humeral head and aligned with the glenoid-centered coordinate system.</p>
7	Glenohumeral	<ul style="list-style-type: none"> • Adduction 	<p>ROM was measured as the angle between the central axis of a humeral stem and a plane parallel to the reamed glenoid face.</p>	<p>Not used</p>
8	Glenohumeral + scapulothoracic + acromioclavicular + sternoclavicular	<ul style="list-style-type: none"> • Humeral elevation 	<p>ISB</p>	<p>ISB</p>

9	Glenohumeral + scapulothoracic	<ul style="list-style-type: none"> • Abduction • Scaption • Forward flexion 	ISB	ISB
10	Glenohumeral	<ul style="list-style-type: none"> • Abduction/adduction • Forward flexion • Extension • Internal rotation with the arm at 90° of abduction • External rotation with the arm at 10° and 90° of abduction 	ISB	ISB
11	Glenohumeral	<ul style="list-style-type: none"> • Adduction in the scapular plane • Internal rotation behind the back • Horizontal adduction • Horizontal abduction at 30° and 60° scaption 	Developed	Developed CS for each motion

12	Glenohumeral + scapulothoracic	<ul style="list-style-type: none"> • Scapular-plane abduction 	<p>The origin of the humerus was located at the centroid of the head of the humerus. The origin of the scapula was defined as the midpoint of the line from the superior and inferior bony edges of the glenoid</p>	<p>The origin of the humerus was located at the centroid of the head of the humerus. The y-axis was defined as being parallel to the shaft of the humerus, and the z-axis was defined as a line through the intertubercular groove from the origin. The origin of the scapula was defined as the midpoint of the line from the superior and inferior bony edges of the glenoid, with the y-axis pointed superiorly and the z-axis pointed anteriorly</p>
13	Glenohumeral	<ul style="list-style-type: none"> • Scapular-plane abduction with elbow fully extended and externally rotated in the thumb-up position. • External rotation of shoulder with elbow flexed at 90° and shoulder abducted at 90°. 	<p>Following a previously reported method (Geomagic studio; Geomagic, USA, Morrisville, NC).</p>	<p>Following a previously reported method (Geomagic studio; Geomagic, USA, Morrisville, NC)</p>
14	Scapulothoracic	<ul style="list-style-type: none"> • Neutral • Full active forward elevation position. 	ISB	ISB
15	Scapulothoracic + acromioclavicular	<ul style="list-style-type: none"> • Neutral • Full active forward elevation position. 	ISB	ISB

16	Acromioclavicular	<ul style="list-style-type: none"> • 0° • Full abduction 	<p>The equator of the cut surface of the clavicle was compared with the full abduction model to analyze the rotation. The center of the cut surface of the clavicle was also compared with the full abduction model to analyze translation.</p>	Not used
17	Glenohumeral	<ul style="list-style-type: none"> • Scapular plane full abduction • Full axial rotation 	ISB	ISB
18	Glenohumeral	<ul style="list-style-type: none"> • Scapular plane full abduction • Full axial rotation 	ISB	ISB
19	Glenohumeral + Acromioclavicular	<ul style="list-style-type: none"> • Scapular-plane abduction with elbow fully extended and externally rotated in the thumb-up position. • Axial rotation with the elbow at 90° from 	ISB	ISB

20	Glenohumeral + Acromioclavicular	<ul style="list-style-type: none"> • Four planes of arm elevation (adduction, flexion, abduction, and extension), with the arm successively held in maximum internal, neutral, and maximum external axial rotation. • Activities of daily living (mimicking eating and hair combing, reaching with their hand the middle of the opposite side of their back, opposite axilla, and front and back pockets) • Sports activities (tennis forehand and backhand strokes with a tennis racket, ball throwing, hockey shooting with a hockey stick, and punching a bag). 	ISB	ISB
----	----------------------------------	---	-----	-----

21	Scapulothoracic	<ul style="list-style-type: none"> • Scapular plane elevation and lowering. 	<p>The humeral origin was placed at the centroid of the humeral head. The scapular origin was defined as the midpoint of the line connecting the most superior and inferior bony edges of the glenoid.</p>	<p>Anatomic coordinate systems of the humerus and the scapula. the humeral origin was placed at the centroid of the humeral head. The y- axis was parallel to the humeral shaft and the z-axis was defined as a line through the intertubercular groove from the origin. The scapular origin was defined as the midpoint of the line connecting the most superior and inferior bony edges of the glenoid, and the y- and z-axes were pointed superiorly and anteriorly, respectively</p>
22	Glenohumeral + scapulothoracic	<ul style="list-style-type: none"> • Scapular plane elevation. 	<p>The humeral origin was placed at the centroid of the humeral head. The scapular origin was defined as the midpoint of the line connecting the most superior and inferior bony edges of the glenoid.</p>	<p>Anatomic coordinate systems of the humerus and the scapula. the humeral origin was placed at the centroid of the humeral head. The y- axis was parallel to the humeral shaft and the z-axis was defined as a line through the intertubercular groove from the origin. The scapular origin was defined as the midpoint of the line connecting the most superior and inferior bony edges of the glenoid, and the y- and z-axes were pointed superiorly and anteriorly, respectively</p>

23	Acromioclavicular + sternoclavicular	<ul style="list-style-type: none"> Scapular plane elevation. 	ISB	ISB
24	Glenohumeral	<ul style="list-style-type: none"> Scapular plane elevation. 	<p>The humeral origin was placed at the centroid of the humeral head. The scapular origin was defined as the midpoint of the line connecting the most superior and inferior bony edges of the glenoid.</p>	<p>Anatomic coordinate systems of the humerus and the scapula. the humeral origin was placed at the centroid of the humeral head. The y- axis was parallel to the humeral shaft and the z-axis was defined as a line through the intertubercular groove from the origin. The scapular origin was defined as the midpoint of the line connecting the most superior and inferior bony edges of the glenoid, and the y- and z-axes were pointed superiorly and anteriorly, respectively</p>
25	Glenohumeral	<ul style="list-style-type: none"> Active external rotation at 90° of shoulder abduction. 	<p>Glenoid: the origin of the glenoid coordinate system is set at the center of gravity of the glenoid surface. Humerus: ISB</p>	<p>Glenoid: the z-axis was defined as the line normal to the glenoid plane, pointing laterally. The x-axis was defined as the line perpendicular to the z-axis and the glenoid longitudinal axis, which connects the superior and inferior poles of the glenoid, pointing forward. The y-axis was defined as the common line perpendicular to the glenoid x- and z-axes, pointing superiorly. The origin of the glenoid coordinate system was set at the center of gravity of the glenoid surface. Humerus: ISB</p>

26	Glenohumeral	<ul style="list-style-type: none"> • Scapular plane elevation • Propulsion • Sideways lean • Weight-relief raise 	ISB	ISB
27	Glenohumeral	<ul style="list-style-type: none"> • Abduction in the scapular plane. 	Superior bony edge and inferior glenoid edge	<p>The glenoid plane was defined to be parallel to a line from the superior bony edge to the inferior glenoid edge and including the line defining the perpendicular short axis of the glenoid. The glenoid center was defined as the midpoint of the line from the superior bony edge to the inferior glenoid edge</p>
28	Glenohumeral	<ul style="list-style-type: none"> • Flexion/extension, • Adduction/abduction, • External/internal rotation with the arm at side 	NA	Not used
29	Glenohumeral	<ul style="list-style-type: none"> • Flexion/extension, • Abduction/adduction • Internal/external rotation at 0° of abduction. 	NA	Not used

2.3.4 CT Scanning Use

Computed tomography has been used in various ways and for several reasons. The main three reasons are categorized into: understanding the etiology of diseases associated with the shoulder (12 studies), characterizing normal motion (11 studies), or improving surgical treatments (5 studies) (1 is 'other'). Table 2.4 summarises the “gap” in the literature each study proposed to address, and the study purpose and outcome measures. Computed tomography was used, along with another imaging modality (i.e., biplane fluoroscopy, x-ray, and motion capture) in 16 studies to characterize motion. Eleven of these 16 studies used biplane fluoroscopy imaging, three studies used x-ray scanning and two studies used tracking systems along with CT imaging. Thirteen studies used CT scanning alone, two of which used a 4DCT scanner. Detailed information about the imaging technique used in each study, CT scanner type and radiation dose are shown in Table 2.5. Twenty-two studies stated the type of CT scanner used and only four studies reported radiation dose.

Table 2.4: Studies Purpose and Outcome Measures			
Article #	Gap/Significance	Purpose	Outcome Measures
1	It is unclear what kind of motion takes place in the AC (acromioclavicular) joint when the Bell-van Riet test is performed.	To determine the motion pattern of the AC joint during adduction of the arm, with and without resisted superior elevation using 4-dimensional computed tomographic scanner.	AC joint width, anteroposterior translation, super-inferior translation and opening of the superior aspect of the joint of neutral, adduction, and loaded positions
2	Controversy still exists whether the clinical syndrome called 'minor anterior glenohumeral instability' can be validly termed as an instability.	To quantify in vivo the 3D translation of the humeral head on the glenoid and to determine the displacements between the articular surfaces at the contact area.	Values of the rotation angle, the direction vector, and the shift of the humeral motion on the glenoid from pose 1 to pose 2 of normal and pathological shoulders.
3	No studies have comprehensively examined isolated GH (glenohumeral) abduction (separate from ST abduction) in patients who have undergone repair for shoulder instability.	To compare the amount of GH abduction during arm abduction in the affected and unaffected shoulders of 3 groups of patients with shoulder instability: failed surgical stabilization, successful surgical stabilization, and unstable shoulder with no prior surgical intervention.	GH abduction for the normal and affected sides in the 0° -0°, 30° - 30°, and overhead positions.

4	Alternative approaches for reporting scapular motion limit the physiological meaning of the rotations as they are not described relative to an anatomical coordinate system and incorporate thoracic motion into their values.	1) To describe the use of this radiographic-based technique (rib-based thorax coordinate system) for measuring thorax motion and to assess the accuracy of this approach. 2) To present preliminary data on ST (scapulothoracic) motion using this new approach.	Misalignment of rib-based coordinate systems relative to the conventional thorax coordinate system (ISB). ST and humerothoracic motions were determined.
5	Accurately measuring in-vivo GH joint motion remains a challenging endeavor.	To measure in-vivo GH joint motion using a developed a technique for tracking the position of the humerus and scapula from biplane X-ray images based on their 3D shape and texture.	Superior/inferior humeral translation relative to the scapula during elevation, and anterior/posterior humeral translation relative to the scapula during external rotation in both the repaired and contralateral shoulders.
6	No study has accurately measured the position of the GH joint during an anterior dislocation involving an engaging Hill-Sachs lesion and a glenoid bone defect or the resulting locked position of the GH joint after an anterior dislocation.	To develop a method to assess the 3D locked position of the GH joint in 3 groups with RASI: patients with “normal” laxity, patients with hyperlaxity, and patients with epilepsy.	Average GH rotations and translations observed in the locked position.

7	<p>A previous in-vitro biomechanical study with cadaveric shoulders has suggested that the use of two peripheral fixation screws (versus the typical usage of four screws) does not compromise primary stability of the baseplate in the context of baseplate micromotion. However, whether the same is true when the center of rotation (COR) is lateralized has not been reported.</p>	<p>1) To develop shoulder specific rTSA (reverse total shoulder arthroplasty) finite element models capable of predicting impingement-free adduction ROM and baseplate micromotion under standardized loads. 2) To measure the effect of COR lateralization on impingement-free adduction ROM and baseplate micromotion, and 3) to measure the effect of using only two (superior/inferior) versus four fixation screws on baseplate micromotion at various COR lateralization distances.</p>	<p>Relationships between lateralization, adduction ROM, the number of fixation screws and micromotion of the baseplate (initial implant fixation) were characterized.</p>
8	<p>The coupled rotations of the scapula and clavicle have not yet been dynamically characterized during humeral elevation.</p>	<p>To quantify shoulder kinematics in cadaveric specimens during passive humeral elevation and compare the rotations of the scapula and clavicle as a function of humeral elevation were in 3 planes.</p>	<p>The scapular motion relative to the trunk or humeral elevation in the coronal, scapular, and sagittal planes. The clavicular motion relative to the trunk for humeral elevation in the coronal, scapular, and sagittal planes. GH to ST ratios.</p>
9	<p>The relative effect of the plane of elevation on GH translation and scapulohumeral rhythm remains unknown.</p>	<p>To measure 3D GH translations and rotations during abduction, scaption, and forward flexion in healthy subjects.</p>	<p>GH rotation and translation in healthy individuals during motion in three arm elevation planes. Scapulohumeral rhythm for motions performed.</p>

<p>10</p>	<p>No study has investigated how different configurations of lateralization or neck-shaft angle (NSA) affect shoulder ROM in different scapular morphologies.</p>	<p>To evaluate the effects of lateralization of the COR and NSA on shoulder ROM after reverse shoulder arthroplasty (RSA) in patients with different scapular morphologies.</p>	<p>Effect of different configurations of lateralization and NSA on ROM.</p>
<p>11</p>	<p>No study has assessed the combined effect of change in humeral version and NSA on shoulder ROM and impingement in rTSA.</p>	<p>To evaluate whether a change in humeral NSA and retroversion prevents impingement between humeral socket and scapular neck in rTSA and 2) to investigate the effect of change in neck–shaft angle and retroversion on adduction, internal rotation behind the back and horizontal adduction and horizontal abduction at 30° and 60° scaption using 3D-simulations.</p>	<p>ROM in terms of horizontal adduction, and horizontal abduction at 30° and 60° scaption, adduction in the scapular plane, internal rotation at the back for different NSA of 135°, 145° and 155° and retroversion angles of 0°, 10°, 20°, 30° and 40°.</p>
<p>12</p>	<p>Alteration in shoulder kinematics has been suggested as one cause of symptoms in shoulders with rotator cuff tears (RCTs). However, only a few studies comparing symptomatic and asymptomatic RCTs using kinematic analysis have been performed.</p>	<p>To compare 3D scapular and GH kinematics during scapular-plane abduction between symptomatic or asymptomatic RCTs and healthy shoulders using 3D/2D registration techniques with biplane fluoroscopic images.</p>	<p>Scapular angular values (including scapulohumeral rhythm) and humeral kinematics relative to scapula.</p>

13	The in vivo dynamics of the 3D movement of the humerus relative to the glenoid have not yet been fully described.	To measure and analyze changes in GH translation in patients with shoulder dislocation and compare these changes with healthy shoulder.	Superior/inferior and anterior/posterior translations for GH for both shoulders during motions.
14	Several studies have identified factors causing scapular dyskinesis. However, the relationship between scapular fracture and scapular dyskinesis has not been established.	1) To assess and quantify dynamic scapular dyskinesis using a 3D motion analysis technique with a computerized simulation system; and 2) to determine whether scapular or clavicular fracture can cause scapular dyskinesis.	3D translational and rotation movement of the scapula in scapular and clavicular fracture patients.
15	There are few reports of 3D kinematics including scapular dyskinesis in AC dislocation patients treated with a hook plate.	To analyze the 3D kinematics of the scapula after hook-plated AC dislocation without CC ligament repair in vivo to evaluate scapular dyskinesis and to digitize the motion of the hook plate in the subacromial space.	3D rotational and translation motion of scapula. 3D translation and angulation of hook plate.
16	No study has analyzed the real motion of the AC joint after hook plate fixation.	To analyze the real motion of the AC joint after hook plate fixation by describing the change in 3D motion of the distal clavicle compared with the normal (without hook plate fixation) shoulder.	Translational and rotational motions of the distal clavicle during abduction. The angle between the humeral shaft in the neutral position and full abduction.

<p>17</p>	<p>There have been no previously published reports that approximate 30–35° of the external rotation of the humerus relative to the scapula occurring during active abduction, as measured by 3D-to-2D model-to-image registration techniques.</p>	<p>To evaluate the kinematics of healthy shoulders during dynamic full axial rotation and scapular plane full abduction using 3D-to-2D model-to-image registration techniques.</p>	<p>3D translation of the humerus relative to the scapula during dynamic scapular plane full abduction and full axial rotation.</p>
<p>18</p>	<p>Few studies have evaluated the external rotation of the humerus relative to the scapula in RCTs during active abduction using 3D-to-2D model-to-image registration techniques.</p>	<p>To evaluate the kinematics of RCTs during dynamic scapular plane full abduction and full axial rotation using 3D-to-2D model-to-image registration techniques.</p>	<p>3D translation of the humerus relative to the scapula during dynamic scapular plane full abduction and full axial rotation.</p>
<p>19</p>	<p>No previous studies on the acromiohumeral distance (AHD) in shoulders with large-to-massive full-thickness RCTs.</p>	<p>To use 3D-to-2D model-to-image registration techniques to measure the AHD in RCTs and healthy shoulders during dynamic scapular plane full abduction and full axial rotation, with the goal of determining how the AHD patterns differed between RCTs and healthy shoulders.</p>	<p>AHD distance as a function of humeral abduction angle and glenohumeral external rotation angle of control and RCTs groups.</p>

<p>20</p>	<p>Combination of biplane fluoroscopy and CT-scan provides accurate 3D measurement of the AHD during dynamic tasks. However, participants performed only two and six trials in previous experiments to respect the recommended radiation exposure per year.</p>	<p>To evaluate a technique for measuring the AHD in 3D and the distances between all bony parts of the humeral head and the acromion during dynamic tasks in the entire shoulder range of motion, activities of daily living, and sports activities.</p>	<p>AHD distance and bone distance maps for performed motions.</p>
<p>21</p>	<p>It remains controversial whether scapular kinematics are symmetric.</p>	<p>To compare 3D scapular kinematics of dominant and nondominant shoulders during dynamic scapular plane elevation and lowering using 3D - 2D model registration techniques.</p>	<p>Scapular angular values during elevation and lowering and scapulohumeral rhythm of dominant and nondominant shoulders.</p>
<p>22</p>	<p>No previous studies reported external rotation of the humerus using 3D/2D model image registration techniques.</p>	<p>To measure superior/inferior translation and external rotation of the humerus relative to the scapula during dynamic scapular plane elevation.</p>	<p>Superior/Inferior translation of the humerus. External/Internal rotation of the humerus.</p>

<p>23</p>	<p>Several groups have reported shoulder kinematics using model-image registration, but no attempt has been made so far to analyze clavicle kinematics.</p>	<p>To evaluate side-to-side differences in the 3D clavicle kinematics during dynamic scapular plane elevation in normal shoulders using model-image registration techniques.</p>	<p>Protraction, elevation, and forward rotation of the clavicle as a function of humeral elevation angle of dominant and non-dominant.</p>
<p>24</p>	<p>Studies evaluating glenohumeral kinematics using model-image registration have employed different methods to calculate humeral translations relative to scapula. Differences between kinematic outputs of these various approaches has not been compared.</p>	<p>To compare GH translations calculated using the following approaches: 1) relative position of the origins of the humeral and scapular models 2) contact points of the two models and 3) relative positions based upon the calculated glenohumeral center of rotation.</p>	<p>GH translations measured and compared by the three methods.</p>
<p>25</p>	<p>Although GH instability is common, the mechanism of instability remains unclear.</p>	<p>To quantitatively evaluate humeral head translation during active external rotation with abduction in patients with GH instability by use of 4-dimensional computed tomography scans.</p>	<p>Translation of humeral head of intact and affected shoulder throughout the motion</p>

<p>26</p>	<p>Previous work relied on either marker-based motion capture for kinematic measures, or ultrasound imaging for arthrokinematics measures, which are 2D and acquired in statically held positions.</p>	<p>To use a fluoroscopy-based approach to accurately quantify GH kinematics during manual wheelchair use and compare tasks for a subset of parameters theorized to be associated with mechanical impingement.</p>	<p>Mean and maximum GH internal/external rotation, superior/inferior position, and anterior/posterior position were determined for each participant for a given task.</p>
<p>27</p>	<p>It is difficult to measure dynamic GH translation, and reports of quantitative 3D measurement of shoulder motion during clinically relevant motions are only beginning to appear.</p>	<p>To investigate GH translation in vivo during active shoulder abduction in the scapular plane.</p>	<p>Humeral translation relative to the glenoid center in the superior/inferior direction.</p>
<p>28</p>	<p>There are no guidelines for the ideal configuration of both humeral and glenoid positioning to obtain the best functional results in elevation and rotation.</p>	<p>To evaluate the influence of humeral neck shaft angle and glenoid lateralization on ROM as well as impingement in RSA design.</p>	<p>Influence of humeral inclination and glenoid lateralization on ROM of motions performed.</p>

<p>29</p>	<p>Numerous strategies have been described to reduce mechanical abutment on the scapular neck. However, whether these strategies can also reduce friction-type scapular notching has not yet been investigated.</p>	<p>To evaluate the effect of the size of glenoid component and type of glenosphere on impingement-free ROM in extension and internal and external rotation, in a virtual RSA model, and 2) to determine the optimal configuration to reduce the incidence of inferior scapular impingement.</p>	<p>Effect of glenosphere type and size on impingement-free ROM and COR offset position.</p>
------------------	---	---	---

Table 2.5: CT Scanner Information			
Article #	Imaging Technique	Scanner Type	Radiation Dose
1	4DCT	Aquilion One (Toshiba Medical Systems, Otawarashi, Tochigi-ken, Japan)	2.5 to 3.5 mSv per scan
2	CT	HiSpeed CT/I, General Electric)	Not stated
3	CT	Not stated	Mean radiation 1,190.4 mGy-cm
4	CT + biplane fluoroscopy	Not stated	Not stated
5	CT + biplane fluoroscopy	Not stated	Not stated
6	CT	Not stated	Not stated
7	CT	Ingenuity CT (Philips Healthcare, Amsterdam, Netherlands)	Not stated
8	CT + electromagnetic tracking system	Not stated	Not stated
9	CT + biplane fluoroscopy	Aquilion 64, Toshiba America Medical Systems, Tustin, California	Not stated
10	CT	Not stated	Not stated
11	CT	Siemens Somatom Plus S scanner (Siemens Medical System, Erlangen, Germany)	Not stated

12	CT + biplane fluoroscopy	Aquilion One; Toshiba	Not stated
13	CT + biplane fluoroscopy	SOMATOM Sensation 16; Siemens Medical Solutions, Malvern, PA	Not stated
14	CT	LightSpeed pro64; Siemens, Erlangen, Germany	Not stated
15	CT	LightSpeed pro64; Siemens, Erlangen, Germany	Not stated
16	CT	Optima CT 660 scanner (GE Healthcare Japan Corp, Hino-shi, Tokyo, Japan)	Not stated
17	CT + x-ray	Aquilion, Toshiba, Tochigi, Japan	Not stated
18	CT + x-ray	Aquilion, Toshiba, Tochigi, Japan	Not stated
19	CT + x-ray	Aquilion, Toshiba, Japan	Not stated
20	CT+ optoelectronic cameras	General Electric Medical System, Milwaukee, USA	Not stated
21	CT + biplane fluoroscopy	Infinix Activ, Toshiba, Tochigi, Japan	Not stated
22	CT + biplane fluoroscopy	Infinix Activ	Not stated
23	CT + biplane fluoroscopy	Not stated	Not stated

24	CT + biplane fluoroscopy	Infinix Activ, Toshiba, Tochigi, Japan	Not stated
25	4DCT	Aquilion ONE; Canon Medical Systems, Otawara, Japan	Was controlled to not exceed 10 mSv. The value was close to the average effective dose of normal chest CT scans (7 mSv).
26	CT + biplane fluoroscopy	128-slice SOMATOM Definition Edge; Siemens Healthcare	Total effective dose from the CT scan and fluoroscopy trials was calculated to be 6.8 mSv and 1.0 mSv
27	CT + biplane fluoroscopy	LightSpeed Plus, GE Yokokawa Medical System	Not stated
28	CT	Not stated	Not stated
29	CT	Not stated	Not stated

2.3.5 Motion Description

The examined papers used different perspectives to report the shoulder motions investigated (Table 2.6). The first column of Table 2.6 describes the motions examined in each study according to the authors definition. The second column attempts to employ standard terminology and reclassifies each motion as described in the paper according to standard terms (scaption, abduction/adduction, internal/external rotations, and flexion/extension). Table 2.6 shows several instances where the same motion examined is described using different terminology when comparing papers. For example, Fung et al. described abduction as “elevation in the coronal plane” (Fung et al., 2001), but Giphart et al., described the same motion as “abduction” (Giphart et al., 2013). Similarly, Kim et al used the terms “neutral” and “forward elevation” (E. Kim et al., 2017; Kim et al., 2018) which, from the study images, appear to be 0° and maximum flexion. Once the motions had been re-mapped, the type of motion examined in each study was categorized as planar (Table 2.7) or combined motion (Table 2.8) in reference to the glenohumeral joint. Fifteen studies examined planar motions only, nine studies examined combined motions, four studies examined a combination of planar and combined motions. In one study, the motions were specific to the population group and did not fit under any of the categories (Mozingo et al., 2019). Also, the reported range of motion across the studies was different (Table 2.9). Twelve papers reported the motions within defined degrees of freedom (extension 0° to 120°), whereas 17 papers reported the motions to “maximum” or “full” range of motion. Thirteen papers reported forearm rotation (palm position) and elbow position when examining motions like abduction, scaption and flexion/extension. Only five studies presented pictures of the motion despite the ambiguous description of motions.

Table 2.6: Description of motion examined		
Article #	Described Motion	Proposed Nomenclature of Described Motion
1	Arm elevated to 90° in the sagittal plane with adduction (loaded and unloaded)	Adduction of the shoulder while 90° in flexion (loaded and unloaded)
2	(1) 90° abduction and 90° external rotation, (2) the late cocking position with the arm maximally externally rotated was assessed on an individual basis	(1) 90° abduction and 90° external rotation, (2) ~90° abduction with maximum extension and external rotation
3	(1) 0° of abduction and 0° of external rotation, (2) 30° of abduction and 30° of external rotation, (3) overhead position - the highest degree of abduction and external rotation that they could attain with their palms facing downward	(1) 0° of abduction and 0° of external rotation, (2) 30° of abduction and 30° of external rotation, (3) Maximum abduction and external rotation with 90° elbow flexion
4	Coronal-plane abduction, beginning with the subject's arm at his/her side and ending at approximately 120° of humerothoracic abduction	Abduction from 0° to 120°
5	(1) Coronal-plane elevation from a resting position (arm at the subject's side) to approximately 120° of humerothoracic elevation, (2) external rotation with the arm adducted from a resting position of full internal rotation to maximal external rotation. Each task was performed with the subject holding a 3-pound hand weight.	(1) Abduction from 0° to 120° (3lbs loaded) (2) external rotation from maximum internal rotation to maximum external rotation (3lbs loaded)
6	Mean locked position was of 12° of abduction, 90° of external rotation, and 21° of extension	Mean locked position was of 12° of abduction, 90° of external rotation, and 21° of extension
7	Adduction	Adduction

8	Raised to maximum elevation in the (1) coronal plane, (2) scapular plane, (3) sagittal plane	(1) Abduction from 0° to maximum, (2) scaption from 0° to maximum (3) flexion from 0° to maximum
9	Range of motion: (1) scaption, (2) forward flexion, (3) abduction	(1) Scaption from 0° to maximum (2) flexion from 0° to maximum, (3) abduction from 0° to maximum
10	ROM of (1) Abduction, (2) adduction, (3) forward flexion, (4) extension, (5) internal rotation with the arm at 90° of abduction, (6) external rotation with the arm at 10° of abduction, (7) external rotation with the arm at 90° of abduction	(1) Abduction, (2) adduction, (3) flexion, (4) extension, (5) internal rotation with the arm at 90° of abduction, (6) external rotation with the arm at 10° of abduction, (7) external rotation with the arm at 90° of abduction
11	ROM in terms of horizontal adduction, and horizontal abduction at 30° and 60° scaption, adduction in the scapular plane, internal rotation at the back	(1) Abduction/adduction from 0° to maximum at 90° flexion, 30° scaption, and 60° scaption, (2) maximum internal rotation with arm behind back
12	For scapular-plane abduction, the arm was placed at the side and lifted to maximum elevation with the arm rotated externally	Scaption from 0° to maximum with maximum external rotation
13	(1) Scapular plane abduction with elbow fully extended and externally rotated in the thumb-up position, (2) external rotation of shoulder with elbow flexed at 90 and arm abducted at 90.	(1) Scaption with elbow fully extended and externally rotated in the thumb-up position, (2) external rotation with 90° abduction and 90° forearm flexion
14	(1) Neutral, (2) full active forward elevation position	(1) 0° flexion, (2) maximum flexion
15	(1) Neutral, (2) full active forward elevation position	(1) 0° flexion, (2) maximum flexion
16	(1) Zero degree, (2) full abduction	(1) 0° abduction, (2) maximum abduction

17	(1) Scapular plane full abduction, (2) full axial rotation in the adducted position with the elbow at 90° from full internal rotation to full external rotation.	(1) Maximum scaption, (2) maximum internal rotation to maximum external rotation at 0° abduction with 90° forearm flexion
18	(1) Scapular plane full abduction, (2) full axial rotation in the adducted position with the elbow at 90° from full internal rotation to full external rotation.	(1) Maximum scaption, (2) maximum internal rotation to maximum external rotation at 0° abduction with 90° forearm flexion
19	(1) Scapular plane full abduction with elbow fully extended and externally rotated in the thumb-up position, (2) full axial rotation in the adducted position with the elbow at 90° from full internal rotation to full external rotation.	(1) Maximum scaption with elbow fully extended and externally rotated in the thumb-up position, (2) maximum internal rotation to maximum external rotation at 0° abduction with 90° forearm flexion
20	Four planes of arm elevation (adduction, flexion, abduction, and extension). Three elevations were performed in each plane of elevation with the arm successively held in maximum internal, neutral, and maximum external axial rotation. Activities of daily living, and sports activities	(1-3) Adduction from 0° to maximum, (4-6) flexion from 0° to maximum, (7-9) abduction from 0° to maximum, (10-12) extension from 0° to maximum. Each with maximum internal rotation, no rotation, and maximum external rotation
21	Elevation and lowering in the scapular plane were performed between the arm at side and maximum elevation positions with the elbow fully extended and the arm externally rotated.	Scaption from 0° to maximum and maximum to 0° with maximum external rotation
22	Elevation in the scapular plane was performed from the arm at the side to maximum elevation with the elbow fully extended and the arm externally rotated.	Scaption from 0° to maximum with maximum external rotation

23	Scapular plane abduction was performed between arm at side and maximum elevation with the elbow fully extended and the arm externally rotated.	Scaption from 0° to maximum with maximum external rotation
24	Elevation in the scapular plane was performed between arm at side and maximum elevation positions with the elbow fully extended and the arm externally rotated	Scaption from 0° to maximum and maximum to 0° with maximum external rotation
25	At 90° of shoulder abduction, rotate the shoulder externally from the neutrally rotated position to the maximum externally rotated position	0° to maximum external rotation at 90° abduction
26	Scapular plane elevation (scaption), MWC propulsion, and two pressure relief maneuvers which included a sideways lean and weight-relief raise	Scaption, MWC propulsion, and two pressure relief maneuvers which included a sideways lean and weight-relief raise
27	Active abduction in neutral rotation from 0-150° in the plane of the scapula.	Scaption from 0° to 150°
28	Flexion/extension, adduction/abduction, external/internal rotation with the arm at side	Flexion/extension, abduction/adduction, and internal/external rotation at 0° of abduction.
29	Flexion/extension, abduction/adduction, and internal/external rotation at 0° of abduction.	Flexion/extension, abduction/adduction, and internal/external rotation at 0° of abduction.

Table 2.7: Planar Glenohumeral Motions Examined							
Article #	Scaption (SCAP)	Abduction (ABD)	Adduction (ADD)	Flexion (FLEX)	Extension (EXT)	External Rotation (ER)	Internal Rotation (IR)
1				x			
2							
3							
4		x					
5		x				x	
6							
7			x				
8	x	x		x			
9	x	x		x			
10		x	x	x	x		
11		x					
12							
13	x						
14				x			
15				x			
16		x					
17	x					x	
18	x					x	
19	x					x	

20		x	x	x	x		
21							
22							
23							
24							
25							
26							
27	x						
28		x	x	x	x	x	x
29		x	x	x	x	x	x

Table 2.8: Combined Glenohumeral Motions Examined

Article #	SCAP & ER	ABD & IR	ABD & ER	ABD, ER & EXT	ABD & FLEX	ADD & FLEX	ADD & IR	ADD & IR	FLEX & IR	FLEX & ER	EXT & IR	EXT & ER	IR w/ Arm Behind Back
1													
2			x	x									
3			x										
4													
5													
6				x									
7													
8													
9													
10		x	x										
11					x	x							x
12	x												
13		x											

14													
15													
16													
17													
18													
19													
20		x	x				x	x	x	x	x	x	
21	x												
22	x												
23	x												
24	x												
25			x										
26													
27													
28													
29													

Table 2.9: Range of Motion Reporting				
Article #	Picture	Maximum	ROM (Range of Motion)	Motion of palm (Internal/External Rotation)
1	x		x	
2			x	x
3			x	x
4			x	
5			x	
6			x	x
7			x	
8		x		
9		x		
10			x	x
11		x		
12		x		x
13			x	x
14	x	x		
15	x	x		
16		x		
17		x		
18		x		
19		x		x
20		x		x
21		x		x
22		x		x
23		x		x
24		x		x
25	x	x		x
26	x	x		

27			X	
28			X	
29			X	

2.4 Discussion

The objective of this study was to examine the extent and range of methods employing CT imaging to measure shoulder kinematics in research studies. Kinematic knowledge is essential for accurate diagnosis and surgical treatment of joint diseases. The results of this structured review indicate that CT has been used extensively to evaluate shoulder motion under normal and abnormal conditions. However, after examining these studies and comparing their methodologies, inconsistencies exist and there are significant gaps that need to be addressed.

Most of the studies examined in this review were conducted in Japan. More than half of the examined patients/participants were adult males with a mean age of ≥ 40 years. However, the age group of two studies was not reported, and the sex of 125 participants of the overall 397 participants in this review was not stated. This poses a problem to the generalizability of the findings, as females have a greater magnitude of shoulder motion than males (Barnes et al., 2001). Matsuki et al. (Matsuki et al., 2012) excluded females due to ionizing radiation exposure, but the radiation dose was not reported. Other studies failed to explain why females might have not been examined.

When examining the articles included in this review, 40% of the studies evaluated healthy participants' shoulder kinematics. Eight studies compared their results to the contralateral shoulder and five studies compared their results to a control group. This is an essential part of research design as it allows researchers to minimize the effect of dependent variables. Examining the contralateral shoulder reduces the sample size of a study and the variability of individual differences or noise as the results have been compared within the same person. However, it is important to note that from a statistical standpoint, the right and left shoulder of the same individual is not an independent sample (the right and left arm of the same individual is more similar than

between two different individuals), therefore, careful statistical consideration is necessary. Scanning both the right and left upper limb exposes the participant to more ionizing radiation. It would be interesting to investigate if a reduced radiation dose can be achieved by scanning both shoulders simultaneously.

Overall, the glenohumeral joint was the most studied, as it was investigated in 22 studies, followed by the scapulothoracic joint that was investigated eight times. Since the glenohumeral joint is the most dislocated joint of the human body, accounting for up to 45% of dislocations (Chang et al., 2020), and is susceptible to a variety of injuries, it has been the focus of many researchers. It has been evaluated (using CT) to measure shoulder kinematics in healthy participants (Dal Maso et al., 2016; Elwell et al., 2017; Fung et al., 2001; Giphart et al., 2013; Jeon et al., 2016; Kozono et al., 2017; Matsuki et al., 2016, 2012; Nishinaka et al., 2008), patients with instability (Baeyens et al., 2001; Bakshi et al., 2016; D. S. Kim et al., 2017; Matsumura et al., 2019), rotator cuff tears (Bey et al., 2008; Kijima et al., 2015; Kozono et al., 2018a, 2018b) and osteoarthritis (Läderrmann et al., 2019; Werner et al., 2018, 2017). The normal motion of the sternoclavicular joint has not been assessed using CT but has been used as a landmark to understand the motion of other joints (Fung et al., 2001; Matsuki et al., 2014). Researchers should pay more attention to the scapulothoracic, acromioclavicular and sternoclavicular joints. These joints should be studied and evaluated in both healthy participants and those with different health conditions to better understand and develop treatment plans for patients to restore range of motion after an injury.

Shoulder kinematics has been evaluated using different measuring systems and imaging techniques. Although some studies did not use coordinate systems to measure range of motion (instead, extracted measurements from 2D CT images), 14 studies used the framework

recommended by the ISB to develop a coordinate system (Lo and Xie, 2012). The ISB coordinate system and an advanced framework for measuring upper extremity kinematics (Gopura et al., 2016) was developed by the International Shoulder Group to encourage and facilitate feedback and discussion among clinicians and researchers (Lo and Xie, 2012). Thus, researchers are encouraged to use this framework to improve communication among researchers and clinicians. Nonetheless, this standardized system only partially addresses the intra-subject variability, which is known to emerge from four different factors. These factors include non-standardized protocols, different data processing methods, incorrect positioning of the center and the actual inconsistency in movements (Williams et al., 2006).

Computed tomography has been used to measure shoulder kinematics in various ways and for different reasons. 3DCT and 3DCT with biplane fluoroscopy are the two primary imaging techniques that have been equally used to understand shoulder motion under different conditions. Mostly, it has been used to understand abnormal and normal shoulder kinematics. The majority of the studies reviewed failed to report participants' exposure to radiation dose. Researchers must communicate the effective radiation dose to minimize, monitor and raise awareness of patient dose. In addition, this will help the scientific community develop a standardized radiation exposure index for different imaging modalities, including computed tomography.

There were many discrepancies in the reporting of the examined motions. Different authors used different perspectives and planes to report similar motions, which contributes to confusion and misunderstanding of the actual examined motion. Also, the complexity of motions (one vs. multiple motions in one movement) is different across the studies and the description of the range of motion was ambiguous, as some studies did not report the degree in which the range of motion was performed. Moreover, there were inconsistencies in reporting forearm rotation (palm position)

and elbow position when examining motions like abduction, scaption and flexion/extension. This is important because it affects shoulder movement and motion analysis, especially if the publication does not provide images of the movement. Researchers within the field faced difficulties in understanding and differentiating between motions. With the current situation, it is difficult for researchers and clinicians to compare and develop standardized protocols and indexes for future studies. Thus, consistent motion reporting using the standard range of motion rather than describing the planes of the motions should be adopted. Often, it is not only the lack of consistent language used in individual studies, but also the complete omission of data that makes it difficult to compare or contrast findings between studies (if it is not clear they are even examining the same thing). Future studies should also include photos of the movement and report the palm and elbow position to better understand and evaluate the kinematics of the shoulder joints. This will potentially help develop treatment plans for patients to restore range of motion after an injury.

2.5 Limitations

This review has several limitations. First, the review focuses only on the CT imaging technique and its use to evaluate shoulder kinematics, yet shoulder kinematics has been measured using other techniques, including motion capture analysis, MRI and 3DCT with and without bi-plane fluoroscopy. Another limitation is that only two databases were used through the literature search (Embase and PubMed), although these databases are comprehensive and inclusive of most of the research papers. The authors excluded one article which met the inclusion criteria but included children participants. The authors also did not systematically or critically evaluate the articles themselves or comment on the use of cadavers in comparison to living participants.

2.6 Conclusion

The shoulder is a complex structure that enables a wide range of motion and provides structural support and maneuverability to perform daily activities and sports. Based on the results of this review, participants of published studies are predominantly males and radiation dose has not been reported in most of the studies. In addition, researchers should pay more attention to the scapulothoracic, acromioclavicular and sternoclavicular joints. Moreover, researchers are encouraged to provide a clear description, along with pictures, of the motions being examined. This makes it easier for other researchers and clinicians to compare and develop standardized protocols. Researchers are also encouraged to use ISB recommendations to improve communication among researchers and clinicians and increase validity and reliability. This will potentially reduce variation in care provided, improve care coordination, and modify care to evidence-based practice.

This review shows that 3DCT and 3DCT with biplane fluoroscopy are the two primary imaging techniques that have been equally used in the literature. Recent studies have started to use 4DCT to assess the glenohumeral joint (Matsumura et al., 2019), scapulothoracic joint (Bell et al., 2015), acromioclavicular (Alta et al., 2012) and sternoclavicular joint (Hislop-Jambrich et al., 2016) of the shoulder. Now that the use of CT imaging approaches to measure shoulder biomechanics has been examined, the findings of this review will be utilized to inform the subsequent study (Chapter 3), which will employ 4DCT imaging to measure GH contact mechanics. In the next study, a clear description of the motion being tested will be provided and dose and scanner type will be listed.

Four-dimensional computed tomography has been used to quantify glenohumeral translation once in the literature during active external rotation with the shoulder abducted (51). However, the study did not assess the internal rotation to back motion, which as discussed earlier, is a significant motion in activities of daily living and its contact mechanics is yet to be measured. Therefore, the contact mechanics of this motion will be assessed in this thesis, and the reliability of the technique will be examined.

2.7 References

- Alta, T.D., Bell, S.N., Troupis, J.M., Coghlan, J.A., Miller, D., 2012. The New 4-Dimensional Computed Tomographic Scanner Allows Dynamic Visualization and Measurement of Normal Acromioclavicular Joint Motion in an Unloaded and Loaded Condition. *Journal of Computer Assisted Tomography* 36, 749–754. <https://doi.org/10.1097/RCT.0b013e31826dbc50>
- Baeyens, J.P., Van Roy, P., De Schepper, A., Declercq, G., Clarijs, J.P., 2001. Glenohumeral joint kinematics related to minor anterior instability of the shoulder at the end of the late preparatory phase of throwing. *Clin Biomech (Bristol, Avon)* 16, 752–757. [https://doi.org/10.1016/s0268-0033\(01\)00068-7](https://doi.org/10.1016/s0268-0033(01)00068-7)
- Bakshi, N.K., Jameel, O.F., Merrill, Z.F., Debski, R.E., Sekiya, J.K., 2016. The Influence of Surgical Stabilization on Glenohumeral Abduction Using 3-Dimensional Computed Tomography in Patients With Shoulder Instability. *Arthroscopy* 32, 1495–1501. <https://doi.org/10.1016/j.arthro.2016.01.021>
- Barnes, C.J., Van Steyn, S.J., Fischer, R.A., 2001. The effects of age, sex, and shoulder dominance on range of motion of the shoulder. *Journal of Shoulder and Elbow Surgery* 10, 242–246. <https://doi.org/10.1067/mse.2001.115270>
- Baumer, T.G., Giles, J.W., Drake, A., Zauel, R., Bey, M.J., 2016. Measuring Three-Dimensional Thorax Motion Via Biplane Radiographic Imaging: Technique and Preliminary Results. *J Biomech Eng* 138. <https://doi.org/10.1115/1.4032058>
- Bell, S.N., Troupis, J.M., Miller, D., Alta, T.D., Coghlan, J.A., Wijeratna, M.D., 2015. Four-dimensional computed tomography scans facilitate preoperative planning in snapping scapula syndrome. *J Shoulder Elbow Surg* 24, e83-90. <https://doi.org/10.1016/j.jse.2014.09.020>
- Bey, M.J., Kline, S.K., Zauel, R., Lock, T.R., Kolowich, P.A., 2008. Measuring dynamic in-vivo glenohumeral joint kinematics: technique and preliminary results. *J Biomech* 41, 711–714. <https://doi.org/10.1016/j.jbiomech.2007.09.029>
- Chang, L.-R., Anand, P., Varacallo, M., 2020. *Anatomy, Shoulder and Upper Limb, Glenohumeral Joint*, StatPearls [Internet]. StatPearls Publishing.
- Clément, J., Ménard, J., Raison, M., Dumais, J., Dubois, L., Rouleau, D.M., 2017. Three-dimensional analysis of the locked position in patients with recurrent shoulder instability. *J Shoulder Elbow Surg* 26, 536–543. <https://doi.org/10.1016/j.jse.2016.07.031>
- Dal Maso, F., Blache, Y., Raison, M., Lundberg, A., Begon, M., 2016. Glenohumeral joint kinematics measured by intracortical pins, reflective markers, and computed tomography: A novel technique to assess acromiohumeral distance. *J Electromyogr Kinesiol* 29, 4–11. <https://doi.org/10.1016/j.jelekin.2015.07.008>
- Elwell, J., Choi, J., Willing, R., 2017. Quantifying the competing relationship between adduction range of motion and baseplate micromotion with lateralization of reverse total shoulder arthroplasty. *J Biomech* 52, 24–30. <https://doi.org/10.1016/j.jbiomech.2016.11.053>
- Fung, M., Kato, S., Barrance, P.J., Elias, J.J., McFarland, E.G., Nobuhara, K., Chao, E.Y., 2001. Scapular and clavicular kinematics during humeral elevation: a study with cadavers. *J Shoulder Elbow Surg* 10, 278–285. <https://doi.org/10.1067/mse.2001.114496>

- Gielen, C.C.A.M., van Bolhuis, B.M., Theeuwes, M., 1995. On the control of biologically and kinematically redundant manipulators. *Human Movement Science* 14, 487–509. [https://doi.org/10.1016/0167-9457\(95\)00025-X](https://doi.org/10.1016/0167-9457(95)00025-X)
- Giphart, J.E., Brunkhorst, J.P., Horn, N.H., Shelburne, K.B., Torry, M.R., Millett, P.J., 2013. Effect of plane of arm elevation on glenohumeral kinematics: a normative biplane fluoroscopy study. *J Bone Joint Surg Am* 95, 238–245. <https://doi.org/10.2106/JBJS.J.01875>
- Gopura, R.A.R.C., Bandara, D.S.V., Kiguchi, K., Mann, G.K.I., 2016. Developments in hardware systems of active upper-limb exoskeleton robots: A review. *Robotics and Autonomous Systems* 75, 203–220. <https://doi.org/10.1016/j.robot.2015.10.001>
- Hislop-Jambrich, J., Troupis, J., Moaveni, A., 2016. The Use of a Dynamic 4-Dimensional Computed Tomography Scan in the Diagnosis of Atraumatic Posterior Sternoclavicular Joint Instability. *Journal of Computer Assisted Tomography* 40, 576–577. <https://doi.org/10.1097/RCT.0000000000000410>
- Jeon, B.-K., Panchal, K.A., Ji, J.-H., Xin, Y.-Z., Park, S.-R., Kim, J.-H., Yang, S.-J., 2016. Combined effect of change in humeral neck-shaft angle and retroversion on shoulder range of motion in reverse total shoulder arthroplasty - A simulation study. *Clin Biomech (Bristol, Avon)* 31, 12–19. <https://doi.org/10.1016/j.clinbiomech.2015.06.022>
- Kijima, T., Matsuki, K., Ochiai, N., Yamaguchi, T., Sasaki, Yu, Hashimoto, E., Sasaki, Yasuhito, Yamazaki, H., Kenmoku, T., Yamaguchi, S., Masuda, Y., Umekita, H., Banks, S.A., Takahashi, K., 2015. In vivo 3-dimensional analysis of scapular and glenohumeral kinematics: comparison of symptomatic or asymptomatic shoulders with rotator cuff tears and healthy shoulders. *J Shoulder Elbow Surg* 24, 1817–1826. <https://doi.org/10.1016/j.jse.2015.06.003>
- Kim, D.S., Lee, B., Banks, S.A., Hong, K., Jang, Y.H., 2017. Comparison of dynamics in 3D glenohumeral position between primary dislocated shoulders and contralateral healthy shoulders. *J Orthop* 14, 195–200. <https://doi.org/10.1016/j.jor.2016.12.014>
- Kim, E., Lee, S., Jeong, H.-J., Park, J.H., Park, S.-J., Lee, J., Kim, W., Park, H.J., Lee, S.Y., Murase, T., Sugamoto, K., Ikemoto, S., 2018. Three-dimensional scapular dyskinesis in hook-plated acromioclavicular dislocation including hook motion. *J Shoulder Elbow Surg* 27, 1117–1124. <https://doi.org/10.1016/j.jse.2017.12.019>
- Kim, E., Park, J.H., Han, B.-R., Park, H.J., Lee, S.Y., Murase, T., Sugamoto, K., Ikemoto, S., Park, S.-J., 2017. In Vivo Analysis of Three-Dimensional Dynamic Scapular Dyskinesis in Scapular or Clavicular Fractures. *Acta Med. Okayama* 71, 151–159. <https://doi.org/10.18926/AMO/54984>
- Kim, Y.S., Yoo, Y.-S., Jang, S.W., Nair, A.V., Jin, H., Song, H.-S., 2015. In vivo analysis of acromioclavicular joint motion after hook plate fixation using three-dimensional computed tomography. *J Shoulder Elbow Surg* 24, 1106–1111. <https://doi.org/10.1016/j.jse.2014.12.012>
- Kozono, N., Okada, T., Takeuchi, N., Hamai, S., Higaki, H., Ikebe, S., Shimoto, T., Miake, G., Nakanishi, Y., Iwamoto, Y., 2017. In vivo kinematic analysis of the glenohumeral joint during dynamic full axial rotation and scapular plane full abduction in healthy shoulders. *Knee Surg Sports Traumatol Arthrosc* 25, 2032–2040. <https://doi.org/10.1007/s00167-016-4263-2>
- Kozono, N., Okada, T., Takeuchi, N., Hamai, S., Higaki, H., Shimoto, T., Ikebe, S., Gondo, H., Nakanishi, Y., Senju, T., Nakashima, Y., 2018a. Dynamic kinematics of the glenohumeral

- joint in shoulders with rotator cuff tears. *J Orthop Surg Res* 13, 9. <https://doi.org/10.1186/s13018-017-0709-6>
- Kozono, N., Okada, T., Takeuchi, N., Hamai, S., Higaki, H., Shimoto, T., Ikebe, S., Gondo, H., Nakanishi, Y., Senju, T., Nakashima, Y., 2018b. In vivo dynamic acromiohumeral distance in shoulders with rotator cuff tears. *Clin Biomech (Bristol, Avon)* 60, 95–99. <https://doi.org/10.1016/j.clinbiomech.2018.07.017>
- Krishnan, R., Björzell, N., Gutierrez-Farewik, E.M., Smith, C., 2019. A survey of human shoulder functional kinematic representations. *Med Biol Eng Comput* 57, 339–367. <https://doi.org/10.1007/s11517-018-1903-3>
- Lädermann, A., Tay, E., Collin, P., Piotton, S., Chiu, C.-H., Michelet, A., Charbonnier, C., 2019. Effect of critical shoulder angle, glenoid lateralization, and humeral inclination on range of movement in reverse shoulder arthroplasty. *Bone Joint Res* 8, 378–386. <https://doi.org/10.1302/2046-3758.88.BJR-2018-0293.R1>
- Lo, H.S., Xie, S.Q., 2012. Exoskeleton robots for upper-limb rehabilitation: state of the art and future prospects. *Med Eng Phys* 34, 261–268. <https://doi.org/10.1016/j.medengphy.2011.10.004>
- Matsuki, K., Kenmoku, T., Ochiai, N., Sugaya, H., Banks, S.A., 2016. Differences in glenohumeral translations calculated with three methods: Comparison of relative positions and contact point. *J Biomech* 49, 1944–1947. <https://doi.org/10.1016/j.jbiomech.2016.03.042>
- Matsuki, K., Matsuki, K.O., Mu, S., Kenmoku, T., Yamaguchi, S., Ochiai, N., Sasho, T., Sugaya, H., Toyone, T., Wada, Y., Takahashi, K., Banks, S.A., 2014. In vivo 3D analysis of clavicular kinematics during scapular plane abduction: comparison of dominant and non-dominant shoulders. *Gait Posture* 39, 625–627. <https://doi.org/10.1016/j.gaitpost.2013.06.021>
- Matsuki, K., Matsuki, K.O., Mu, S., Yamaguchi, S., Ochiai, N., Sasho, T., Sugaya, H., Toyone, T., Wada, Y., Takahashi, K., Banks, S.A., 2011. In vivo 3-dimensional analysis of scapular kinematics: comparison of dominant and nondominant shoulders. *J Shoulder Elbow Surg* 20, 659–665. <https://doi.org/10.1016/j.jse.2010.09.012>
- Matsuki, K., Matsuki, K.O., Yamaguchi, S., Ochiai, N., Sasho, T., Sugaya, H., Toyone, T., Wada, Y., Takahashi, K., Banks, S.A., 2012. Dynamic in vivo glenohumeral kinematics during scapular plane abduction in healthy shoulders. *J Orthop Sports Phys Ther* 42, 96–104. <https://doi.org/10.2519/jospt.2012.3584>
- Matsumura, N., Oki, S., Fukasawa, N., Matsumoto, M., Nakamura, M., Nagura, T., Yamada, Y., Jinzaki, M., 2019. Glenohumeral translation during active external rotation with the shoulder abducted in cases with glenohumeral instability: a 4-dimensional computed tomography analysis. *Journal of Shoulder and Elbow Surgery* 28, 1903–1910. <https://doi.org/10.1016/j.jse.2019.03.008>
- Mozingo, J.D., Akbari-Shandiz, M., Van Straaten, M.G., Murthy, N.S., Schueler, B.A., Holmes, D.R., McCollough, C.H., Zhao, K.D., 2019. Comparison of glenohumeral joint kinematics between manual wheelchair tasks and implications on the subacromial space: A biplane fluoroscopy study. *J Electromyogr Kinesiol* 102350. <https://doi.org/10.1016/j.jelekin.2019.08.004>

- Nishinaka, N., Tsutsui, H., Mihara, K., Suzuki, K., Makiuchi, D., Kon, Y., Wright, T.W., Moser, M.W., Gamada, K., Sugimoto, H., Banks, S.A., 2008. Determination of in vivo glenohumeral translation using fluoroscopy and shape-matching techniques. *J Shoulder Elbow Surg* 17, 319–322. <https://doi.org/10.1016/j.jse.2007.05.018>
- Rau, G., Disselhorst-Klug, C., Schmidt, R., 2000. Movement biomechanics goes upwards: from the leg to the arm. *Journal of Biomechanics* 33, 1207–1216. [https://doi.org/10.1016/S0021-9290\(00\)00062-2](https://doi.org/10.1016/S0021-9290(00)00062-2)
- Viceconti, M., 2011. *Multiscale Modeling of the Skeletal System*. Cambridge University Press, Cambridge. <https://doi.org/10.1017/CBO9781139049627>
- Werner, B.S., Chaoui, J., Walch, G., 2018. Glenosphere design affects range of movement and risk of friction-type scapular impingement in reverse shoulder arthroplasty. *Bone Joint J* 100-B, 1182–1186. <https://doi.org/10.1302/0301-620X.100B9.BJJ-2018-0264.R1>
- Werner, B.S., Chaoui, J., Walch, G., 2017. The influence of humeral neck shaft angle and glenoid lateralization on range of motion in reverse shoulder arthroplasty. *J Shoulder Elbow Surg* 26, 1726–1731. <https://doi.org/10.1016/j.jse.2017.03.032>
- Williams, S., Schmidt, R., Disselhorst-Klug, C., Rau, G., 2006. An upper body model for the kinematical analysis of the joint chain of the human arm. *Journal of Biomechanics* 39, 2419–2429. <https://doi.org/10.1016/j.jbiomech.2005.07.023>
- Wu, G., van der Helm, F.C.T., (DirkJan) Veeger, H.E.J., Makhsous, M., Van Roy, P., Anglin, C., Nagels, J., Karduna, A.R., McQuade, K., Wang, X., Werner, F.W., Buchholz, B., 2005. ISB recommendation on definitions of joint coordinate systems of various joints for the reporting of human joint motion—Part II: shoulder, elbow, wrist and hand. *Journal of Biomechanics* 38, 981–992. <https://doi.org/10.1016/j.jbiomech.2004.05.042>

Chapter 3: Four-Dimensional Computed Tomography Scanning

Allows for the Visualization and Measurement of Glenohumeral

Joint Arthrokinematics

In this chapter, the knowledge learned in Chapter 2 will be utilized to develop a technique that employs four-dimensional computer tomography scanning to measure congruency and contact centroid translation of the glenohumeral joint during internal rotation to the back in seven healthy participants. In addition, the reliability of the used technique will be measured.

3.1 Introduction

The glenohumeral joint is the most mobile joint in the human body, making it more susceptible to injury and pathology (Lefèvre-Colau et al., 2018; Massimini et al., 2014; Patel et al., 2018). The main goal of treating any shoulder injury or pathology is to restore normal glenohumeral biomechanics and arthrokinematics (Bey et al., 2010). Characterizing normal glenohumeral arthrokinematics of the glenoid with the humerus in healthy adults can help clinicians and researchers in the development of pre- and post-operative treatment plans and enhance implant designs to achieve desirable outcomes.

Numerous studies have measured the biomechanics of the glenohumeral joint under in-vitro (cadaveric specimens) and in-vivo (medical imaging modalities) conditions. However, quantifying glenohumeral biomechanics remains challenging due to associated limitations with current techniques. For example, cadaveric specimens cannot stimulate accurate muscle and joint forces (Greis et al., 2002; Gupta and Lee, 2005; Yu et al., 2005). Imaging techniques, such as magnetic resonance imaging (MRI) have a lower resolution than three-dimensional computed

tomography (3DCT) (Graichen et al., 2005, 2000; Hinterwimmer et al., 2003; Pappas et al., 2006; Werner et al., 2006), and both modalities have limited dynamic imaging capabilities (Baeyens et al., 2001). Although bi-plane fluoroscopy is a dynamic imaging modality, is limited by its 2D nature, making it difficult to detect complex musculoskeletal movements and abnormalities (Mahfouz et al., 2005; Mandalidis et al., 1999; Pfirrmann et al., 2002; Talkhani and Kelly, 2001). Thus, the previous measurement methods cannot accurately assess in-vivo, three-dimensional (3D) glenohumeral contact patterns during dynamic motions.

Recently, four-dimensional computed tomography (4DCT) (time + 3DCT) technology has emerged and may be a useful alternative to 3DCT. This new technique produces 3DCT images that demonstrate movement in real-time (Bell et al., 2015). Recently, studies have used 4DCT scanning to assess the glenohumeral joint (Matsumura et al., 2019), scapulothoracic joint (Bell et al., 2015), acromioclavicular joint (Alta et al., 2012) and sternoclavicular joint (Hislop-Jambrich et al., 2016). 4DCT have been used as a motion measuring tool of the glenohumeral and acromioclavicular joint (Alta et al., 2012; Matsumura et al., 2019), as a preoperative planning tool in snapping scapula syndrome (Bell et al., 2015), and as a diagnostic tool of the sternoclavicular joint instability (Hislop-Jambrich et al., 2016). Glenohumeral translation was assessed during active external rotation with the shoulder abducted by tracking the center of the best-fitting sphere of the articular surface of the humerus (51). None of these studies have evaluated the contact patterns and mechanics of the GH joint during active internal rotation to the back. As discussed in Chapter 1, this motion is significant in activities of daily living and is limited after reverse shoulder arthroplasty (RSA) as the implant is limited to rotate/spin. Quantifying normal arthrokinematics can explain the importance of translation in providing to the range of motion.

Therefore, the objectives of this study are 1) describe a technique which employs 4DCT to quantify in vivo GH contact patterns during dynamic shoulder motion, and 2) quantify normal GH joint contact mechanics and translation in the healthy adult during internal rotation to the back.

3.2 Methods

3.2.1 Study Protocol

After approval of Western Research Board, seven participants (average age 29 ± 9 years old) were recruited from a tertiary academic upper extremity orthopedic centre. Inclusion criteria included males over the age of 18 with no previous shoulder injury. Exclusion criteria included females and everyone under the age of eighteen. Females were excluded due to higher breast-tissue sensitivity to ionizing radiation than males.

Following consents, participants underwent static (neutral) and dynamic 4DCT scanning (Revolution CT Scanner, GE Healthcare, Waukesha, Wisconsin, USA) of their dominant shoulder while positioned supine on their side. Dynamic 4DCT started with elbow fixed at 90° , shoulder adducted, and palm flat on stomach. Participants were then instructed to actively elevate and internally rotate the shoulder to position the dorsum (the back of the hand) behind their back (Figure 3.1). This motion is called internal rotation to the back. To examine participants' natural range of motion and joint mechanics, the motion performed was physically unconstrained. A live demonstration and practice were performed prior to scanning to ensure the performance of the correct motion. During the scan, the CT technologist remained with the participant to direct them throughout the motion as well as count out loud to ensure the completion of the motion in the allotted time (21 seconds). The maximum radiation dose any subject received was 17.3 mSv. On average, radiation dose for abdomen and chest CT are 10 mSv and 7 mSv, respectively.

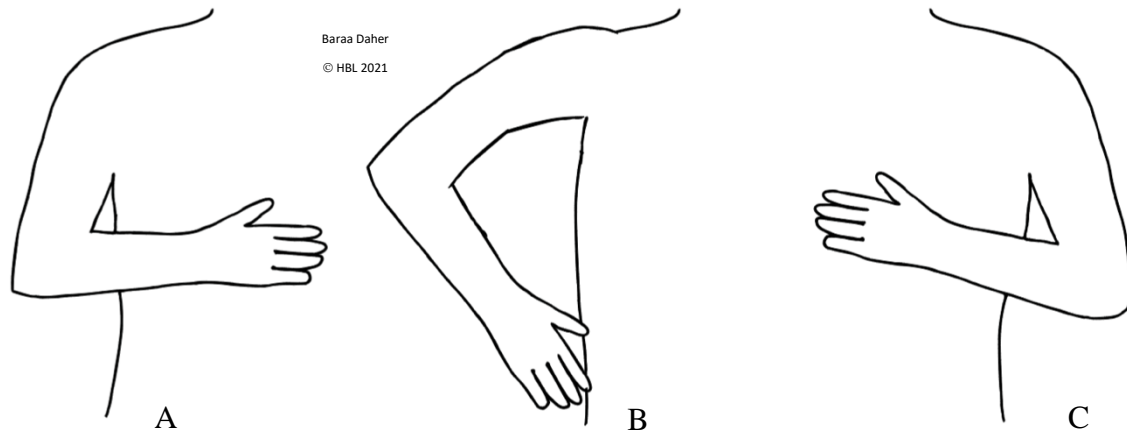


Figure 3.1: Internal rotation to the back: (A) Anterior view of the motion's starting point (B) Anterior view of the motion halfway through (C) Posterior view of the motion's ending point

3.2.2 Three-Dimensional Reconstruction and Registration

The static CT frame obtained from the scan, along with dynamic frames of the motion, were used to reconstruct 3D models of the glenoid and humerus using 3D Slicer software version 4.11.0, an open source for medical imaging processing, using a semi-automatic segmentation procedure (available at <https://www.slicer.org>) (Fedorov et al., 2012) (Figure 3.2). The static models of the glenoid and humerus were registered to the position of the dynamic frames after a landmark course alignment registration was performed using surface-based registration (iterative closest point (ICP)) algorithm (Besl and McKay, 1992). The registered models were visualized using Paraview version 4.4.0 (Kitware, Inc., New York, New York, www.paraview.org).

3.2.3 Measuring Glenohumeral Joint Congruency

Glenohumeral joint congruency was measured using a previously developed inter-bone distance algorithm to analyze the contact area of the glenohumeral joint (Lalone et al., 2013). The algorithm calculates minimum inter-bone distances between opposing bone surfaces using a point-to-point distance measurement. To display inter-bone distances, a colour scale from 0 to 6.0 mm (0 mm, red; 6 mm, blue) was selected. Distances greater than 6 mm are represented as dark blue. In addition to measuring the inter-bone distance, Joint Space Area (JSA, mm²), defined as the area on the surface of the glenoid that is within 4.0 mm of the opposing surface for the glenohumeral joint, was measured and normalized relative to the area of each participant's fossa. This analysis was conducted on each frame of the dynamic motion and visualized using a congruency contour map.

3.2.4 Measuring Glenohumeral Arthrokinematics

Glenohumeral arthrokinematics were determined by tracking the centroid of the JSA. The centroid was determined by finding the geometric average of the x, y, and z coordinates of the points on the surface of the glenoid that were within 4 mm of the humeral head. The translation of the centroid of contact was tracked throughout the motion for all participants. To describe the translation of this centroid on the glenoid surface, a local coordinate system was generated based on manually selected anatomical landmarks. The three selected landmarks were along the outer edge of the glenoid, specifically the most superior point, the most inferior point, and the most posterior point. The origin was defined as the midpoint between the inferior and superior landmarks. The y-axis was defined as the line connecting the inferior and superior landmarks, pointing superiorly. The x-axis was defined as the line perpendicular to the plane formed by the

three landmarks, pointing laterally. The z-axis was the common line perpendicular to both the x- and y-axes, pointing posteriorly.

The next step was to transform the centroid from global coordinates to the local glenoid coordinate system using MATLAB. The transformation matrix obtained through registration of the dynamic model was multiplied with the matrix defining the local coordinate axes, this results in a matrix that describes the position of the dynamic model relative to global coordinates. This resultant was inversed and multiplied by the centroid position to give the coordinates of the centroid relative to the dynamic scapula. These steps were repeated for all dynamic frames of each patient to get the contact at each point in time. The overall result of these calculations is a 3D contact path of glenohumeral joint contact throughout the motion.

Due to different glenoid sizes amongst subjects, the glenohumeral joint contact data were normalized relative to the size of each participant's glenoid. Specifically, Paraview was used to manually measure the glenoid's maximum superior/inferior (S/I) and anterior/posterior (A/P) dimensions from the CT-based reconstructed bone models. Then, for each participant, the 3D joint contact center coordinates were normalized by dividing the A/P and S/I contact center locations by the maximum A/P and S/I glenoid dimensions, respectively. Therefore, the data is expressed as a percentage of the maximum glenoid dimensions in both the A/P and S/I directions.

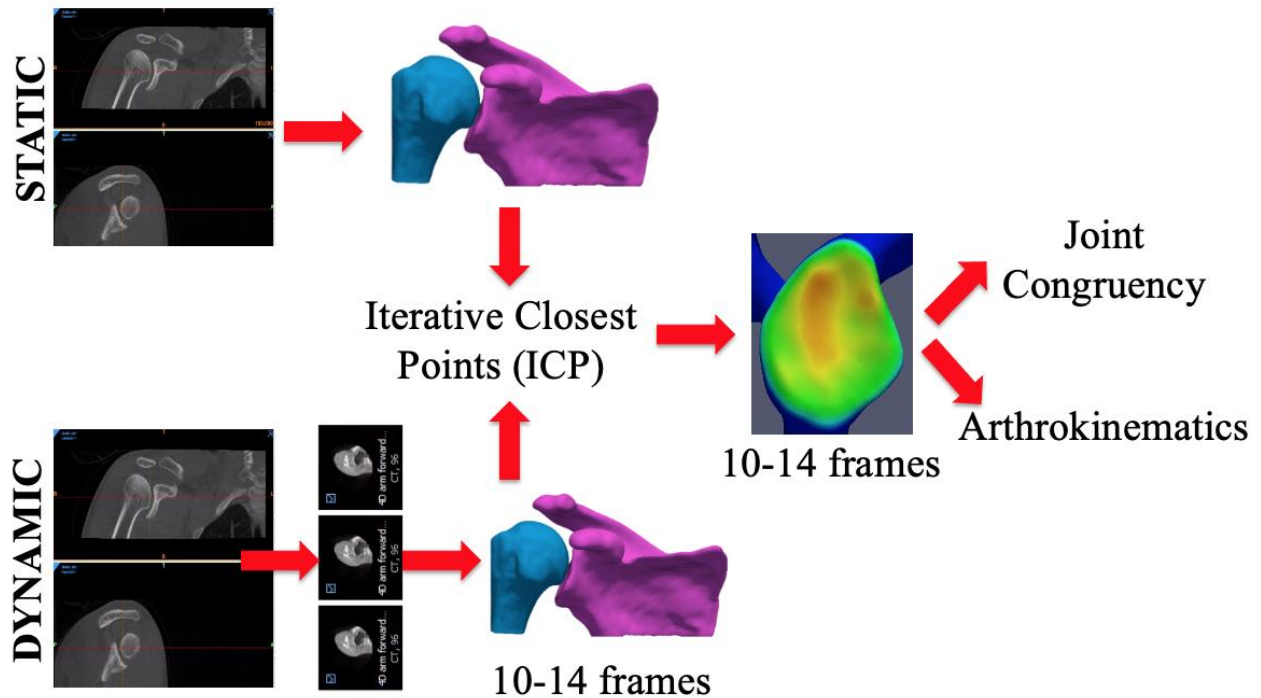


Figure 3.2: Summary of image processing and data analysis

3.2.4 Reliability Analysis

3.2.4.1 Arthrokinematics Reliability

Statistical analysis for intra-observer reliability was conducted using SPSS version 27 (SPSS Inc, Chicago, IL). An intraclass correlation coefficient (ICC) (two-way random model with consistency) was used to measure intra-observer reliability between two trials for one rater of the arthrokinematics of one patient. The translation in the S/I and A/P directions of both trials were compared. ICC values have a poor agreement when <0.50 , moderate agreement when between 0.50 and 0.75, good agreement when between 0.75 and 0.90, and excellent agreement when >0.90 .

3.2.4.2 Model-Making Comparison

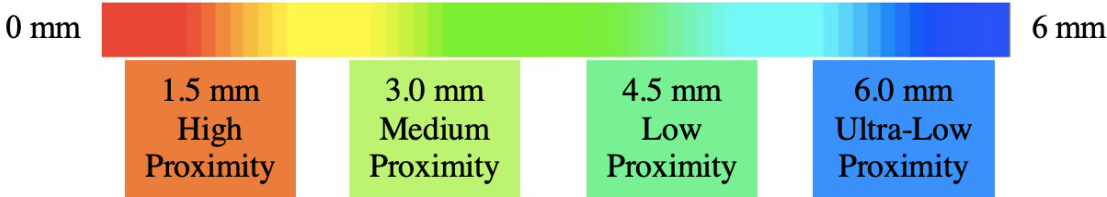
The error associated with model-making between the two trials was calculated using a previously developed inter-bone distance algorithm (Lalone et al., 2013). The algorithm calculated minimum inter-bone distances between surfaces of humeri and scapulas, respectively, using a point-to-point distance measurement. The error values for both bones were calculated by averaging the inter-bone distances between surfaces of the two trials. For visualization, proximity maps showing the inter-bone distances between trials were created and a colour scale displaying the distances from 0 to 1.0 mm (0 mm, blue; 1 mm, red) was selected.

3.3 Results

3.3.1 Glenohumeral Joint Congruency

Proximity maps of the glenohumeral joint for seven healthy participants throughout the motion are shown in Table 3.1A and Table 3.1B. Table 3.1A presents proximity maps for frames 0-12 and Table 3.1B presents proximity maps for frames 14-26. Overall, the proximity maps indicate more contact at the beginning of the motion and towards the end, when participants' hand is behind their back reaching for maximum internal rotation. The joint congruency maps and JSA show that the contact patterns of the joint change as the shoulder moves throughout the motion. Percent contact area for n=7 is presented in Table 3.2.

Table 3.1A: Proximity maps of frames 0-12 for n=7 during internal rotation to the back. A colour scale displays inter-bone distances from 0 to 6.0 mm (0 mm, red; 6 mm, blue)



Participant	Frame 0	Frame 2	Frame 4	Frame 6	Frame 8	Frame 10	Frame 12
1							
2							
3							

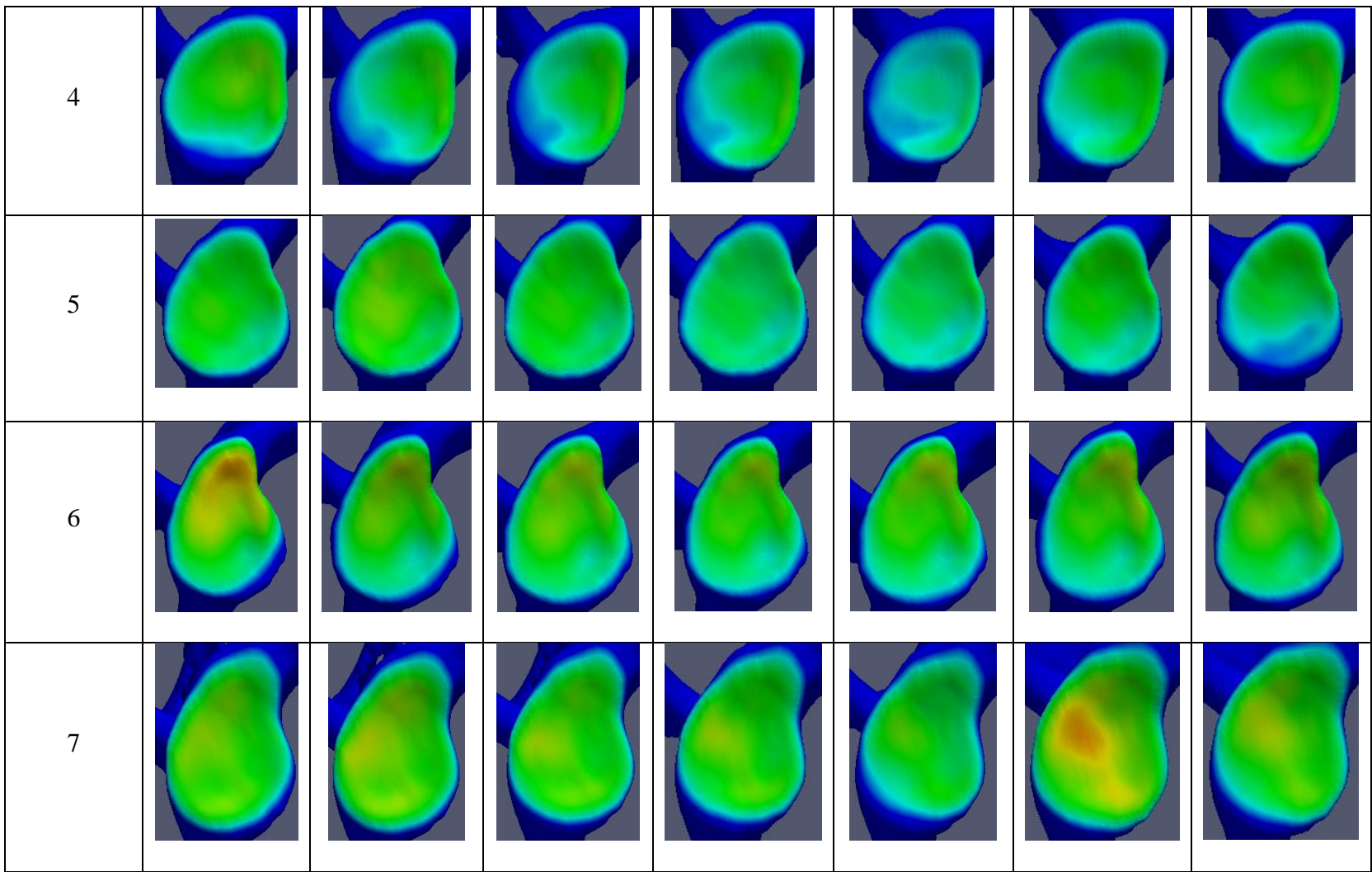


Table 3.1B: Proximity maps of frames 14-26 for n=7 during internal rotation to the back. A colour scale displays inter-bone distances from 0 to 6.0 mm (0 mm, red; 6 mm, blue)



Participant	Frame 14	Frame 16	Frame 18	Frame 20	Frame 22	Frame 24	Frame 26
1							
2							
3							

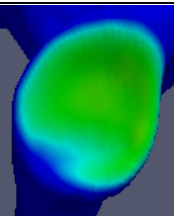
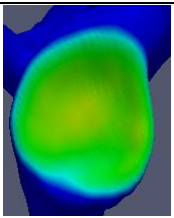
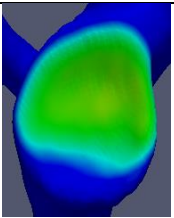
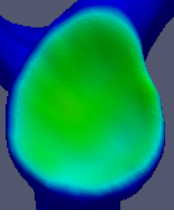
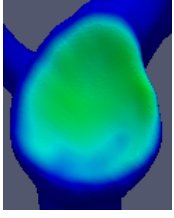
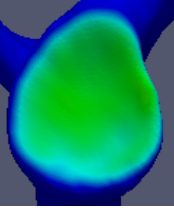
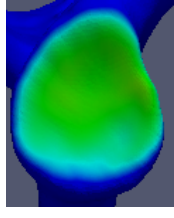
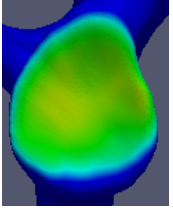
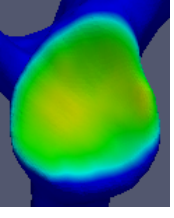
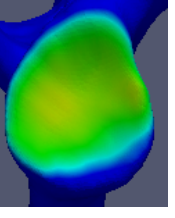
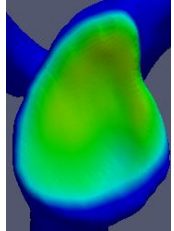
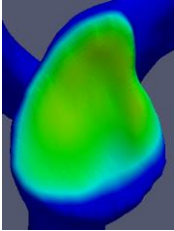
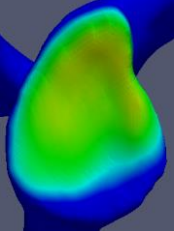
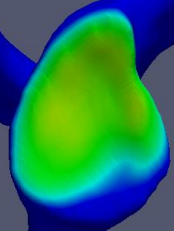
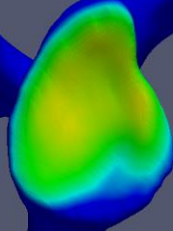
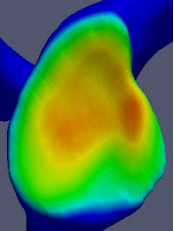
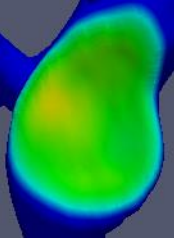
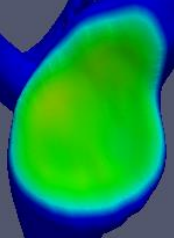
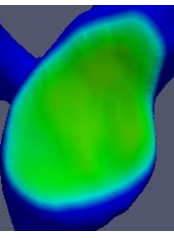
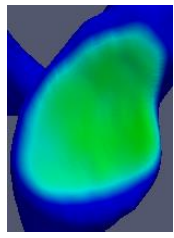
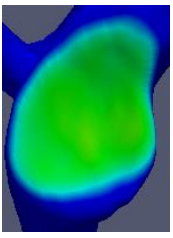
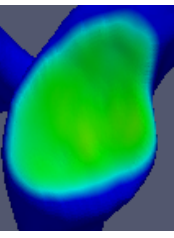
4							
5							
6							
7							

Table 3.2: Percent contact area for n=7 during internal rotation to the back

		Frame													
		0	2	4	6	8	10	12	14	16	18	20	22	24	26
Contact Area (%)	Participant 1	76.5	77.5	69.8	68.5	67.2	67.0	64.2	60.1	60.1	72.3	68.6	70.3	66.7	
	Participant 2	59.0	43.3	74.2	53.0	24.6	31.8	33.7	39.6	55.9	54.1				
	Participant 3	62.4	50.3	73.7	70.2	72.7	56.8	38.8	49.2	51.3	47.3	40.4	54.9		
	Participant 4	58.4	42.5	46.0	51.4	22.9	55.8	64.9	58.4	73.7	54.2				
	Participant 5	72.0	83.8	77.6	59.3	46.0	62.2	44.5	64.7	35.4	57.5	61.3	74.9	76.4	71.9
	Participant 6	72.2	66.1	68.4	66.1	74.9	66.6	64.7	65.6	66.7	72.3	88.1			
	Participant 7	82.5	78.5	73.6	62.1	84.1	74.0	77.1	75.1	70.8	44.3	61.9	61.4		

3.3.2 Glenohumeral Arthrokinematics

The translation of the humerus relative to the glenoid was calculated in the y-axis (superior/inferior, superior positive) and z-axis (anterior/posterior, posterior positive). Figure 3.3 shows that the average humerus translated a total of 4.9 ± 2.8 mm superiorly/inferiorly and 3.1 ± 1.3 mm anteriorly/posteriorly. This is a percent average of $13 \pm 7\%$ and $11 \pm 5\%$, respectively (Figure 3.4). Table 3.3 presents contact pathways of glenohumeral joint contact throughout the motion, total translation in y- and z-directions, and percent difference of total translation in both direction for all participants.

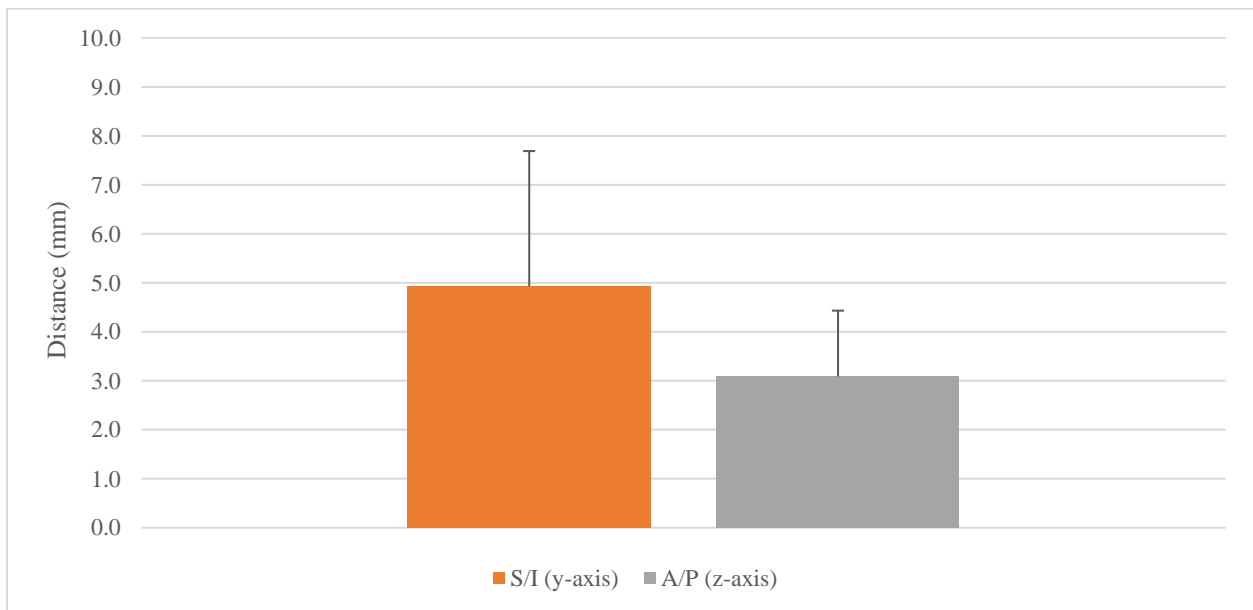


Figure 3.3: Average of total translation in the y- and z-direction of n=7

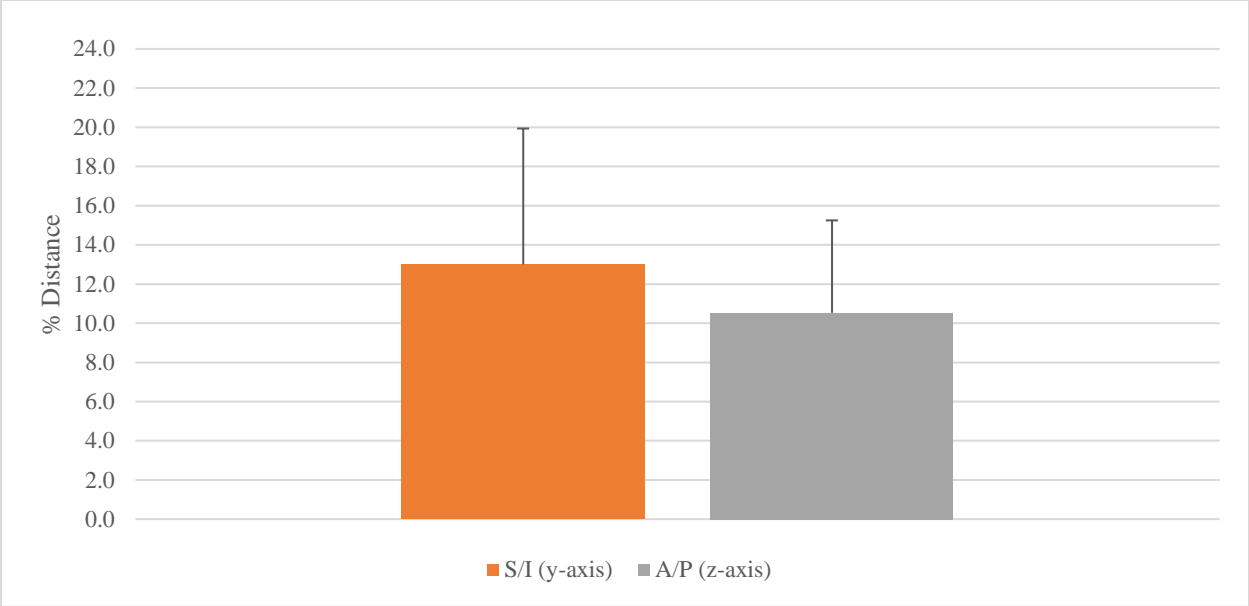
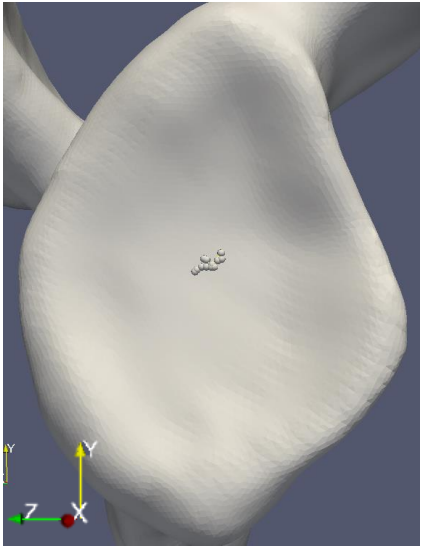
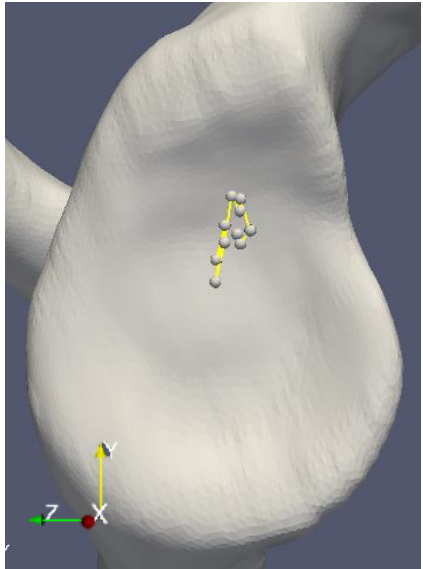
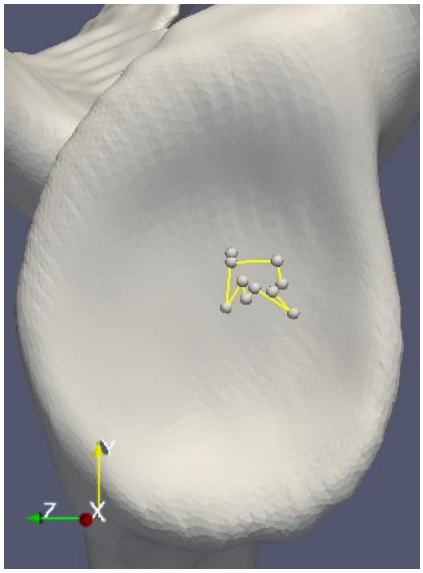


Figure 3.4: Percent average of total translation in the y- and z-direction of n=7

Table 3.3: Contact pathways of glenohumeral joint contact throughout the motion, total translation in y- and z-directions, and percent difference of total translation in y- and z-directions

Participant	Contact Pathway	Y-axis Distance (mm)	Y-axis Total Distance (mm)	Percent Difference (%)	Z-axis Distance (mm)	Z-axis Total Distance (mm)	Percent Difference (%)
1		1.4	38.5	3.7	2.4	33.7	7.2

2	 <p>A 3D visualization of a human torso from a posterior view. A cluster of approximately 10 grey spheres is connected by a yellow line, positioned in the upper back region. A 3D coordinate system is shown at the bottom left, with a red dot at the origin, a yellow arrow pointing up (Y-axis), a green arrow pointing left (Z-axis), and a white arrow pointing right (X-axis).</p>	6.8	39.2	17.3	2.8	30.3	9.3
3	 <p>A 3D visualization of a human torso from a posterior view, similar to the first image. A cluster of approximately 10 grey spheres is connected by a yellow line, positioned in the upper back region. A 3D coordinate system is shown at the bottom left, with a red dot at the origin, a yellow arrow pointing up (Y-axis), a green arrow pointing left (Z-axis), and a white arrow pointing right (X-axis).</p>	9.4	39.7	23.6	5.1	29.6	17.1

4		6.2	36.9	16.8	6.5	28.5	22.7
5		6.6	34.4	18.9	2.5	29.2	8.5

6		3.2	36.3	8.8	1.4	29.1	4.9
7		2.8	36.3	7.7	12.6	27.8	9.4

3.3.3 Reliability Analysis

3.3.3.1 Arthrokinematics Reliability

The intraclass coefficient reported has an excellent agreement within the observer. The ICC value for intra-observer reliability of two trials was 0.951 (95% coefficient 0.877 - 0.981). Table 3.4 presents the two data sets of the same participant at trial one and two. The intraclass coefficient value indicate that intra-rater was excellent for the translation measurements.

3.3.3.2 Model-Making Comparison

The error associated with model making is 0.06 mm for the humerus, and 0.26 mm for the glenoid. Figure 3.5 visualizes the difference of the bone models of both trials. A colour scale displays inter-bone distances from 0 to 1.0 mm (0 mm, blue; 1 mm, red).

Table 3.4: Contact pathways of glenohumeral joint contact throughout the motion, total translation in y- and z-directions, and percent difference of total translation in y- and z-directions

	Contact Pathway	Y-axis Distance (mm)	Y-axis Total Distance (mm)	Percent Difference (%)	Z-axis Distance (mm)	Z-axis Total Distance (mm)	Percent Difference (%)
Trial 1		6.8	39.2	17.3	2.8	30.3	9.3

Trail 2		6.4	39.2	16.4	3.2	30.2	10.6
---------	--	-----	------	------	-----	------	------

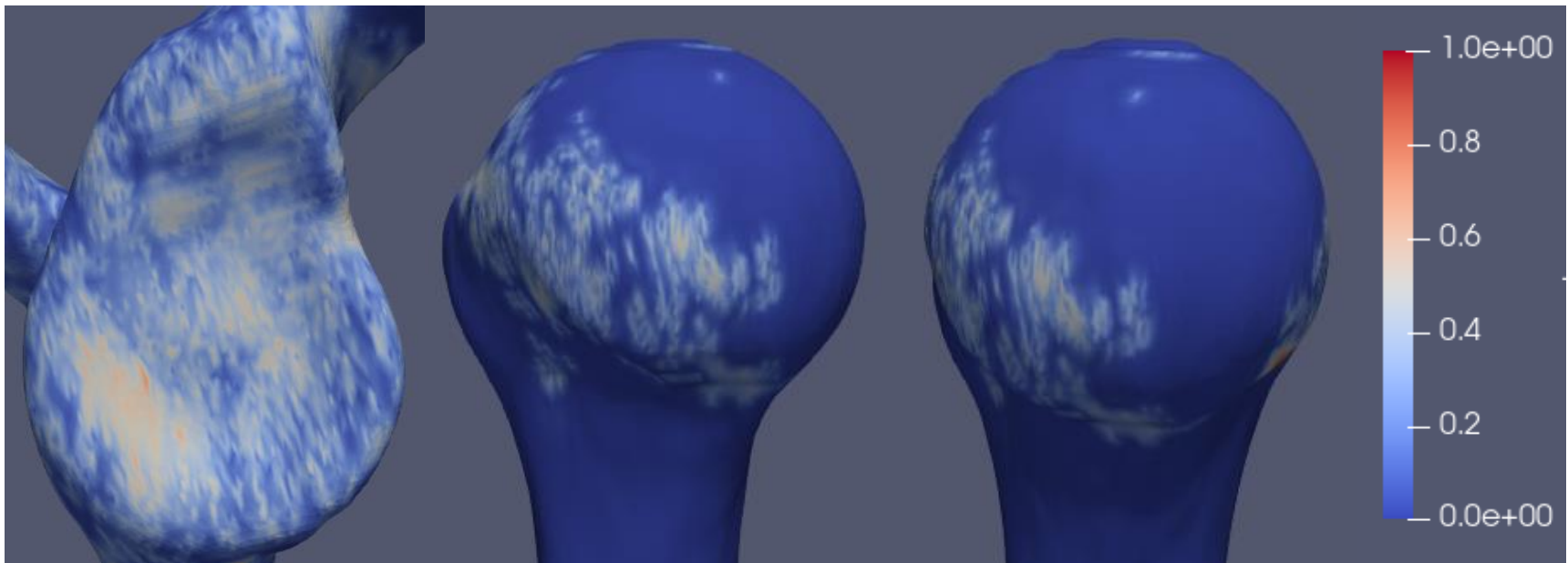


Figure 3.5: Registration differences of the bone models of both trials. A colour scale displays inter-bone distances from 0 to 1.0 mm (0 mm, blue; 1 mm, red)

3.4 Discussion

This study successfully 1) describes a technique which uses 4DCT to quantify in vivo glenohumeral contact patterns during dynamic shoulder motion, and examines the reliability of the proposed technique, and 2) quantifies normal glenohumeral arthrokinematics and translations in the healthy adult (n=7) during internal rotation to the back. As mentioned in Chapter 1, the internal rotation to the back motion is significant in activities of daily living, such as washing the back and opposite shoulder, using a back pocket, managing toileting and clasping a brassiere (Kim et al., 2020). This motion is limited after a RSA surgery as a consequence of inverting the anatomic concavities of the glenoid and humerus that creates a fixed structure in which is limited to only rotate/spin (Roche and Crosby, 2018). Therefore, quantifying normal arthrokinematics can explain the importance of translation to achieve a healthy range of motion and eventually improve implant designs.

The proximity maps and JSA of seven healthy glenohumeral joints show a general trend throughout the motion. Closer contact patterns and higher joint surface area can be noted at the beginning of the motion when compared to values throughout the motion. Contact patterns and JSA start decreasing as participants elevated and internally rotated the shoulder around the thorax. As participants reach their maximum internal rotation to the back, contact patterns and JSA start increasing. Arthrokinematics data show that on average, joint contact center moved predominantly in the S/I direction during internal rotation to the back. The average humerus translated a total of 4.9 ± 2.8 mm in the S/I direction, and 3.1 ± 1.4 mm in the A/P direction. Overall, five of seven participants had glenoid contact location at the anterior half of the glenoid, one at the superior half, and one at the center of the glenoid. Standard-deviation values in both S/I and A/P directions of centroid locations can be explained by the variable contact mechanics between subjects throughout

the motion. In addition, the results of this work explain the importance of translation throughout the motion to achieve maximum range of motion. Inverting the anatomy in RSA restricts the shoulder from translating, thus limiting its range of motion during internal rotation to the back.

Glenohumeral joint contact patterns have been measured in a number of cadaveric studies (Creighton et al., 2007; Ghodadra et al., 2010; Gupta and Lee, 2005; Lin et al., 2013; Soslowsky et al., 1992; Warner et al., 1998) and have added important knowledge to the literature. However, in-vitro, cadaveric studies cannot accurately replicate the shoulder's in-vivo environment in addition to specimen's properties changes that may occur during testing. Under in-vivo conditions, glenohumeral arthrokinematics have previously been quantified using static CT and bi-plane fluoroscopy during coronal-plane abduction and scapular plane elevation/depression with external humeral rotation (Bey et al., 2010; Massimini et al., 2014). Bey et al (Bey et al., 2010) quantified and compared in-vivo glenohumeral contact mechanics during dynamic coronal-plane abduction of repaired and contralateral shoulders after rotator cuff repair. The joint contact center location of the closest 200 mm² contact area between the humerus and glenoid was tracked to describe the translation and position of the centroid of contact. Massimini et al (Massimini et al., 2014) used a similar technique to that described by Bey and colleagues (Bey et al., 2010) to determine dynamic in-vivo glenohumeral contact mechanics in the healthy adult during scapular plane elevation/depression with external rotation of the humus. During abduction, Bey et al (Bey et al., 2010) found the joint contact center translated predominantly in the S/I direction compared to the A/P direction. The contact center travelled approximately a total of 8.0 ± 2.0 mm in the S/I direction, and 4.0 ± 2.0 mm in the A/P direction. During scapular plane elevation/depression with external humeral rotation, Massimini et al (Massimini et al., 2014) also found the joint contact center translated predominantly in the S/I direction compared to the A/P direction. The contact

center travelled a total of 18.3 ± 10.6 mm in the S/I direction, and 4.5 ± 10.9 mm in the A/P direction. This is a percent average of $36.6 \pm 11.1\%$ and $21.9 \pm 8.3\%$ in the S/I and A/P directions, respectively. The different results in the literature and this study may be explained as a result of the following variations between the studies: 1) the current study assessed internal rotation to the back, where previous studies assessed abduction and scapular elevation, respectively, 2) the humerus during the current study was internally rotated, whereas in previous studies it was either neutrally or externally rotated, 3) subject age group of the current study was 29 ± 9 years, whereas in previous studies the age groups were 26 ± 2.4 and 65 ± 10.4 years, and 4) the current study used 4DCT scanning to quantify arthrokinematics, whereas previous studies used CT and bi-plane fluoroscopy. As mentioned in Chapter 1, bi-plane fluoroscopy is limited by its 2D nature, making it difficult to detect complex musculoskeletal movements and abnormalities (Baumer et al., 2016; Bey et al., 2008; Dal Maso et al., 2016; Matsuki et al., 2016; Matsumura et al., 2019; Mozingo et al., 2019). Four-dimensional computed tomography overcomes this limitation and has promising clinical outcomes for the visualization and measurement of musculoskeletal kinematics. A recent study used 4DCT scanning to measure glenohumeral translation during active external rotation with the shoulder abducted (Matsumura et al., 2019). Matsumoto et al (Matsumura et al., 2019) found that the humeral head center translated 1.7 mm in the S/I direction and 3.4 mm in the A/P direction. This study not only assessed a different motion than the current study, but also tracked the center of the best-fitting sphere of the humeral head surface rather than the center of contact like the current study. In addition, the reliability of the techniques used was not assessed like the case of the current study. The approach utilized to quantify glenohumeral arthrokinematics using 4DCT scanning in the current study has shown to be reliable based on the data analyzed. The error associated with model making is 0.06 mm for the humerus, and 0.26 mm for the glenoid. The

glenoid was more likely to be affected by image resolution due to lower bone mineral density of the glenoid when compared to the humerus (glenoid: $356 \text{ mg} \cdot \text{cm}^{-3}$, humeral head: $1000 \text{ mg} \cdot \text{cm}^{-3}$) (Alidousti et al., 2017; Lehtinen et al., 2004).

3.5 Limitations

The technique developed in this study to quantify in-vivo glenohumeral contact patterns using 4DCT scanning overcomes the shortcomings of previous quantification methods and assesses a new motion. However, there are a few study design limitations. Although a CT technologist remained with the participant to direct them throughout the motion, this is an unconstrained motion in which participants were not required to follow a specific path while performing the motion. This resulted in motion variability, and thus high standard deviation. In addition, since this was a dynamic study, participants reached their maximum range of motion at different points in time, thus less/more frames to analyze, making it impossible to compare one-to-one frames across participants. The data relies on the accuracy of surface models and image resolution, which has not been validated, but has shown to be reliable. This study did not evaluate the translation in the medial/lateral direction as arthrokinematics was quantified. Furthermore, manual segmentation and registration of this study was time consuming, thus limiting the sample size that could be analyzed. On average, each participant required roughly 60 hours to analyze. Lastly, current study excluded females due to higher breast-tissue sensitivity to ionizing radiation than males.

3.6 Conclusion

The limitations of current techniques for measuring shoulder motion can be circumvented when using 4DCT scanning. Four-dimensional computed tomography (time + 3DCT) can be used to visualize and measure movement in real-time. This work quantified glenohumeral arthrokinematics using 4DCT as a novel approach for obtaining glenohumeral motion information. The objectives were met by describing and using a technique that utilizes 4DCT to measure normal glenohumeral joint motion during internal rotation to the back in terms of joint congruency and centroid contact location. Arthrokinematics data show that on average, joint contact center moved predominantly in the S/I direction during internal rotation to the back. The average humerus translated a total of 4.9 ± 2.8 mm in the S/I direction, and 3.1 ± 1.3 mm in the A/P direction. Current study indicates the importance of translation to achieve maximum internal rotation to the back, which is restricted after RSA thus limiting the range of motion. The use of 4DCT as a biomechanical measuring tool has shown to be a reliable technique in quantifying joint congruency and centroid translation of the glenohumeral joint.

3.7 References

- Alidousti, H., Giles, J.W., Emery, R.J.H., Jeffers, J., 2017. Spatial mapping of humeral head bone density. *J Shoulder Elbow Surg* 26, 1653–1661. <https://doi.org/10.1016/j.jse.2017.03.006>
- Alta, T.D., Bell, S.N., Troupis, J.M., Coghlan, J.A., Miller, D., 2012. The New 4-Dimensional Computed Tomographic Scanner Allows Dynamic Visualization and Measurement of Normal Acromioclavicular Joint Motion in an Unloaded and Loaded Condition. *Journal of Computer Assisted Tomography* 36, 749–754. <https://doi.org/10.1097/RCT.0b013e31826dbc50>
- Baeyens, J.-P., Van Roy, P., De Schepper, A., Declercq, G., Clarijs, J.-P., 2001. Glenohumeral joint kinematics related to minor anterior instability of the shoulder at the end of the late preparatory phase of throwing. *Clinical Biomechanics* 16, 752–757. [https://doi.org/10.1016/S0268-0033\(01\)00068-7](https://doi.org/10.1016/S0268-0033(01)00068-7)
- Baumer, T.G., Giles, J.W., Drake, A., Zauel, R., Bey, M.J., 2016. Measuring Three-Dimensional Thorax Motion Via Biplane Radiographic Imaging: Technique and Preliminary Results. *J Biomech Eng* 138. <https://doi.org/10.1115/1.4032058>
- Bell, S.N., Troupis, J.M., Miller, D., Alta, T.D., Coghlan, J.A., Wijeratna, M.D., 2015. Four-dimensional computed tomography scans facilitate preoperative planning in snapping scapula syndrome. *J Shoulder Elbow Surg* 24, e83-90. <https://doi.org/10.1016/j.jse.2014.09.020>
- Besl, P.J., McKay, N.D., 1992. A method for registration of 3-D shapes. *IEEE Transactions on Pattern Analysis and Machine Intelligence* 14, 239–256. <https://doi.org/10.1109/34.121791>
- Bey, M.J., Kline, S.K., Zauel, R., Kolowich, P.A., Lock, T.R., 2010. In Vivo Measurement of Glenohumeral Joint Contact Patterns. *EURASIP J Adv Signal Process* 2010, 162136. <https://doi.org/10.1155/2010/162136>
- Bey, M.J., Kline, S.K., Zauel, R., Lock, T.R., Kolowich, P.A., 2008. Measuring dynamic in-vivo glenohumeral joint kinematics: technique and preliminary results. *J Biomech* 41, 711–714. <https://doi.org/10.1016/j.jbiomech.2007.09.029>
- Creighton, R.A., Cole, B.J., Nicholson, G.P., Romeo, A.A., Lorenz, E.P., 2007. Effect of lateral meniscus allograft on shoulder articular contact areas and pressures. *J Shoulder Elbow Surg* 16, 367–372. <https://doi.org/10.1016/j.jse.2006.06.004>
- Dal Maso, F., Blache, Y., Raison, M., Lundberg, A., Begon, M., 2016. Glenohumeral joint kinematics measured by intracortical pins, reflective markers, and computed tomography: A novel technique to assess acromiohumeral distance. *J Electromyogr Kinesiol* 29, 4–11. <https://doi.org/10.1016/j.jelekin.2015.07.008>
- Fedorov, A., Beichel, R., Kalpathy-Cramer, J., Finet, J., Fillion-Robin, J.-C., Pujol, S., Bauer, C., Jennings, D., Fennessy, F., Sonka, M., Buatti, J., Aylward, S., Miller, J.V., Pieper, S., Kikinis, R., 2012. 3D Slicer as an Image Computing Platform for the Quantitative Imaging Network. *Magn Reson Imaging* 30, 1323–1341. <https://doi.org/10.1016/j.mri.2012.05.001>
- Ghodadra, N., Gupta, A., Romeo, A.A., Bach, B.R., Verma, N., Shewman, E., Goldstein, J., Provencher, M.T., 2010. Normalization of glenohumeral articular contact pressures after Latarjet or iliac crest bone-grafting. *J Bone Joint Surg Am* 92, 1478–1489. <https://doi.org/10.2106/JBJS.I.00220>

- Graichen, H., Hinterwimmer, S., von Eisenhart-Rothe, R., Vogl, T., Englmeier, K.-H., Eckstein, F., 2005. Effect of abducting and adducting muscle activity on glenohumeral translation, scapular kinematics and subacromial space width in vivo. *J Biomech* 38, 755–760. <https://doi.org/10.1016/j.jbiomech.2004.05.020>
- Graichen, H., Stammberger, T., Bonel, H., Karl-Hans Englmeier, null, Reiser, M., Eckstein, F., 2000. Glenohumeral translation during active and passive elevation of the shoulder - a 3D open-MRI study. *J Biomech* 33, 609–613. [https://doi.org/10.1016/s0021-9290\(99\)00209-2](https://doi.org/10.1016/s0021-9290(99)00209-2)
- Greis, P.E., Scuderi, M.G., Mohr, A., Bachus, K.N., Burks, R.T., 2002. Glenohumeral articular contact areas and pressures following labral and osseous injury to the anteroinferior quadrant of the glenoid. *J Shoulder Elbow Surg* 11, 442–451. <https://doi.org/10.1067/mse.2002.124526>
- Gupta, R., Lee, T.Q., 2005. Positional-dependent changes in glenohumeral joint contact pressure and force: possible biomechanical etiology of posterior glenoid wear. *J Shoulder Elbow Surg* 14, 105S-110S. <https://doi.org/10.1016/j.jse.2004.10.005>
- Hinterwimmer, S., Von Eisenhart-Rothe, R., Siebert, M., Putz, R., Eckstein, F., Vogl, T., Graichen, H., 2003. Influence of adducting and abducting muscle forces on the subacromial space width. *Med Sci Sports Exerc* 35, 2055–2059. <https://doi.org/10.1249/01.MSS.0000099089.49700.53>
- Hislop-Jambrich, J., Troupis, J., Moaveni, A., 2016. The Use of a Dynamic 4-Dimensional Computed Tomography Scan in the Diagnosis of Atraumatic Posterior Sternoclavicular Joint Instability. *Journal of Computer Assisted Tomography* 40, 576–577. <https://doi.org/10.1097/RCT.0000000000000410>
- Kim, M.S., Jeong, H.Y., Kim, J.D., Ro, K.H., Rhee, S.-M., Rhee, Y.G., 2020. Difficulty in performing activities of daily living associated with internal rotation after reverse total shoulder arthroplasty. *Journal of Shoulder and Elbow Surgery* 29, 86–94. <https://doi.org/10.1016/j.jse.2019.05.031>
- Lalone, E.A., McDonald, C.P., Ferreira, L.M., Peters, T.M., King, G.W., Johnson, J.A., 2013. Development of an image-based technique to examine joint congruency at the elbow. *Comput Methods Biomech Biomed Engin* 16, 280–290. <https://doi.org/10.1080/10255842.2011.617006>
- Lefèvre-Colau, M.-M., Nguyen, C., Palazzo, C., Srour, F., Paris, G., Vuillemin, V., Poiraudau, S., Roby-Brami, A., Roren, A., 2018. Recent advances in kinematics of the shoulder complex in healthy people. *Annals of Physical and Rehabilitation Medicine* 61, 56–59. <https://doi.org/10.1016/j.rehab.2017.09.001>
- Lehtinen, J.T., Tingart, M.J., Apreleva, M., Warner, J.J.P., 2004. Total, trabecular, and cortical bone mineral density in different regions of the glenoid. *Journal of Shoulder and Elbow Surgery* 13, 344–348. <https://doi.org/10.1016/j.jse.2004.01.012>
- Lin, T., Javidan, P., McGarry, M.H., Gonzalez-Lomas, G., Limpisvasti, O., Lee, T.Q., 2013. Glenohumeral contact pressure in a simulated active compression test using cadaveric shoulders. *J Shoulder Elbow Surg* 22, 365–374. <https://doi.org/10.1016/j.jse.2012.02.003>
- Mahfouz, M., Nicholson, G., Komistek, R., Hovis, D., Kubo, M., 2005. In vivo determination of the dynamics of normal, rotator cuff-deficient, total, and reverse replacement shoulders. *J Bone Joint Surg Am* 87 Suppl 2, 107–113. <https://doi.org/10.2106/JBJS.E.00483>

- Mandalidis, D.G., Mc Glone, B.S., Quigley, R.F., McInerney, D., O'Brien, M., 1999. Digital fluoroscopic assessment of the scapulohumeral rhythm. *Surg Radiol Anat* 21, 241–246. <https://doi.org/10.1007/BF01631393>
- Massimini, D.F., Warner, J.J.P., Li, G., 2014. Glenohumeral joint cartilage contact in the healthy adult during scapular plane elevation depression with external humeral rotation. *Journal of Biomechanics* 47, 3100–3106. <https://doi.org/10.1016/j.jbiomech.2014.06.034>
- Matsuki, K., Kenmoku, T., Ochiai, N., Sugaya, H., Banks, S.A., 2016. Differences in glenohumeral translations calculated with three methods: Comparison of relative positions and contact point. *J Biomech* 49, 1944–1947. <https://doi.org/10.1016/j.jbiomech.2016.03.042>
- Matsumura, N., Oki, S., Fukasawa, N., Matsumoto, M., Nakamura, M., Nagura, T., Yamada, Y., Jinzaki, M., 2019. Glenohumeral translation during active external rotation with the shoulder abducted in cases with glenohumeral instability: a 4-dimensional computed tomography analysis. *Journal of Shoulder and Elbow Surgery* 28, 1903–1910. <https://doi.org/10.1016/j.jse.2019.03.008>
- Mozingo, J.D., Akbari-Shandiz, M., Van Straaten, M.G., Murthy, N.S., Schueler, B.A., Holmes, D.R., McCollough, C.H., Zhao, K.D., 2019. Comparison of glenohumeral joint kinematics between manual wheelchair tasks and implications on the subacromial space: A biplane fluoroscopy study. *J Electromyogr Kinesiol* 102350. <https://doi.org/10.1016/j.jelekin.2019.08.004>
- Pappas, G.P., Blemker, S.S., Beaulieu, C.F., McAdams, T.R., Whalen, S.T., Gold, G.E., 2006. In vivo anatomy of the Neer and Hawkins sign positions for shoulder impingement. *J Shoulder Elbow Surg* 15, 40–49. <https://doi.org/10.1016/j.jse.2005.04.007>
- Patel, R.M., Gelber, J.D., Schickendantz, M.S., 2018. The Weight-Bearing Shoulder: *Journal of the American Academy of Orthopaedic Surgeons* 26, 3–13. <https://doi.org/10.5435/JAAOS-D-15-00598>
- Pfarrmann, C.W.A., Huser, M., Székely, G., Hodler, J., Gerber, C., 2002. Evaluation of complex joint motion with computer-based analysis of fluoroscopic sequences. *Invest Radiol* 37, 73–76. <https://doi.org/10.1097/00004424-200202000-00004>
- Roche, C., Crosby, L., 2018. Kinematics and biomechanics of reverse shoulder arthroplasty, in: *Othopaedic Knowledge Update: Shoulder and Elbow*. pp. 45–54.
- Soslowsky, L.J., Flatow, E.L., Bigliani, L.U., Pawluk, R.J., Ateshian, G.A., Mow, V.C., 1992. Quantitation of in situ contact areas at the glenohumeral joint: A biomechanical study. *Journal of Orthopaedic Research* 10, 524–534. <https://doi.org/10.1002/jor.1100100407>
- Talkhani, I.S., Kelly, C.P., 2001. Movement analysis of asymptomatic normal shoulders: a preliminary study. *J Shoulder Elbow Surg* 10, 580–584. <https://doi.org/10.1067/mse.2001.118481>
- Warner, J.J., Bowen, M.K., Deng, X.H., Hannafin, J.A., Arnoczky, S.P., Warren, R.F., 1998. Articular contact patterns of the normal glenohumeral joint. *J Shoulder Elbow Surg* 7, 381–388. [https://doi.org/10.1016/s1058-2746\(98\)90027-1](https://doi.org/10.1016/s1058-2746(98)90027-1)

- Werner, C.M.L., Weishaupt, D., Blumenthal, S., Curt, A., Favre, P., Gerber, C., 2006. Effect of experimental suprascapular nerve block on active glenohumeral translations in vivo. *J Orthop Res* 24, 491–500. <https://doi.org/10.1002/jor.20011>
- Yu, J., McGarry, M.H., Lee, Y.-S., Duong, L.V., Lee, T.Q., 2005. Biomechanical effects of supraspinatus repair on the glenohumeral joint. *J Shoulder Elbow Surg* 14, 65S-71S. <https://doi.org/10.1016/j.jse.2004.09.019>

Chapter 4: General Discussion and Conclusions

This chapter summarizes the work performed to complete the objectives and hypotheses stated in Chapter 1 of this thesis. It discusses major conclusions, strengths and limitations of each study.

Lastly, an outline of future work and directions is provided.

4.1 Summary and Conclusions

The shoulder is the most mobile joint in the human body with a wide, coupled and constrained motion (Lefèvre-Colau et al., 2018; Patel et al., 2018). Its special range of motion makes the assessment of shoulder biomechanics a challenging task, especially under in-vivo conditions. Current non-invasive tools for assessing shoulder biomechanics range from static medical imaging, such as radiographs, MRI and 3DCT, to dynamic medical imaging, such as four-dimensional computed tomography (4DCT) scanning. Four-dimensional computed tomography is a dynamic CT imaging technique, which allows for evaluation of continuous shoulder motion, as opposed to sequential static 3DCT. New studies are emerging that employ 4DCT and replace traditional study designs that combine biplane fluoroscopy and computed tomography. These studies would benefit from the valuable work that has been done in the past to inform this new generation of CT motion analysis. As such, this thesis 1) assessed the use of CT to measure shoulder kinematics, 2) proposed and used a technique that employed 4DCT to quantify glenohumeral joint congruency and arthrokinematics, and 3) tested the reliability of the proposed method.

The first objective of this thesis was to examine the extent and range of methods employing CT imaging to measure shoulder kinematics in research studies using a systematic literature search and structured data extraction process. The hypothesis was that the use of CT imaging in the literature to assess the kinematics of the shoulder presents inconsistencies and significant gaps of data reporting due to non-standardized protocols. Using a systematic literature search and structured data extraction method, Chapter 2 reviewed the extent and range of study designs measuring shoulder kinematics using CT imaging. This chapter addressed the current gaps in data reporting, and concluded with recommendations for future studies using CT. The objective of this chapter was achieved, and the hypothesis was confirmed. Based on the results of the review, participants of published studies were predominantly males, which poses a problem to the generalizability of the findings, as females have a greater magnitude of shoulder motion than males (Barnes et al., 2001). Matsuki et al. (Matsuki et al., 2012) excluded females due to ionizing radiation exposure, but failed to report the radiation dose. In fact, radiation dose was not reported in most of the studies and the reasons for not including females were not addressed. A sample size of males and females should be recruited when applicable, or a clear reason should be outlined to explain the exclusion of a certain sex in a study. In addition, radiation dose should be communicated to minimize, monitor, and raise awareness of patient dose. This will help the scientific community develop a standardized radiation exposure index for different imaging modalities, including computed tomography. The glenohumeral joint was the most studied among other joints, thus future studies should examine other shoulder joints, such as the scapulothoracic, acromioclavicular and sternoclavicular joints. Furthermore, the kinematics of the shoulder joints were examined using the recommendations by the International Society of Biomechanics (ISB) in 14 of the 29 studies included in the review. Researchers are encouraged to use ISB

recommendations to improve communication among researchers and clinicians and increase validity and reliability. This will potentially reduce variation in care provided, improve care coordination, and modify care to evidence-based practice. Lastly, many discrepancies in the reporting of the examined motions were noted in this chapter. Different authors used different perspectives and planes to report similar motions, which contributes to confusion and misunderstanding of the actual examined motion. Researchers are encouraged to provide a clear description, and/or pictures, of the motions being examined. This makes it easier for other researchers and clinicians to compare and develop standardized protocols. The findings and knowledge learned in this chapter was utilized to inform the study design of Chapter 3.

In Chapter 3, the radiation dose was effectively communicated, and the exclusion of females was explained to the higher breast-tissue sensitivity to ionizing radiation than males. In addition, a clear description of the motion examined was provided. The objectives of Chapter 3 were 1) to describe a technique which employs 4DCT to quantify in vivo glenohumeral contact patterns during dynamic shoulder motion, and examine the reliability of the proposed technique, and 2) To quantify normal glenohumeral joint congruency and arthrokinematics in the healthy adult during internal rotation to the back. The importance of this motion has been discussed in Chapter 1 and how it is limited after a reverse shoulder arthroplasty (RSA) surgery that creates a fixed structure in which is limited to only rotate/spin (Roche and Crosby, 2018). Chapter 3 used 4DCT scanning to measure joint contact patterns and mechanics. The outcomes of proximity maps and joint surface area (JSA) of seven healthy glenohumeral joint showed a general trend throughout the motion. Closer contact patterns and higher joint surface area can be noted at the beginning of the motion when compared to values throughout the motion. Contact patterns and JSA started decreasing as participants elevated and internally rotated the shoulder around the

thorax. Contact patterns and JSA increased again as participants reached their maximum internal rotation to the back. Arthrokinematics data showed that on average, joint contact center moved predominantly in the S/I direction during internal rotation to the back. The average humerus translated a total of 4.9 ± 2.8 mm in the S/I direction, and 3.1 ± 1.3 mm in the A/P direction. Overall, five of seven participants had glenoid contact location at the anterior half of the glenoid, one at the superior half, and one at the center of the glenoid. The results of this work explained the importance of translation throughout the motion to achieve maximum range of motion. Inverting the anatomy in RSA restricts translation of the shoulder, thus limiting range of motion during internal rotation to the back. In addition, the reliability of the technique used to quantify glenohumeral joint congruency and arthrokinematics using 4DCT scanning was assessed and has shown to be reliable based on the data analyzed.

4.2 Strengths and Limitations

The studies conducted in this thesis have several strengths, including the assessment of the literature employing CT scanning and the identification of current gaps and discrepancies in study designs (Chapter 2). In addition, this thesis described, implemented, and proved the reliability of a technique that employs 4DCT scanning to measure glenohumeral joint congruency and arthrokinematics during internal rotation to the back (Chapter 3). Chapter 2 informs researchers of current gaps in the literature and recommends that future studies use a comprehensive, descriptive study designs to allow researchers and clinicians to compare and develop standardized protocols and indexes. As mentioned earlier, this chapter recommends that researchers 1) include a sample size of both sex, 2) report radiation dose, 3) examine other shoulder joints in addition to glenohumeral, 4) use ISB's recommendations, and 5) provide a clear description, and/or pictures,

of the motions being examined. Chapter 3 utilized these recommendations to measure glenohumeral joint congruency and arthrokinematics using 4DCT during internal rotation to the back. Four-dimensional computed tomography scanning allows for in-vivo testing of human participants as it is a non-invasive imaging modality. In addition, 4DCT allows for dynamic, real-time visualization and measurement throughout the motion, which overcomes the shortcomings of current static imaging modalities, such as static 3DCT, MRI and radiography. It also overcomes the limited field of view of bi-plane fluoroscopy imaging. The dynamic imaging of 4DCT enables accurate visualization and measurement of shoulder motion which could be missed by static imaging techniques or limited field of view of other dynamic techniques. Therefore, this imaging modality provides further insight into true shoulder motion. In addition, this study examines internal rotation to the back, a motion that previous research have not examined. The reliability of the approach used is another strength of this chapter, as shown by the excellent agreement in intraclass correlation coefficient test and the low error in the model making process. The in-vivo nature and unconstrained motion of this study allowed participants to perform the shoulder motion as close to natural as possible. In addition, participants of this study did not encounter problems or difficulties fitting in the scanner while performing the motion. For these purposes, the proposed technique employing 4DCT imaging visualized and measured true, dynamic shoulder motion in this thesis.

While the findings and technique of this thesis are promising, the research conducted are not void of limitations. The review of Chapter 2 has several limitations including the focus on computed tomography imaging techniques only, though shoulder kinematics has been measured using other in-vivo techniques. Another limitation of the review is that only two databases were used through the literature search (Embase and PubMed), although these databases are

comprehensive and inclusive of most of the research papers. The authors also did not systematically or critically evaluate the articles themselves or comment on the use of cadavers in comparison to living participants.

While conducting the study of Chapter 3, it was learned that some the recommendations outlined in Chapter 2 are difficult to meet. The 4DCT scanner has a field of view of 16 cm in which ISB's recommended distal landmarks of the humerus were out of the field of view. In addition, the study excluded females due to higher breast-tissue sensitivity to ionizing radiation than males. The effective radiation dose would have been 20.9 mSv for females, compared to 17.3 mSv for males. Joint congruency and arthrokinematics of only the glenohumeral joint were quantified in this study, as the translation of the contact center of this joint was the focus of interest. Another limitation of this chapter is the unconstrained motion that resulted in motion variability, but true shoulder motion. In addition, since this was a dynamic study, participants reached their maximum range of motion at different points in time, thus less/more frames to analyze, making it impossible to compare one-to-one frames across participants. Furthermore, the data relies on the accuracy of surface models and image resolution, which has not been validated, but has shown to be reliable. This study did not evaluate the translation in the medial/lateral direction as arthrokinematics in the A/P and S/I directions were the focus of interest. Lastly, manual segmentation and registration in this study were time consuming, thus limiting the sample size that could be analyzed. On average, each participant required about 60 hours to analyze. Future work will focus on reducing the time required to analyze 4DCT scans.

4.3 Current and Future Directions

The review conducted in Chapter 2 informs scientists of current gaps in the literature and recommends that future studies 1) include a sample size of both sex, 2) report radiation dose, 3) examine other shoulder joints in addition to glenohumeral, 4) use ISB's recommendations, and 5) provide a clear description, and/or pictures, of the motions being examined. Future studies would benefit from these recommendations by improving communication among researchers and clinicians. This will allow for the comparison and development of standardized protocols and indexes, which will reduce variation in care provided, improve care coordination, and modify care to evidence-based practice.

The approach of analyzing 4DCT scans in Chapter 3 is time consuming and labour intensive, as it involves extensive manual segmentation and registration. Thus, limiting the number of scans analyzed by decreasing the sample size or the number of frames that could be analyzed. Future work will include the development and application of machine learning and artificial intelligent algorithm for automatic segmentation and semi-automatic registration as an efficient data analysis strategy. These approaches will not only allow for faster reconstruction rate but also increase the accuracy and quality of 3D models, as well as enable the analysis of larger sample size. In addition, the radiation dose of future studies will significantly drop as lower resolution will not propose an issue while artificial intelligent takes on the segmentation process. This will allow for the inclusion of females and the recruitment of larger sample size, in addition to the examination of multiple motions.

4.4 Conclusions

Despite the extent in which the shoulder complex has been examined, extensive gaps and discrepancies still exist in the literature. The recommendations made in this thesis are designed to increase the efficiency and effectiveness of future studies. When applicable, these recommendations were followed while conducting the second study which employed 4DCT scanning. Four-dimensional computed tomography has shown to be a reliable tool for the visualization and measurement of dynamic in-vivo glenohumeral joint congruency and arthrokinematics during internal rotation to the back. The results of this work show the importance of contact center translation throughout the motion to achieve maximum range of motion. Inverting the anatomy and high constraint in RSA restricts the shoulder from translating, thus limiting its range of motion during internal rotation to the back. The knowledge advancement of this work can further advance the field of biomechanics by contributing to the understanding of 4DCT as a measurement tool in the field. A greater understanding of the arthrokinematics of the glenohumeral joint can contribute to the improving of implant designs, treatment plans, and post-surgery outcomes.

4.5 References

- Barnes, C.J., Van Steyn, S.J., Fischer, R.A., 2001. The effects of age, sex, and shoulder dominance on range of motion of the shoulder. *Journal of Shoulder and Elbow Surgery* 10, 242–246. <https://doi.org/10.1067/mse.2001.115270>
- Lefèvre-Colau, M.-M., Nguyen, C., Palazzo, C., Srour, F., Paris, G., Vuillemin, V., Poiraudreau, S., Roby-Brami, A., Roren, A., 2018. Recent advances in kinematics of the shoulder complex in healthy people. *Annals of Physical and Rehabilitation Medicine* 61, 56–59. <https://doi.org/10.1016/j.rehab.2017.09.001>
- Matsuki, K., Matsuki, K.O., Yamaguchi, S., Ochiai, N., Sasho, T., Sugaya, H., Toyone, T., Wada, Y., Takahashi, K., Banks, S.A., 2012. Dynamic in vivo glenohumeral kinematics during scapular plane abduction in healthy shoulders. *J Orthop Sports Phys Ther* 42, 96–104. <https://doi.org/10.2519/jospt.2012.3584>
- Patel, R.M., Gelber, J.D., Schickendantz, M.S., 2018. The Weight-Bearing Shoulder: *Journal of the American Academy of Orthopaedic Surgeons* 26, 3–13. <https://doi.org/10.5435/JAAOS-D-15-00598>
- Roche, C., Crosby, L., 2018. Kinematics and biomechanics of reverse shoulder arthroplasty, in: *Othopaedic Knowledge Update: Shoulder and Elbow*. pp. 45–54.

Curriculum Vitae

Name: Baraa Daher

Post-Secondary Education and Degrees: Bachelor of Science
Western University, London, Ontario
2014-2018

Masters of Engineering Science in Biomedical Engineering
Western University, London, Ontario
2019-2021

Honours and Awards: Dean's Scholar
Western University, London, Ontario
2017-2018

Western University Excellence Scholarship
Western University, London, Ontario
2014-2015

Related Work Experience: Lead Teaching Assistant
Department of Software Engineering
Western University, London, Ontario
2020-2021

Teaching Assistant
Department of Applied Math
Western University, London, Ontario
2020-2021

Teaching Assistant
Department of Physics and Astronomy
Western University, London, Ontario
2019-2021

Teaching Assistant
Department of Biology
Western University, London, Ontario
2019-2021

Collaborative Musculoskeletal Health Research (CMHR) Trainee
Western University, London, Ontario
2019-2021

Western Engineering Outreach Instructor
Western University, London, Ontario
2019

Western Engineering Summer Academy Instructor
Western University, London, Ontario
2018, 2019

Research Assistant
Department of Mechanical and Materials Engineering
Western University, London, Ontario
2018-2021

Research Assistant
London Health Science Centre, London, Ontario
2017

Research Assistant
Brescia University Collage
Western University, London, Ontario
2016-2017

Research Assistant
Department of Physiology and Pharmacology
Western University, London, Ontario
2016

Publications:

Baraa Daher, Hames Hunter, George S. Athwal, Emily Lalone (2021). How does Computed Tomography Inform our Understanding of Shoulder Kinematics? A Structured Review. *Journal of Medical and Biological Engineering and Computing*, Under Revision.

Andrea Kassay, Baraa Daher, Emily Lalone (2020). An Analysis of Wrist and Forearm Range of Motion Using the Dartfish Motion Analysis System. *Journal of Hand Therapy*. 34(4):604-611.

Presentations:

First Listed Author. Four-Dimensional Computed Tomography Scans Allow Dynamic Visualization and Measurement of Glenohumeral Joint Arthrokinematics Joint Kinematics. Baraa Daher, George S. Athwal, Emily Lalone. Orthopaedic Research Society. 2022.

First Listed Author. Four-Dimensional Computed Tomography Scans Allow Dynamic Visualization and Measurement of Glenohumeral Joint Arthrokinematics Joint Kinematics. Baraa Daher, George S. Athwal, Emily Lalone. Canadian Biomaterials Society – Southwestern Ontario Student Chapter (CBS-SEOSC). 2021.

First Listed Author. Four-Dimensional Computed Tomography Scans Allow Dynamic Visualization and Measurement of Glenohumeral Joint Arthrokinematics Joint Kinematics. Baraa Daher, George S. Athwal, Emily Lalone. Biomedical Engineering Seminar Series. 2021.

First Listed Author. Four-Dimensional Computed Tomography Scans Allow Dynamic Visualization and Measurement of Scapulothoracic Joint Kinematics. Baraa Daher, George S. Athwal, Emily Lalone. Imaging Network Ontario (ImNO). 2021.

First Listed Author. Four-Dimensional Computed Tomography Scans Allow Dynamic Visualization and Measurement of Scapulothoracic Joint Kinematics. Baraa Daher, George S. Athwal, Emily Lalone. Canadian Bone and Joint Conference. 2020.

First Listed Author. Four-Dimensional Computed Tomography Scans Allow Dynamic Visualization and Measurement of Scapulothoracic Joint Kinematics. Baraa Daher, George S. Athwal, Emily Lalone. Biomedical Engineering Seminar Series. 2020.

First Listed Author. The Field of Biomedical Engineering. Baraa Daher. Ontario Tech University. 2020.

Posters:

First Listed Author. Four-Dimensional Computed Tomography Scans Allow Dynamic Visualization and Measurement of Scapulothoracic Joint Kinematics. Baraa Daher, George S. Athwal, Emily Lalone. Canadian Orthopaedic Research Society (CORS). 2020.

First Listed Author. Four-Dimensional Computed Tomography Scans Allow Dynamic Visualization and Measurement of Scapulothoracic Joint Kinematics. Baraa Daher, George S. Athwal, Emily Lalone. Imaging Network Ontario (ImNO). 2020.

First Listed Author. Four-Dimensional Computed Tomography Scans Allow Dynamic Visualization and Measurement of Scapulothoracic Joint Kinematics. Baraa Daher, George S. Athwal, Emily Lalone. Ontario Biomechanics Conference (OBC). 2020.